The Role of Mitochondrial Dynamics on Neurodegenerative Processes of Multiple Sclerosis in Respose to Inflammation and Endoplasmic Reticulum Stress

by

Xiaodan Deng

A thesis submitted in partial fulfillment of the requirements for the degree of

Master of Science

Centre for Neuroscience
University of Alberta

Abstract

Biopsies and post-mortem tissue of patients with multiple sclerosis (MS) as well as inflammatory demyelinating animal models show that endoplasmic reticulum (ER) stress is a hallmark of the progression of these pathologies. Moreover, MS biopsies and animal models of neuroinflammatory diseases have detected axonal damage associated with mitochondria fragmentation and impaired distribution as an early event in absence of demyelination. It is thought that a combination of these phenomena makes cells more susceptible to inflammatory–mediated neurodegeneration and subsequent progression of the disease. Recent studies have demonstrated that Rab32, a small GTPase in the Ras protein family, plays a role in regulating mitochondrial mobility and ER stress induced apoptosis. Liang *et al.* showed that Rab32 expression sharply increases in response to acute brain inflammation, but subsequently drops. Based on the finding that activation of Rab32 induces ER stress related apoptosis and facilitates mitochondrial fragmentation via activation of dynamin-related protein 1 (Drp1), we hypothesize that Rab32 could play a role in altering the axonal mitochondrial distribution and inducing neurodegeneration in MS. In this study, we probed and measured the levels of Rab32 protein and functional related proteins Rab38 and Rab7L1, ER stress and apoptosis related proteins in acute as well as chronic lesions and normal-appearing white matter (NAWM) of inflamed MS brain tissues by Western blot and immunohistochemistry. Indeed, we found that high levels of Rab32 coincide with ER stress-associated apoptosis in acute lesions and its activation leads to shorter neurites with fragmented mitochondria in human neurons. Moreover, abnormal expression and activity of Rab32 accelerates apoptosis of human neurons, suggesting a role for Rab32 in neurodegenerative progression of MS.

Acknowledgements

I would like to send a big thank you to my supervisor, Dr. Fabrizio Giuliani for all his support and encouragement. I couldn't have finished this meaningful work without him. I would also like to thank Dr. Thomas Simmen for his supervision and support throughout my project. Thank you to my committee members, Drs. David Westaway and Thomas Simmen, for their time, advice and effort contributing to my project.

I feel so grateful to have worked with some excellent lab members over the past few years, Yohannes, Diane and Laura, and for their support and advice during my master project. Carolina, Emily, Arun and many others provided valuable advice and assistance with my experiments. For Jasmine and Megan, I appreciate all your effort along the way.

I would like to thank Dr. Jack Jhamandas and his lab, Dr. Christopher Power and his lab, Dr. Bradley Kerr and his lab, and Dr. Jian-Qiang Lu for their donations of MS tissue, antibodies, advice and technical support.

Last but not least, I must thank my family and friends who encouraged and supported me during perusing my master's study. Their kindness and love give me the strength to continue with my future endeavors.

TABLE OF CONTENTS

LIST OF TABLES

LIST OF FIGURES

LIST OF ABBREVIATIONS

AD	Alzheimer's disease
AKAP	A-kinase anchoring protein
ALS	Amyotrophic Lateral Sclerosis
ANOVA	One-way analysis of variance
APP	Amyloid precursor protein
ATF6	Transcription factor-6
ATP	Adenosine tri-phosphate
Aβ	Amyloid β
BBB	Blood brain barrier
BiP	Binding immunoglobin protein
Cdk1	Cyclic-dependent kinase 1
CHOP	C/EBP homologous protein
CNS	Central nerves system
DNA	Deoxyribonucleic acid
DRG	Dorsal root ganglion
Drp1	Dynamin-related protein 1
EAE	Experimental autoimmune encephalomyelitis
EDSS	Expanded Disability Status Scale
ER	Endoplasmic reticulum
ETC	Electron transport chain
EVI5	Ecotropic viral integration site 5
FAD	Focal axonal degeneration
Fis1	Mitochondrial fission protein 1
GAP	GTPase-activating protein
GED	GTPase effector domain
G-protein	Guanosine nucleotide-binding protein
Grp75	Mortalin or glucose-related protein 75
Grp94	Glucose-related protein 94
GTPase	Guanosine triphosphate hydrolase

GWAS	Genome-wide association study
H&E	Hematoxylin and eosin
HD	Huntington's disease
HFN	Human fetal neuron
HLA	Human leukocyte antigen
HR1 or 2	Heptad repeat domain 1 or coiled-coil domain 1 or 2
Hsp70	Heat shock protein 70
I	Isoleucine
iPSC	Induced pluripotent stem cell
IRE1	Inositol-requiring protein-1
L	Leucine
LFB	Luxol fast blue
MAM	Mitochondria-associated ER membrane
Mff	Mitochondrial fission factor
Mfn1 or 2	Mitofusin 1 or 2
MRI	Magnetic resonance imaging
mRNA	Messenger ribonucleic acid
MS	Multiple Sclerosis
N	Asparagine
Na^+/K^+ ATPase	Sodium/potassium ATPase
NAWM	Normal-appearing white matter
nf	Normalization factor
NO	Nitric oxide
Opa1	Optic atrophy 1
PACS2	Phosphofurin acidic cluster sorting protein 2
PD	Parkinson's disease
PERK	Protein kinase RNA-like ER kinase
PINK1	Putative kinase 1
PKA	Protein kinase A or cyclic AMP dependent protein kinase A
PP-MS	Primary-progressive multiple sclerosis
PR-MS	Progressive-relapsing multiple sclerosis
PS1 or 2	Presenilin 1 or 2

Q	Glutamine
Ran	Ras-related nuclear protein
ROS	Reactive oxygen species
RR-MS	Relapsing-remitting multiple sclerosis
S	Serine
SNPs	Single-nucleotide polymorphisms
SOD1	Superoxide dismutase 1
SP-MS	Secondary-progressive multiple sclerosis
T	Threonine
TRAF2	TNF receptor-associated factor 2
WT	Wild type
XBP-1	X-box binding protein 1

CHAPTER 1:

Introduction

1. INTRODUCTION

1.1 Multiple Sclerosis

1.1.1 Overview

Probably the very first case of Multiple Sclerosis (MS) documented is a girl in Holland who developed an acute sickness in 1395 at her age of 16 whose symptoms included blindness, loss of balance, weakness and pain [1]. In the next few centuries, similar cases occurred. In 1868, Dr. Jean-Martin Charcot, who is regarded as "the father of neurology", examined a young woman with a tremor, noted her neurological abnormalities in speech and eye movement, and found the characteristic scars in her autopsy brain. He collected clinical symptoms and the post-mortem pathological evidences of many patients with similar neurological disabilities including cognitive and motor impairments. He concluded this was a disease of which some reliable indicators were intention tremor, nystagmus and scanning speech, and proposed naming this disease 'multiple sclerosis (MS)' [1, 2]. In the following decades, great progresses were made in understanding the pathological mechanisms of MS and establishing therapies and symptomatic treatments with development of imaging techniques and advance of basic science research.

Nowadays, MS is considered a complex chronic inflammatory disease of the central nerves system (CNS) [3] and its diagnosis is facilitated by the use of neuroimaging techniques such as magnetic resonance imaging (MRI). MS symptoms are heterogeneous depending on the location of the lesions within the CNS and vary as time goes on. Patients with MS can suffer almost any of neurological symptoms, which include motor,

coordination, visual and cognitive impairments in most cases. The most common symptoms are numbness, vision impairment, motor impairment and spasticity [4].

1.1.1.1 Facts of MS

MS is the first cause of non-traumatic disability among young adults in North America and Europe and affects over two million people worldwide [5-10]. According to the recent announcement made by MS Society of Canada, 100,000 Canadians are currently living with MS, and this is one of the highest rates in the world. Disease onset is usually between age 15 and 40, whereas children as young as two can be diagnosed with pediatric MS and more likely to be suffering from seizures, and brainstem and cerebellar symptoms [11]. Similar to other autoimmune diseases, MS has a higher prevalence in females and the reason is possibly related to seasonal effects and hormonal fluctuations [4, 12].

1.1.1.2 Measurements of Disabilities in MS Patients

A method to evaluate patient's neurological disability in MS, known as the Expanded Disability Status Scale (EDSS), was developed by Dr. John F. Kurtzke, who is a neuroepidemiologist and a neurology professor at Georgetown University in the United States [13]. The EDSS was established to quantify disability in eight functional systems of the human body, including pyramidal, cerebellar, brainstem, sensory, bowel and bladder, visual and other functions [13]. The functional system score scale goes from 1 to 10, where 0 represents normal neurological exam, 1.0 to 4.5 indicates people with MS

who are fully ambulatory, 5.0 to 9.5 defines MS patients with impaired ambulation, and the highest score 10 represents “death caused by MS” [13].

1.1.1.3 Clinical Subtypes of MS

It is recognized that MS has four clinical courses [14]. Around 85% of patients experience relapsing-remitting MS (RR-MS), where acute worsening of symptoms occurs, followed by symptom reduction or remission [4]. The majority of these patients eventually develop a secondary-progressive course (SP-MS), where even though relapses can occur, recovery is incomplete with a gradual progression of disability [4]. These patients are considered to be at an advanced clinical stage with increased disability and higher EDSS score. In contrast, 10-15% of patients have a primary progressive course (PP-MS) characterized by slow progression of disability without relapse [14]. Few patients present a progressive relapsing course (PR-MS) where relapses can occur on a background progression [14]. In RR-MS patients, some symptoms disappear during the remission period between two relapses [14]. However in some cases, permanent neurological impairment persists and leads to severe disability and eventually death at an advanced disease stage [14]. In MS patients, combinations of these disease courses may also occur and the disease course is extremely variable among different individuals [4].

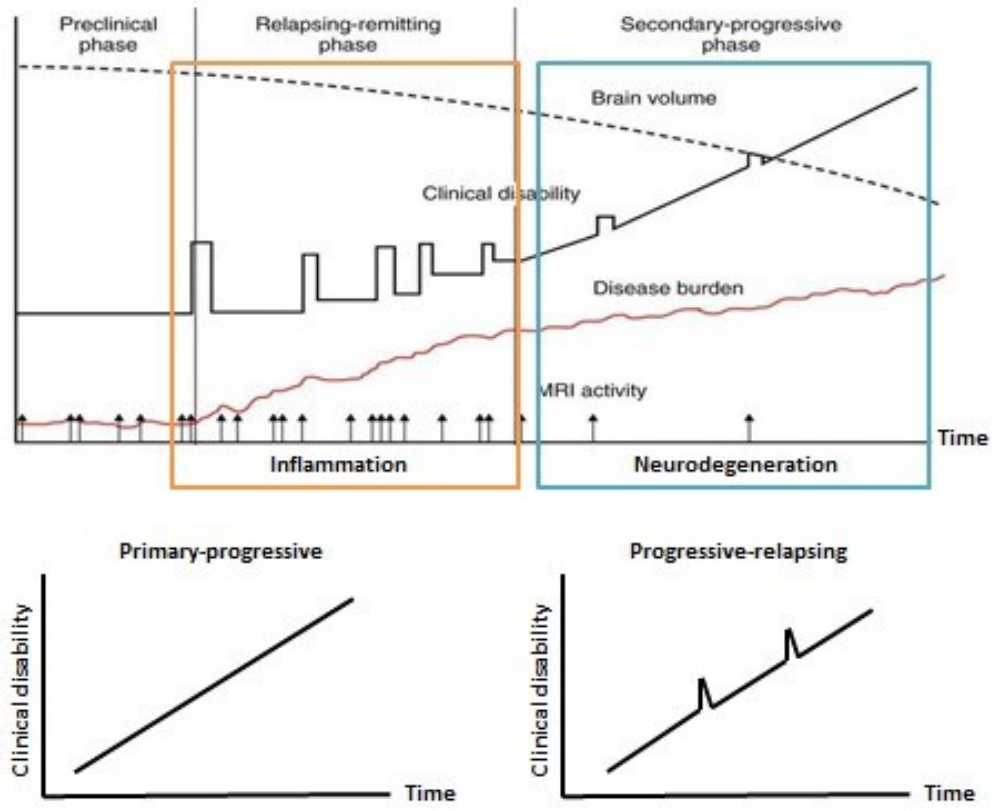

Figure 1.1 Different clinical courses and progression of MS. Clinical disability of patients with 4 different MS clinical courses is illustrated over time. The most common, relapsing-remitting MS, starts with massive inflammation and progresses to secondary progressive MS where increased lesion volume, tissue damage and disability are dominant. Adapted from [15].

1.1.2 Etiology of MS

1.1.2.1 Environmental Effects

The etiology of MS has been widely studied, however no apparent candidate appear to completely describe the cause of the disease [16]. There are increasing amount of evidence suggesting that a number of environmental factors are important in the development of MS [11]. Lower prevalence is seen nearer the equator and in Asian countries, compared to the regions close to the poles both in Europe and North America

[17-21]. The reasons for this difference can be genetic and/or environmental [22]. Studies have shown that migrants moving from high MS prevalence regions to lower risk regions particularly before the age of 15 may have lowered chance of contracting the disease, while a reverse migration will retain the lower MS risk with unclear age effect [23-30]. MS incidence was three-fold higher in women than in men, but the gender difference is a common factor in most autoimmune diseases [31, 32]. Two studies from the Ascherio group have shown that low vitamin D intake and the lack of serum vitamin D are associated with high risk of developing MS, indicating Vitamin D as the cause of the latitude effect [33, 34]. However, to date these researches remain inconclusive [35-38]. Cigarette smoking increases the risk of autoimmune diseases [39, 40], having a proinflammatory effect [41, 42] and increasing the permeability of the blood brain barrier (BBB) [43, 44], with subsequent induction of inflammation within the CNS and development of MS [5]. Viral and bacterial infections have been investigated as a possible cause for disease onset [45, 46]. Early infection by so-called long-acting viruses that remain hidden in the body for years induces latent immunological changes in the body and is present in many patients with MS [47]. These viruses eventually result in autoimmune demyelination and subsequently the appearance of disease symptoms [47]. This finding suggests that early exposure to these viruses could play an important role in the development of MS [47].

1.1.2.2 Genetic Effect

The genetic contribution to the susceptibility and age of disease onset is also undeniable [48]. Studies in twins demonstrate a concordance rate of more than 25% in

monozygotic compared to less than 3% for dizygotic twins in the normal population for MS, indicating that genetics contributes to the etiology of the disease [49]. In the early 1970s, the human leukocyte antigen (HLA) gene cluster on chromosome 6p21.3 was discovered to be an MS susceptibility locus through the use of a classic case–control association approach [50]. Later, examination of common genetic variants among numerous individuals termed as genome-wide association study (GWAS) was conducted in a large group of MS patients to understand the association between single-nucleotide polymorphisms (SNPs) and disease traits. According to the most recent and reliable result of the GWAS in 2011, approximately 50 non- HLA genetic risk factors have been identified to be associated with MS [48]. However, no further molecular analysis of these risk genes in altering MS occurrence and progression has been done. With a large proportion of the disease heritability still unclear, more studies are now focusing on the identification of causal alleles, associated pathways, epigenetic mechanisms, and gene–environment interactions [48].

Because of complexity and under-development of MS pathogenesis, there is currently no cure for MS [51]. However, several treatments have been established to improve patients' quality of life. Different types of these treatments include disease-modifying therapies that reduce the occurrence of relapses and lesions and slow down the aggravation of disabilities, and numerous medications and physiotherapies in treating MS symptoms [52]. The fact that there is currently no cure for MS suggests a need to develop effective therapeutic compounds and biomarkers based on a better understanding of the disease pathogenesis.

1.1.3 Pathology of MS

1.1.3.1 Inflammation

The term 'inflammation', which comes from the Latin *inflammare* meaning "to set on fire", was first documented by Aulus Celsus, a Roman encyclopaedist, 2000 years ago according to four cardinal signs: redness, swelling, heat and pain [53]. The definition of inflammation based on a combination of clinical signs and symptoms underestimates the cellular processes and signals that do not give rise to any of the symptoms [54]. Before 19th century, inflammation was described as an acute and complex biological response of the body's immune system to foreign harmful stimuli or one's own damaged cells, which should have more of a protective effect on injury than a pathological impact. However, since it is observed that tissues and organs in inflammation lose some of their functions, it is obvious that the inflammatory response has its pros and cons [54]. When inflammation starts, activated immune cells invade the inflamed tissue where antigens are targeted and cells with these antigens present are killed. Damaged cells are then recognized by the immune system and produce molecules to attract more cells and induce further killing. The accumulated inflammatory response affects surrounding cells and tissues, and leads to permanent damage. Modern molecular analysis suggests that inflammation is characterized by a constellation of more complex mechanisms including pro-inflammatory signaling molecules mediated responses in absence of activated immune cell invasion [55].

1.1.3.2 Neuroinflammation-mediated MS Pathogenesis

The pathology of MS is characterized by inflammation-initiated multiple lesions with demyelination and axonal injury within the CNS. However, in recent years, evidence has accumulated, supported by neuroimaging, that the progression of disability does not correlate with the number of demyelinated plaques, but rather with the level of total axonal damage and loss [56, 57]. The observed axonal injury and neurodegeneration in MS are believed to be inflammation-mediated [57, 58]. As mentioned above, the inflammatory response is an early, non-specific reaction of the immune system to tissue damage or pathogen invasion [14, 59]. Neuroinflammation is caused by unexpected activation of peripheral leukocytes migrating into an aberrantly compromised CNS [4, 60]. The most accepted hypothesis is that T lymphocytes, myeloid cells and B cells are activated by an unknown antigen in the periphery. Then they up-regulate their surface molecules and efficiently adhere to the endothelial cells of the BBB in agreement with the local chemokine gradients [61]. BBB is a complex structure that protects the CNS from the circulatory system and absorbs nutrients, resists toxin from the blood and releases wastes from the brain. The integrity of BBB is vital to a normal homeostasis of the CNS. In MS, activated lymphocytes attach, roll and adhere to the BBB, secrete matrix metalloproteinase to alter the extracellular milieu and increase the permeability of BBB, and finally enter the CNS through trans-endothelial migration [55, 61]. These cells are thought to enter the CNS due to the similarity of the unknown activating antigen to a CNS antigen, possibly myelin antigen [62]. This misrecognition is known as molecular mimicry, where a CNS protein is misinterpreted and targeted as a viral or bacterial antigen by the immune system [6, 63, 64]. Once in the CNS, the infiltrating T cells are

re-activated by resident antigen-presenting cells. The presented antigen can be a myelin-specific protein and can stimulate T cells to destroy myelin within the CNS, leaving axons vulnerable to further attacks from T cells or other neurotoxic agents. Furthermore, chronic activation of CNS-resident cells in response to pro-inflammatory cytokine secretion and epitope spreading were shown to participate in the killing, which may take place independent of ongoing peripheral events [61]. Astrocytes, which are an essential component of the BBB, may also provide the endothelial cells with signals corresponding to the pro-inflammatory environment, further facilitating leukocyte transmigration [65].

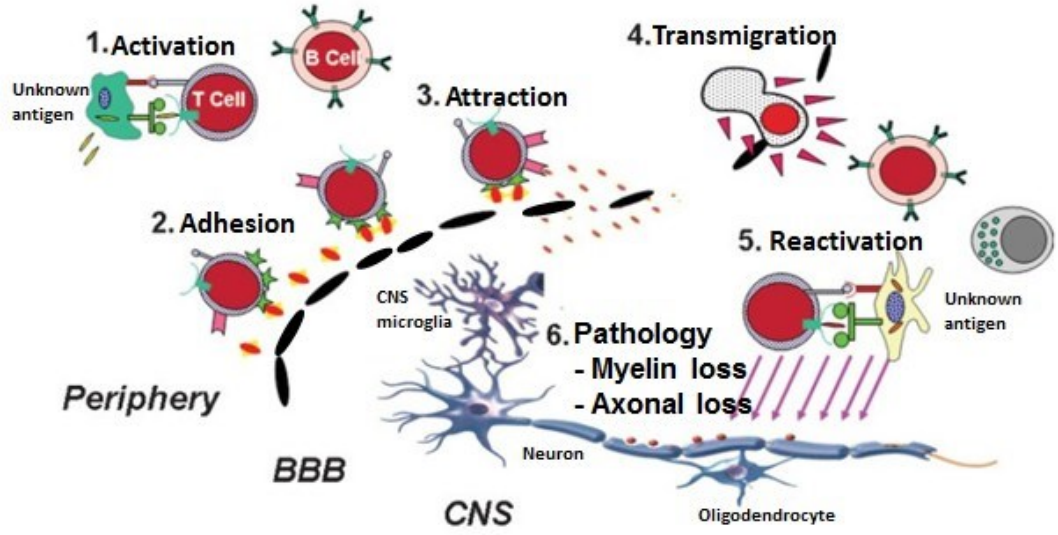

Figure 1.2 Neuroinflammatory mechanism of MS pathology in the CNS.
Peripheral immune cells are activated in response to an unknown antigen, increase their surface molecules and adhere to the endothelial cells of the BBB responding to local chemokine gradients. Secretion of matrix proteases increases permeability of the BBB and allows invasion into the CNS. Invaded cells are reactivated in response to a similar antigen as in the periphery, and lead to pathological alterations in the CNS facilitated by chronically activated resident microglia. Adapted from [61].

Recent pathological studies further emphasize the role of an adaptive immune response in the axonal damage within the CNS. A relationship between the severity of meningeal inflammation and the neuronal and axonal loss has been established [66, 67]. Similarly, amyloid precursor protein (APP) accumulations in axons was observed in chronic lesions correlating to the adaptive immune cell infiltration, indicating an acute axonal damage [68, 69]. In addition, Kerschensteiner and Misgeld group have shown that macrophage-derived toxins trigger mitochondrial dysfunction and focal axonal degeneration (FAD) with or without demyelination [58]. Therefore, the studies have indicated that the inflammation-mediated axonal injury are highly induced as the disease progresses, and the injured neurons become more susceptible to inflammation, further inducing neurodegeneration [6].

1.1.3.3 Inflammation and Disease Progression of MS

Neuroinflammation is considered to be the initial event in triggering MS pathology [61]. However, the mechanism of auto-activation of immune cells in healthy individuals is still unknown[61]. A potential event in triggering "self-immunity" might be genetic dysfunction of important molecules that leads to pro-inflammatory signal and increased susceptibility to immune cell attack. Supportive findings to genetic associations in MS patients have been described by GWAS study [70]. Moreover, in most MS patients, initial inflammatory response gradually decreases with time while neurodegeneration becomes dominant and irreversible at late stage, leading to severe disability [6]. It is considered that inflammation initiates axonal injury and neuron damage, whereas

subsequent progression and accumulated neurodegeneration does not rely on continuously active inflammatory responses.

1.2 Mitochondria-Mediated Neuropathology in MS

The neurodegeneration in MS, which is mostly characterized by the axonal degeneration within the CNS, is traditionally described as a progressive loss of myelin leading to impaired propagation of action potentials across the demyelinated regions of the axon, causing the neuronal dysfunction [6]. The demyelinated axons become transected and dystrophic [6, 71] and cumulative axonal loss is considered to be the possible reason for progressive and irreversible neurological disability in MS [6, 72]. However, it is still not clear whether demyelination is a prerequisite for axonal injury. It has been shown that a genetic mutation can cause axonal swellings and lead to premature neuron death without myelin damage [58, 73]. Another possible cause of axonal degeneration not associated with myelin loss might be represented by the abnormal function of cellular organelles, such as mitochondria.

1.2.1 Mitochondrial Dysfunction in MS

1.2.1.1 Mitochondria

Mitochondria are a type of membrane-bound intracellular organelle ubiquitously found in most eukaryotic cells. They function as the major energy supplier in cellular metabolisms and signal transportations, and are essential for maintaining ionic homeostasis and structural integrity [74]. A mitochondrion is composed of four sub-compartments including the outer membrane, the inter-membrane space, the inner

membrane and the matrix, and each carries out specialized functions. The mitochondrial outer membrane encloses the entire organelle and has high similarity in molecular composition and function to the eukaryotic plasma membrane [75]. It protects proteins in the inter membrane space from leaking into the cytosol and communicate with other membrane-enclosed structures in cells to adjust ionic homeostasis [75]. The inter membrane space contains vital ions and sugars diffused from cytosol and mitochondrial-specific proteins facilitating metabolic reactions on inner membrane [75]. The inner membrane is one of the most essential compartments in mitochondria facilitating cellular energy regulation, where multiple enzymes, ion channels and transporters locate and form the electron transport chain (ETC) [75]. Cristae, which are a typical membrane-folding structure of the inner membrane, significantly enlarge surface area of the membrane and enhance multiple reactions carried out on the membrane [75]. The matrix is the "storage room" for mitochondrial proteins, especially enzymes involve in the breakdown of carbohydrates and fatty acids and adenosine tri-phosphate (ATP) production with the aid of the ATP synthase located in the inner membrane [75]. It maintains osmotic balances and contains species-specific mitochondrial genome that is essential for mitochondrial inheritance and production of several proteins important in oxidative phosphorylation [75].

1.2.1.2 Dysfunction of Mitochondria in Neurodegenerative Disorders

In human, normal morphology and function of mitochondria is crucial for one's health. The high energy demand of the CNS makes it particularly vulnerable to alterations in mitochondria [76]. In the CNS, impaired mitochondrial functions and

properties would make neurons intrinsically susceptible to cellular stress and genetic mutation, thus triggering neuronal apoptosis and degeneration of other CNS cells, unhealthy aging, permanent disability and death [77]. Studies have shown that mitochondrial impairment is associated with some most frequent neurodegenerative diseases. Induced oxidative stress, the ETC complex deficiency, mitochondrial deoxyribonucleic acid (DNA) mutation and distorted calcium homeostasis are the major pathological changes in mitochondria leading to neuronal loss in Alzheimer, Huntington and Parkinson's diseases (AD, HD & PD) [78]. In Amyotrophic Lateral Sclerosis (ALS), reactive gliosis mediated inflammation and glutamatergic toxicity through the blockage of presynaptic receptors trigger excessive calcium influx and oxidative stress in mitochondria, causing degenerative damage in motor neurons and subsequent disabilities [79]. Neuroinflammation, which is a major neuropathological mediator in most neurodegenerative diseases, contributes to alterations in mitochondrial function and gene expression. Thus, it is not surprising that mitochondrial impairment is associated with neuroinflammation-initiated MS [80].

1.2.1.3 Dysfunction of Mitochondria in MS

In the early phase of MS, inflammation is initial and usually transient [80]. However, the progression of the disease does not stop or even slow-down along with the attenuation of inflammatory responses and reduced number of relapses, and eventually chronic axonal neurodegeneration becomes dominant [60]. This suggests irreversible pathological change in MS is triggered but not necessarily maintained by inflammation.

Evidence is emerging that mitochondrial impairment plays a vital role for disease progression and possibly contributes to neurodegenerative processes in MS [76]. In MS, neuroinflammation mediated by active microglia in the CNS triggers the production and release of highly reactive free radicals including reactive oxygen species (ROS) and nitric oxide (NO). [81, 82]. These molecules can also oxidize and damage proteins, nucleic acids, polysaccharides and lipids, resulting in mitochondrial DNA mutation and organelle damage in both myelinated and demyelinated axons [77, 82, 83]. Evidences have shown that the activity of complex IV of mitochondrial respiratory chain and its catalytic component COX-I is defected in response to soluble products of active microglia/macrophages in post-mortem tissue of MS patients and the inflammatory lesions of a commonly used MS animal model, experimental autoimmune encephalomyelitis (EAE) [58, 84]. In EAE, pathological alteration of mitochondria happens even when peripheral immune cells are only present in meninges before invasion into the CNS parenchyma, suggesting the diffusing radicals ROS and NO secreted by these immune cells play a vital role in early mitochondrial damage [66, 85]. However, no study was performed to assess the activation of CNS-resident microglia before leukocyte infiltration on oxidative damage of mitochondria in EAE [76]. Furthermore, inflammatory factors present in the CNS may alter neuronal mitochondrial distribution and accelerate mitochondria-mediated apoptosis, which has been observed in ALS and encephalitis [86, 87].

In MS, a particular pathological event is demyelination of intact axons. The absence of myelin triggers the re-distribution of ion channels, in particular sodium channels [88]. The alteration of ion channels is proposed to cause an increased intra-axonal energy

demand and subsequent induction and redistribution of mitochondria to provide energy for cell damage recovery [89]. In chronic MS lesions where inflammation is remarkably less than in acute MS lesions, axonal degeneration still progress. An explanation for the axonal degeneration independent of inflammatory responses is that mitochondrial re-alignment triggered by initial inflammation is impaired, thus not sufficient to fulfil the requirement of ATP production in these axons [82]. It is suggestive that this failure of mitochondrial activity may be due to organelle damage sustained previously during acute inflammatory response [76].

Mitochondrial DNA mutation is another mechanism leading to mitochondrial impairment mediated neurodegeneration. ROS and NO released by active microglia induce damage to neuronal mitochondrial DNA, which contributes to suppressed activities of complexes I, III and IV involved in oxidative phosphorylation reactions and subsequent reduction of ATP production [83]. Moreover, decreased expression of a transcriptional co-activator in MS neurons blocks the transcription of important oxidative phosphorylation subunits and antioxidants, causing mitochondrial impairment and energy deficiency [83]. Overall, mitochondria play an important role in MS pathogenesis and neurodegenerative progression.

1.2.2 Mitochondrial Dynamics in MS

1.2.2.1 Mitochondrial Membrane Dynamics

A neuron is a specialized type of cell with a typically long fiber raised from the cell body named axon that conducts electrical impulses for information transmission to other CNS cells. Because of the long asymmetrical structure of neurons, mitochondria

generated in the cell body need to be delivered throughout the whole cell in response to local energy demand [90, 91]. The movement of mitochondria along axons is known as "mitochondrial membrane dynamics" and is facilitated by microtubule, cytoskeleton, motor proteins, and mitochondrial fission/fusion machineries mainly composed of dynamin and related guanosine triphosphate hydrolase (GTPase) [92, 93].

In response to alteration in local energy demand, mitochondria tend to fragment into small motile mitochondria while transporting along axons, and fuse into large stationary mitochondria at energy demanding sites [92, 93]. The fragmentation of mitochondria is called fission, which is critically regulated by dynamin-related protein 1 (Drp1), a ubiquitous protein related to dynamin [94]. Drp1, mainly located in the cytosol, is composed of an N-terminal GTP-binding domain, a central domain responsible for oligomerization, and a C-terminal assembly or GTPase effector domain (GED) for regulating GTPase activity and mitochondrial targeting [95]. Upon activation, Drp1 is recruited on ER tubules that wrap around mitochondria and attach to mitochondrial outer membrane facilitated by mitochondrial fission protein 1 (Fis1) or mitochondrial fission factor (Mff) [95, 96]. It then oligomerizes and compresses the mitochondrial scission site through GTPase reactions [95]. Drp1 can be post-translationally regulated in many ways, one well-studied machinery of which is through phosphorylation of serine residues within the GED [95]. Studies have shown that a phosphorylation of Ser616 residue by cyclic-dependent kinase 1 (Cdk1) leads to induced mitochondrial fission by NO, whereas the phosphorylation of Ser637 or Ser656 by protein kinase A (PKA) inhibited mitochondrial fission and cell apoptosis through blockage of Drp1 translocation to mitochondria and its GTPase activity [95]. Other post-translational modifications include sumoylation,

ubiquitination and S-nitrosylation, which are all crucial for maintaining normal mitochondrial function and dynamics [95].

The fusion of mitochondrial outer membrane is mainly facilitated by mitofusins 1 and 2 (Mfn1 & 2). They are transmembrane GTPase located in the mitochondrial outer membrane, and are composed of an N-terminal GTP-binding domain, a coiled-coil domain next to it (HR1), a transmembrane domain and a C-terminal coiled-coil or called heptad repeat domain (HR2) for mitofusin dimerization and assembly of adjacent mitochondria [95]. Mitochondria fragmentation is largely (over 85%) induced in absence of these mitofusins, whereas overexpression leads to long-tubule morphology of mitochondria [97]. Mfn1 has a greater GTPase activity and tether ability to induce mitochondrial fusion compared to Mfn2, while both are required for embryonic development [97, 98]. Besides, Mfn2 plays a role in calcium communication between mitochondria and endoplasmic reticulum (ER) through tethering mitochondria to the ER [99]. A similar machinery is carried out by optic atrophy 1 (Opa1) in fusion of inner mitochondrial membrane. Opa1 is a GTPase in the dynamin family thus contains GED at C-terminal next to a central domain and a GTPase domain in the middle of the protein. The other half of the protein contains a coiled-coil domain similar to mitofusins, hydrophobic segments and a mitochondrial import sequence at the N-terminal [95]. The hydrophobic segments contribute to anchoring Opa1 onto the mitochondrial inner membrane and GTPase functions in fusion reactions [95]. Opa1 is also essential to maintain mitochondrial membrane potential, preventing the release of cytochrome *c* in mitochondrial respiratory chain and subsequent apoptosis, regulating cristae junctions,

preserving mitochondrial DNA and targeting depolarized fragmented mitochondria for autophagy [95].

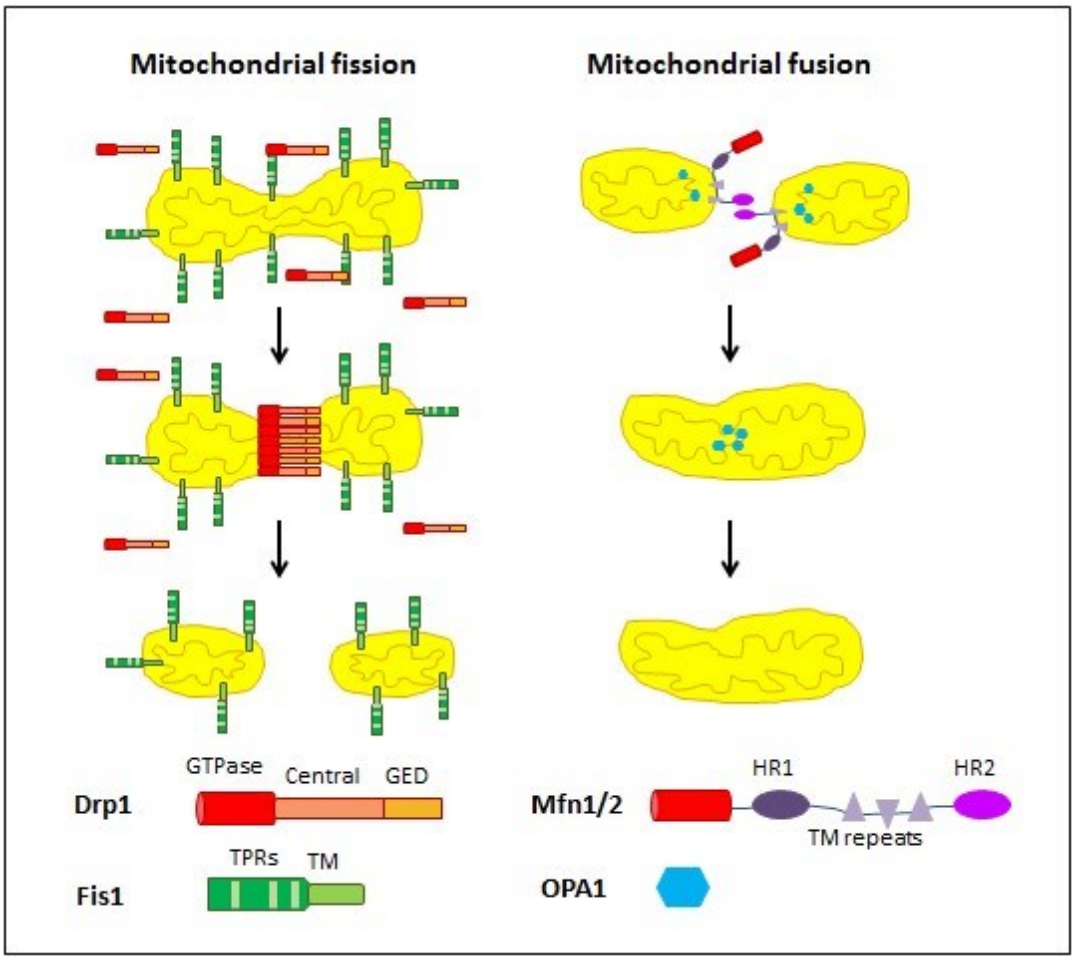

Figure 1.3 Mitochondrial membrane dynamics. Drp1 is a major player in mitochondrial fission in facilitation by Fis1 that performs as a Drp1 docking site at the outer mitochondrial membrane. Mfn1 and Mfn2 carry out outer membrane fusion of mitochondria, while OPA1 functions to fuse inner mitochondrial membrane. Adapted from [95].

1.2.2.2 Dysfunction of Mitochondria in Neurodegenerative Disorders

Normal mitochondrial dynamics are of vital importance for neurons because of their specific cell structure and high energy demands for survival and their specialized

functions. This makes neurons more vulnerable to mitochondrial dynamics defects. The alteration of mitochondrial mobility was observed frequently along with the progression of several neurodegenerative diseases, leading to neuronal dysfunction and apoptosis [92, 100]. While studying autopsy brain tissue of patients with Alzheimer's disease and neurons of transgenic mice, Manczak *et al*. [101] observed alterations of several mitochondrial fission/fusion proteins compared to control: increase in expression of Drp1 and Fis1 and decrease in that of Mfn1, Mfn2 and Opa1. These results suggest that mitochondrial fission and fragmentation are induced in AD associated with amyloid β (Aβ) oligomer accumulation and cleavage of Tau, which triggers neurodegeneration [102]. Similar machinery was observed in neurons of HD patients where mutant huntingtin protein up-regulation and accumulation were present. In ALS where oxidative stress is a primary pathological event triggering disease progression, induced mitochondrial fragmentation and impaired mitochondrial dynamics were observed in motor neurons that express mutant superoxide dismutase (SOD1) in the inter membrane space of their mitochondria [103]. The vulnerability of dopaminergic neurons in substantia nigra to impairment of mitochondrial dynamics is suggested to be lower compared to other midbrain neurons [104]. A study on PD patient fibroblasts revealed that PTEN induced putative kinase 1 (PINK1) mutation promoted mitochondrial fragmentation [105]. In fibroblasts and dopaminergic neurons derived from stem cells of PD patients with LRRK2 mutant, inhibition of Drp1 function reduced excessive autophagy and neuronal damage [106], which suggested that mitochondrial fission could play a role in PD pathogenesis. All in all, mitochondrial dynamics are crucial to maintain neuronal health and are a potential therapeutic target for neurodegenerative diseases.

1.2.2.3 Impaired Mitochondrial Dynamics in MS

As previously stated, MS pathology is considered to be inflammation-initiated. When the neurons in the CNS become inflamed and axonal injury and demyelination take place, mitochondria increase their sizes and activity at docking sites, and redistribute according to cell rescuing signal in response to inflammation.

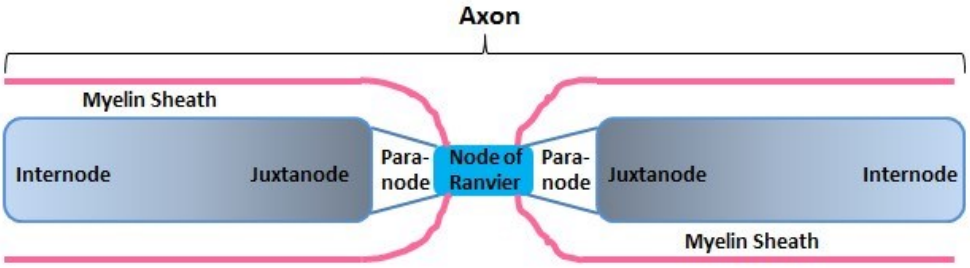

Figure 1.4 Node of Ranvier and surrounding regions.

Within intact myelinated axons, long big stationary mitochondria are sitting and clustering in internodal and juxtanodal regions (Fig. 1.4) and account for more than 90% of total axonal mitochondria [89]. Whereas, in the nodes of Ranvier and paranodal regions, there are fewer and smaller mitochondria [89]. This distribution of mitochondria is in a similar pattern as the sodium/potassium ATPase (Na^+/K^+ ATPase) that is the primary consumer of ATP [89]. When demyelination happens, Na^+/K^+ ATPases are no longer compartmentalized and tend to diffuse and redistribute along axonal membrane. The change of energy demanding sites triggers mitochondrial relocation and an increase of mitochondrial size, density and activity [89]. Following remyelination, the size of mitochondria returns back to normal as seen in myelinated axons, whereas overall

number of mitochondria stays relatively high [89]. A study by Zambonin *et al.* [74] provides evidences of similar alterations in lesions of MS patients. The recovery of mitochondrial content in remyelinated neurons indicates the likelihood of fission-fusion cooperation being responsible for the recovery of destroyed myelin [89]. However, the consistently high number of mitochondria, including both mobile and stationary mitochondria, suggests an impairment of mitochondrial dynamics and energy deficits leading to secondary neuroinflammation and neurodegeneration [89, 107].

However, demyelination as a hallmark of MS is demonstrated not to be a prerequisite for the disease progression [58]. A study of acute lesions in EAE and MS patients performed by Nikic *et al.* [58] revealed that axonal injury or so-called 'focal axonal degeneration (FAD)' is the earliest sign of tissue damage corresponding to initial neuroinflammation and is the key event in triggering disease progression and permanent disability in patients. In these injured axons, mitochondrial pathology played a vital role. In Nikic's study, FAD was assigned into three stages according to axonal morphology in the lesions: stage 0 represents normal-appearing axons, stage 1 represents focal swelling and stage 2 represents axonal fragmentation. In EAE lesions, mitochondrial size decreased as FAD stage increased with mild effect of demyelination, and induced mitochondrial fragmentation was observed in the region of axon within the lesion compared to the outside [58]. A similar pattern was observed in acute human MS lesion where mitochondrial size in intact demyelinated axon is relatively greater than that in normal-appearing myelinated axons [58]. These results represent impaired mitochondrial dynamics in MS pathogenesis in response to inflammation, and suggested a role of imbalanced mitochondrial fission-fusion cooperation in disease onset and degenerative

progression. Moreover, the blockage of mitochondria-mediated metabolic pathways is an early event in FAD and contributes to the initiation of axonal loss in MS [58]. FAD is promoted by inflammatory response to the active immune cells and free radical release, thus, suggesting a role of active microglia and macrophages in alteration of mitochondrial metabolism and redistribution [58, 82, 89]. All these studies conclude and emphasize the importance of normal mitochondrial motility in maintaining healthy neurons, and propose a rational therapeutic target for MS therapies.

1.3 Endoplasmic Reticulum Stress in MS

1.3.1 ER Stress

1.3.1.1 Endoplasmic Reticulum

Endoplasmic Reticulum (ER) is a large, sac-like, membrane-enclosed organelle in most types of human cells interconnecting nucleus and some important cytosolic compartments, including mitochondria and Golgi. The rough ER that locates near the nucleus is composed of ribosomes studded in peri-nuclear face of the membrane that translate messenger ribonucleic acid (mRNA), indicating an important role of the ER in protein synthesis [108]. Free ribosome starts the translation of proteins destined for the secretory pathway through translating a short piece of signal peptide that is recognized and bound by signal recognition particle [108]. The ribosome complex then binds to the rough ER and continues to translate the nascent polypeptide into the internal space of ER membrane called ER lumen, where the peptide is modified into proper structure [108]. This modification process requires an oxidizing environment within the ER for formation of disulfide bonds and multiple molecular chaperones, folding factors and sensors

cooperating and ensuring correct folding of peptides into mature proteins. The other type of ER that lacks bound ribosome is named as smooth ER, locating mainly in cell periphery. A major function of the smooth ER is to synthesize and secret phospholipids, cholesterol and steroids [108]. It also carries out carbohydrate metabolism, detoxification reactions, plasma membrane receptor translocation, and communication among mitochondria and Golgi. Most components of the ER membranes are freely diffusible between the rough and smooth regions, whereas the rough ER contains special proteins for ribosome translocation and binding [108]. Noteworthily, the lumen of the ER contains the highest concentration of Ca2+ within the cell because of active transport of calcium ions by Ca^{2+} ATPases and regulates intracellular calcium homeostasis that is important for cell metabolism, signaling and apoptosis [108].

1.3.1.2 Endoplasmic Reticulum Stress

Disturbances such as viral infection, inflammation, aberrant Ca^{2+} regulation and cellular redox regulation cause accumulation of unfolded and incorrectly folded proteins in ER lumen, and trigger a cellular stress response called ER stress [109]. These accumulated proteins are then directed into ER quality control pathways for re-folding or degradation to adapt to the changing environment and re-establish normal ER function [109]. A molecular chaperone, binding immunoglobulin protein (BiP), is an early signaling marker responding to ER [109]. In the ER lumen, BiP binds to receptors on the membrane surface to inactivate them under non-stressful condition. In response to cellular disturbances, BiP releases from binding receptors thus, in short-term, activates inositol-requiring protein-1 (IRE1). The downstream activation of TNF receptor-

associated factor 2 (TRAF2) signals and activates several kinases, causing expression of host defense genes to warn the cell of changing environment [109]. IRE1 receptor activation also induces the splicing of a transcription factor, X-box binding protein 1 (XBP-1).The spliced and activated XBP-1 facilitates transcription of important ER chaperones, including BiP, that are involved in protein re-folding or degradation to recover normal protein production and save cells [109]. Another ER membrane receptor, transcription factor-6 (ATF6), is activated upon BiP release and relocates to Golgi where it is cleaved by resident proteases [109]. Cleaved ATF6 is then released and migrates into the nucleus where it regulates protective gene expression and facilitates XBP-1 production [109]. Absence of BiP-binding signal also activates protein kinase RNA-like ER kinase (PERK) on the ER membrane, induces phosphorylation of a translation initiation factor elF2α and subsequently inhibits global protein synthesis to reduce protein accumulation in the ER lumen [110]. However, if the accumulation of misfolded proteins is not resolved, a prolonged ER stress signal will implement up-regulation of a pro-apoptotic marker C/EBP homologous protein (CHOP) through increased translation of a transcription factor, ATF4. The overexpressed CHOP blocks the transcription of several genes involved in cell metabolism, anti-apoptosis and calcium homeostasis, thus proceeds to programmed cell death [110]. Indeed, a key event in triggering and accelerating ER stress induced apoptosis is the distorted Ca^{2+} homeostasis, which is caused by excess outflow from the ER lumen into the cytosol. The Ca^{2+} outflow activates multiple kinases and caspases essential for programed cell death, suppresses transcription of regulatory genes, blocks Ca^{2+}-dependent ER chaperone activity and impairs Ca^{2+}-sensitive mitochondrial activities [109, 110].

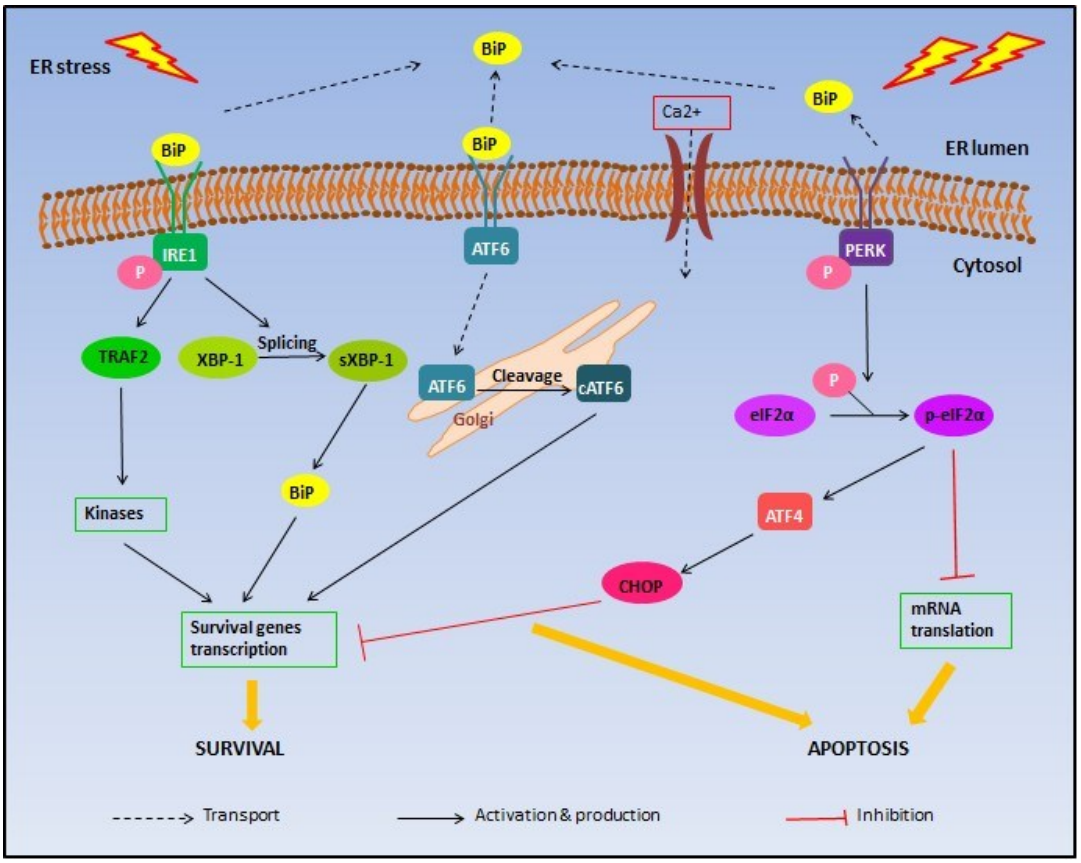

Figure 1.5 Signal transduction pathways associated with ER stress. Accumulation of un- or mis- folded proteins in the ER lumen initiates release of BiP from ER membrane receptors, IRE1, ATF6 and PERK. The release subsequently activates the membrane receptors. Activated and phosphorylated IRE1 activates TRAF2, which in cascade leads to activation of several kinases facilitating transcription of cell survival genes. Active IRE1 also induces post-translational modification of XBP-1, further regulating BiP production and gene transcription. ATF6 is released from the ER membrane upon dissociation with BiP, transports to Golgi where it is cleaved. Cleaved ATP6 then transports to cell nucleus where it regulates gene transcription and XBP-1 production. Active PERK in response to prolonged ER stress signal induces phosphorylation of elF2α, blocking mRNA translation and promote CHOP production. CHOP down-regulates survival gene transcription and signals cell apoptosis. Adapted from [110].

1.3.2 ER Stress in Neurodegenerative Diseases

In several neurodegenerative disorders, including AD, HD, PD and prion disease, accumulation of specific mutant and misfolded proteins is observed in triggering neurodegenerative progression, which proposed a role of ER stress in these diseases [111]. Induction of BiP expression was detected and varied in AD cases at different disease progression stages, suggesting ER stress is an early event in AD pathology [112]. Moreover, in post-mortem brain of AD patients and *in vitro* models, activation of PERK and induced phosphorylation of elF2α correlate with increased Aβ level and hyper-phosphorylated Tau [112, 113]. These findings suggest a link between main pathological alterations and ER stress induced apoptosis in AD [111]. Similar associations were observed in HD and PD with mutation and accumulation of huntingtin and α-synuclein, respectively [111]. In the most common form of prion neurodegenerative disorder in human, Creutzfeldt-Jakob disease, several ER chaperones and sensor proteins including BiP were observed to be up-regulated [114]. ER stress facilitates production of misfolded forms of the prion protein *in vitro*, and the misfolded prion protein further induces ER stress and leads to cell apoptosis [115, 116].

1.3.3 ER Chaperone Alteration in MS

In neurons, the tubular smooth ER distributes throughout axons and distal dendrites, regulating cell metabolisms, mitochondrial function and calcium homeostasis [110]. Axonal damage as an early event in MS neuropathology triggers ER stress to repair injured axons and rescue neurons from further degeneration [110]. With the accumulation

of axonal injury and neuroinflammatory responses, prolonged ER stress initiates cascades of reactions signaling cell apoptosis, and leads to subsequent pathological degeneration in MS [110]. Evidences suggest that increased expression of ER stress-associated proteins contribute to MS pathology [117, 118]. Both immunostaining and real-time PCR results indicate an induction of both BiP and CHOP in grey and white matter of MS patient biopsies and post-mortem brain tissue compared to those of normal control patient brain tissue [117, 118]. Interestingly, in the white matter of MS patient brain, CHOP is significantly induced at peri-lesional area compared to the center region of acute and chronic plaques [117]. In normal-appearing white matter (NAWM), expression level of CHOP is also significantly high compared to controls [117]. Indeed, peri-lesional areas are suffering from active immune cell infiltration and inflammation that diffuse into surrounding NAWM, whereas in the center of the lesions, demyelination and tissue damage are more dominant [84, 117]. Moreover, the preserved high level of CHOP at the center of demyelinating plaques compared to controls indicates that ER stress signaling pathways are a mediator of myelin destruction [117]. Thus, it is possible that CHOP induction observed in MS brain as a marker of ER stress and apoptosis contributes to pre-lesion alterations and lesion development in response to inflammation. A similar study performed in rat EAE model revealed that expression of ER stress-associated chaperons significantly increased in lesion tissue compared to those in normal rat tissue [119]. Conclusion of these findings indicates that ER stress is a potential hallmark of pathological progression in MS in response to inflammation and provides a potential therapeutic target for axonal and neuronal protection in this disease.

1.3.4 ER-Mitochondria Communication

1.3.4.1 Mitochondria-Associated ER Membrane

As stated in previous section (Section 1.3.1.1), ER is in contact with multiple membrane-enclosed intracellular organelle, including mitochondria. The region of the smooth ER membrane that interfaces with mitochondria is known as mitochondria-associated ER membrane (MAM), where protein complexes tether the two organelles dynamically and closely but do not allow them to fuse [120].

The first function of MAM identified is the formation and exchange of lipids. It has been shown that lipid handling at MAM can alter respiratory activity in yeast [121] and mitochondrial membrane dynamics in mice [122]. Later on, with the understanding that ER is the major calcium storage compartment and mitochondrial function relies on calcium signaling and homeostasis, cyclic exchange of calcium between the two organelles has been proposed and studied [123]. Transfer of calcium from the ER to mitochondrial matrix is essential for regulating mitochondrial activities through facilitating multiple enzymes in the electron transport chain. An *in vitro* study on the activity of pyruvate dehydrogenase indicated that this enzyme was hyper-phosphorylated and inactivated under impaired calcium influx into the mitochondria through the ER, which triggers mitochondrial dysfunction in redox reactions and ATP production and subsequent cell survival response to shortage of nutrients [124]. Furthermore, signaling cascades of calcium at the MAM is vital for regulating cell apoptosis. Recent studies showed that MAM becomes tighter and greater in number in response to harmful stimuli such as induced ER stress or nutrient deprivation [120]. The studies also demonstrated that the break-up of ER-mitochondrial network suppresses programmed cell death under

apoptotic signals [125]. A massive calcium signal changes mitochondrial morphology and membrane permeability, which triggers impairment of mitochondrial membrane potential and subsequent disabilities in ATP production and cell metabolisms [126]. It also urges the release of a respiratory chain subunit, which amplifies apoptotic signal through multiple pathways [127]. These findings proposed a tight linkage among ER calcium exchange, mitochondrial activities and cell apoptosis at MAM, highlighting the importance of maintaining normal MAM interaction and function in human health.

1.3.4.2 The MAM and Neurodegeneration

As mentioned in the last section, MAM is essential for cell apoptosis, so it is not surprising to see the association of MAM functions with disease pathology and progression where cell apoptosis is implicated, such as those of neurodegenerative disease. A typical event in triggering cognitive impairments and physical disabilities in AD patients is the progressive loss of hippocampal and cortical neurons [128]. It is believed traditionally that splicing of amyloid precursor protein (APP) into different forms of Aβ as well as Tau hyper-phosphorylation are key pathological characteristics in AD, which cause massive neuron loss. In APP-related pathology of AD, presenilin proteins and several secretases contribute to the splicing machinery whose genetic alterations are indicated to be associated with disease initiation and progression [128]. Studies have shown that presenilin 1 & 2 (PS1, PS2) interact directly with calcium transport IP3 receptors located at MAM to regulate mitochondrial influx of calcium, and mutations of these two proteins in AD enhanced the receptor activity [129]. Moreover, lipid metabolism is distorted in AD, which promotes re-arrangement of MAM lipid

composition, reorients APP transmembrane domain at this region and alters cleavage products of APP according to lipid composition and thickness of inserted membrane [128]. Thus, over-activation and impairment of MAM are proposed to underline pathogenesis of neurodegeneration in AD, and it is suggestive for a role of MAMs in MS neuropathology where calcium homeostasis defects, mitochondrial dysfunction and axonal degeneration occur.

1.4 Rab Proteins

1.4.1 Rab protein structure and reaction machinery

Rab protein family is a member of Ras small molecular weight guanosine nucleotide-binding protein (G-protein) expressed universally in human and other eukaryotic cells [130]. Rab proteins are in the size of 20-25kDa and localize at the cytosolic surface of many cellular organelles [130]. Similar to the structure of other G-proteins, Rab proteins contain a multi-loop structure interacting with GTP and handling its hydrolysis [130]. In active state, Rab binds to GTP and hydrolyze it. During hydrolysis, conformation of the loop region changes to adopt its binding to the hydrolyzed product of GTP, GDP. At the GDP-bound state, Rab is inactivated. Besides this well-conserved structure, Rab has a C-terminal region that is hyper-variable between Rabs of different eukaryotic species and is essential for cellular targeting of individual Rabs [130]. A cysteine motif at the extreme carboxyl terminus is post-translational modified by adding geranyl groups known as isoprenylation, and is conserved for its function in membrane insertion [130]. In addition, by analogy with other Ras proteins, a specific sequence is identified in Rabs termed the "effector" domain [130]. Rabs are able to bind specific effector molecules or proteins to

their "effector" domain in active status, regulating and targeting these molecules to their destination [130]. Most of the effector proteins are involved in regulating protein sorting, recruitment and recycling, as well as vesicle transport, docking and fusion with appropriate membrane compartments [131].

A number of Rab mutations have been established to study the function and mechanism of these proteins. A frequently utilized mutant for Rabs is at amino acid position around 70 where the conservation of a glutamine (Q) to a leucine (L) takes place [130]. This Rab mutant is impaired in GTP hydrolysis thus remains dominantly activated at GTP-bound state [130]. In contrast, a mutation leading to everlasting association of GDP generates dominant inactive Rabs (or dominant negative Rab mutant) through the conversion of a serine (S) or a threonine (T) to an asparagine (N) near amino acid position 20 [130].

1.4.2 Rab protein cellular localization and function

Rab proteins function predominantly in coordinating membrane trafficking and protein delivery because of their ubiquitous distribution to multiple subcellular structures and high-level specificity in membrane transport machinery. According to different cellular compartments they work at, characterized Rab proteins are divided into 13 subfamilies excluding the Ras-related nuclear protein (Ran), summarized by Brighouse *et al.* [132]. Most Rabs transport dynamically among the ER, Golgi, lysosome and plasma membrane. These Rabs play major roles in facilitating the secretory and endocytosis/exocytosis pathways [130]. For example, Rab9 participates in vesicle formation from sorting endosome and transport to fuse with Golgi; Rab5 and Rab7

contribute to retrograde transport of transmembrane proteins from endosomes to Golgi; Rab8 attaches vesicles containing light-perceptive pigment to actin microfilaments; Rab11 facilitates vesicle transport in secretory pathways while Rab5 modulates endocytosis [132]. Several Rabs also participate in endosomal fusion through interaction of their regulatory proteins with membrane fusion proteins [133]. Some of the Rab proteins, such as Rab1 and Rab32, are more stationary at their docking sites compared to those dynamically transporting Rabs, and facilitate vesicle targeting and tethering between contacting compartments [130].

1.4.3 Rab32 family proteins

According to Brighouse's categorizing of Rabs into different subfamilies in terms of their sequence similarity and cellular localizations, Rab32, Rab38, Rab7L1 (Rab29 in rat) are grouped together [132]. A specific sequence characteristic of this group of Rabs is that, in the GTPase domain, these Rabs contain an isoleucine (I) at the amino acid position where other Rabs contain a threonine (T) [134]. This alteration is evolution-adapted and suggests a different binding property or efficiency of these Rabs to GTP/GDP. Besides their sequence specificity, Rabs in Rab32 subfamily function at similar subcellular compartments, such as cargo transport from post-Golgi to melanosomes that are lysosome-related organelles responsible for color and photoprotection [135]. However, recent studies indicate an association of Rab32 with ER and mitochondria where it may be involved in cell survival-related pathways [136, 137].

1.4.3.1 Rab32

Rab32 was first identified in blood platelets and distributed universally in human tissue and organs [134]. An mRNA-level study conducted by Bao *et al.* [134] illustrated that expression of Rab32 was high in heart, liver and kidney, and moderate in pancreas, placenta and lung, while a very mild expression of this protein was detected in brain and skeletal muscle. They also reported that Rab32 protein was fractionated together with granules/mitochondria and membranes, suggesting a potential involvement of this protein in mitochondrial activities [134]. In the same year 2002, Alto *et al.* [137] confirmed the co-localization of Rab32 with mitochondria and, more importantly, discovered a major function of this protein in regulating mitochondrial dynamics and distribution. In Alto's study, Rab32 is characterized to be an A-kinase anchoring protein that target PKA to mitochondria [137]. Rab32, as other AKAPs, contains an amphipathic helix for PKA anchoring that is absent in other Rabs including closely related Rab38 and Rab7L1 [137]. This specific domain allows Rab32 to interact with and recruit PKA to mitochondrial membrane where PKA mediates phosphorylation of mitochondrial dynamics related proteins, such as Drp1 [136, 137].

As stated in section 1.2.2.1, Drp1 is critical for mitochondrial division, size and shape, and distribution throughout the neuron, and the impaired expression and activity of Drp1 contributes to neuronal apoptosis in the progression of several neurodegenerative diseases. A more recent study on the role of Rab32 in regulating apoptosis and MAM properties presented co-localization of Rab32 with both mitochondria and the ER at MAM while highlighted the association of Rab32 with Drp1 [136]. It has been shown that the dominant negative Rab32 T39N mutants (Rab32T39N) and the wild type Rab32

(Rab32WT) co-localize nicely with MAM and mitochondria, where they target PKA to serine 637 in human Drp1 and lead to inactivation of Drp1 through doubling its phosphorylation level [136]. Inactivation of Drp1 facilitates mitochondrial fusion and protects cells from apoptosis by allowing functional complementation of mitochondrial DNA, proteins, and metabolites between adjacent mitochondria [94, 138]. In contrast, a GTP-bound dominant active mutant of Rab32 (Rab32Q85L) leads to a decreased association of PKA with mitochondrial membrane, similar to the effect of Rab32 protein depletion [136, 139]. Moreover, Rab32 protein is identified to modulate MAM by regulating ER calcium handling and disrupts the specific enrichment of calnexin on MAM [136]. Active Rab32 extracts and transports calnexin from MAM to cell periphery, which is believed to be a cell apoptotic signal [136]. Our collaborator, Dr. Thomas Simmen at the University of Alberta, showed that up-regulation of Rab32 was associated with ER stress induction under hypoxia condition in neuronal cells (unpublished data), and over-activated Rab32 distorted mitochondrial membrane potential (unpublished data) and accelerated cell apoptosis [136]. To summarize these findings, it is suggestive that Rab32 regulates mitochondria-associated and ER stress-induced neuronal apoptosis. A proposed machinery of Rab32 in regulating mitochondrial dynamics upon ER stress signal is illustrated in figure 1.6, as suggested by Dr. Simmen [140].

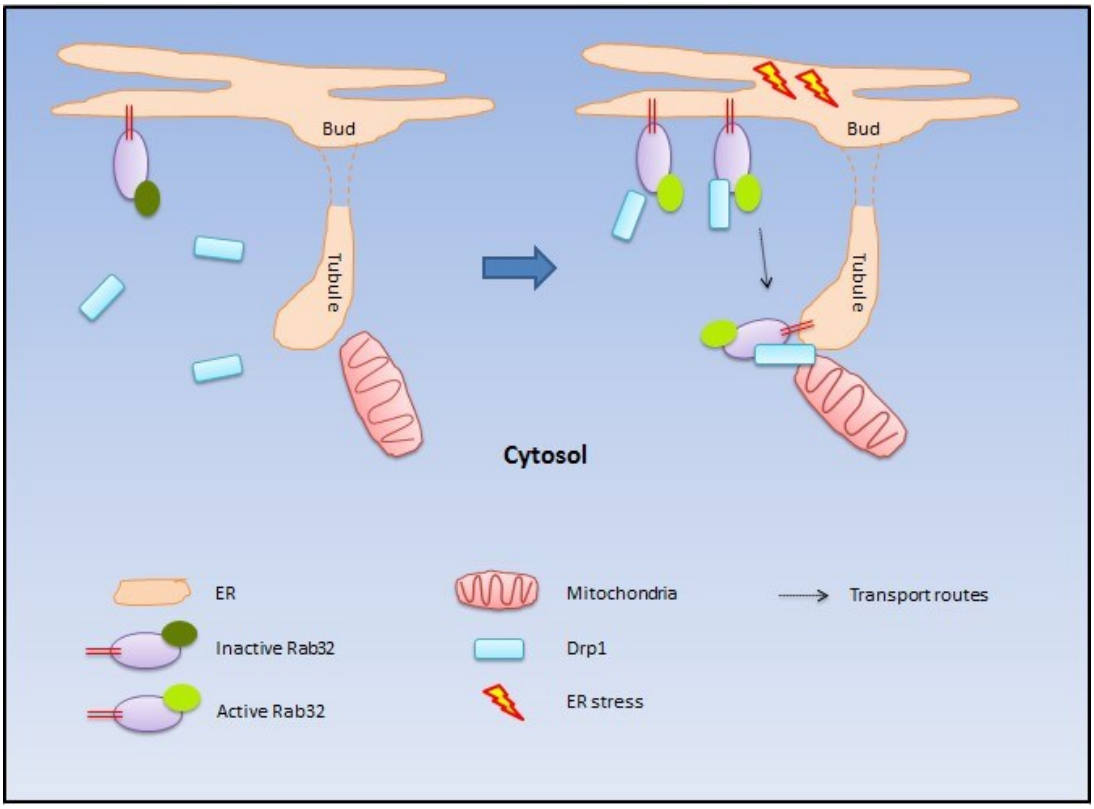

Figure 1.6 Machinery of Rab32-mediated mitochondrial dynamics regulation at MAM. In inactive state, GDP-bound Rab32 sits on the ER membrane. When ER stress initiates, Rab32 are up-regulated on the ER membrane and activated, binding to their effector protein Drp1 and recruiting them to MAM. Adapted from [140].

1.4.3.2 Rab38 and Rab29

Rab38 and Rab7L1 are evolutionarily related to Rab32 according to the phylogenetic analysis of the Rab family proteins [141], and are similar in their localization and functions [132]. Similar to Rab32, Rab38 is mainly involved in facilitating transport cargo among ER, Golgi and melanosome [135], as well as melanosome biogenesis [142]. Interestingly, Rab38 has recently been identified as one of the top markers associated with the age of onset endpoint in the RR-MS and SP-MS [48]. In addition, Rab7L1 is of interest in the disease risk of Parkinson's disease at genetic level [143]. These findings

suggest possible contributions of Rab32 protein subfamily to neurodegenerative mechanisms.

1.6 Summary

Over the past decade, MS researchers have shown much interest in the inflammation-initiated neurodegenerative mechanisms, where mitochondrial dysfunction is suggested to play a significant role. High-level ER stress and impaired mitochondrial dynamics and distribution make cells more susceptible to inflammation, causing neurodegeneration and subsequent progression of the disease and onset of permanent disability. Rab32 protein is indicated to regulate mitochondrial fragmentation-mediated cell death by altering the activation level of Drp1 that is involved in neurodegenerative mechanisms of several CNS disorders. Rab32 also plays a role in apoptosis through its response to ER stress and modulation of mitochondria-ER communication. The evolutionary related Rab38 protein is identified as a risk marker in MS, and together with Rab7L1, may play a similar role to that of Rab32 in regulating mechanisms of cell apoptosis. These findings suggest the involvement of Rab32-like proteins in the neurodegenerative mechanisms of MS where their dysfunction may accelerate disease progression.

1.7 Hypothesis and Specific Aims

According to the literature findings stated above, **I hypothesize that Rab32 plays a role in altering the axonal mitochondrial dynamics and distribution, and subsequent induction of neurodegeneration in MS in response to ER stress and inflammation.** To understand the effect of abnormal expression of Rab32 on pathological changes in MS,

a detailed characterization of its expression and localization in MS patient tissue needs to be established. Specifically, I will detect the expression of Rab32 in and out of lesions of MS brain tissue to have a general understanding of its potential contribution to MS pathology in response to ER stress and inflammation. I will identify its localization within neurons to glean insight of my understanding. Moreover, evaluation of cellular alteration in neurons can provide important information for a potential mechanism of Rab32 in triggering neurodegenerative progression of MS. I will investigate if transient changes in expression and activity of Rab32 impair neurite growth and mitochondrial dynamics within human neurons, and prolonged effect of these changes accelerates neuron apoptosis.

Specific Aims:

1. To detect the expression and variation of Rab32, Rab38 and Rab7L1 proteins in MS brain tissue.
2. To detect the expression and variation of ER stress and apoptotic markers in MS brain tissue and speculate the association of Rab32 with these markers in acute and chronic lesions.
3. To detect the expression of Rab32 in neurons of MS brain tissue and analyze mitochondrial morphology and dynamics in neurons that express mutant, WT or depletion of target Rab proteins.
4. To evaluate the rate of apoptosis of neurons that express mutant, WT or depletion of target Rab proteins.
5. To propose a potential mechanism of Rab32 protein in neurons of MS patients.

CHAPTER 2:

Materials and Methods

2. MATERIALS AND METHODS

2.1 MATERIALS AND REAGENTS

The materials, chemicals, and reagents used for this thesis were purchased from suppliers indicated below and used according to the manufacturers' recommendations with modifications stated otherwise.

Table 2.1 Chemicals and Reagents

Chemical/Reagent	**Supplier**
2-Mercaptoethanol	Bio-Rad
4-(2-hydroxyethyl)-1-piperazieethanesulfonic acid (HEPES)	Sigma-Aldrich
4',6-Diamidino-2-Phenylindole, Dihydrochloride (DAPI)	Life Technologies
Acrylamide (30%)	Bio-Rad
AIM-V Medium (1X)	GIBCO Life Technologies
Ammonium Persulfate (APS)	Bio-Rad
Ampicillin	Sigma-Aldrich
Bovine Serum Albumin (BSA)	Sigma-Aldrich
Bromophenol Blue	Bio-Rad
Cytoseal XYL	Richard-Allan Scientific
Cytosine Arabinoside (AraC)	Sigma-Aldrich
Dimethyl Sulfoxide (DMSO)	EMD
DNase I	Roche Diagnostics
Dulbecco's Modified Eagle Medium (DMEM, + high glucose)	GIBCO Life Technologies
Eosin Y solution, alcoholic	Sigma-Aldrich
Ethanol	Commercial Alcohols
Fetal Bovine Serum (FBS)	GIBCO Life Technologies
Ficoll-Paque PLUS	GE Healthcare
Fungizone	GIBCO Life Technologies
Glycerol	Bio-Rad

Goat serum	GIBCO Life Technologies
Hank's Balanced Salt Solution (HBSS)	GIBCO Life Technologies
Hematoxylin Solution, Mayer's	Sigma-Aldrich
Isopropanol	Fisher Scientific
L-glutamine	GIBCO Life Technologies
Luria Broth Base, Miller	BD Biosciences
Luria-Bertani (LB) Agar, Miller	BD Biosciences
Luxol® fast blue solution	Sigma-Aldrich
MEM Nonessential Amino Acids (NEAA)	GIBCO Life Technologies
Methanol	Fisher Scientific
Minimum Essential Medium (MEM)	GIBCO Life Technologies
MitoTracker Red CMX Ros	Invitrogen
Mouse serum	Sigma-Aldrich
N-2 supplement	GIBCO Life Technologies
Nitrocellulose Trans-blot	Bio-Rad
Paraformaldehyde (PFA)	Sigma-Aldrich
Penicillin-Streptomycin Solution	GIBCO Life Technologies
Phosphate Buffer Saline with Calcium and Magnesium (PBS++)	Cellgro Mediatech, Inc.
Phosphate Buffered Saline (PBS, pH 7.4)	Sigma-Aldrich
Poly-l-ornithine	Sigma-Aldrich
Precision Plus Protein Dual Colour Standards	Bio-Rad
ProLong Antifade Resin (PLAF)	Invitrogen Molecular Probes
Recovery cell-culture freezing media	GIBCO Life Technologies
Retinoic Acid (RA)	Sigma-Aldrich
RPMI medium 1640 (1X, +L-glutamine)	GIBCO Life Technologies
Saponin	Fluka
Sodium Bicarbonate	EMD
Sodium Chloride	Fisher Scientific
Sodium citrate dihydrate	Sigma-Aldrich
Sodium Dodecyl Sulphate (SDS)	Bio-Rad

Sodium pyruvate	GIBCO Life Technologies
Sucrose	Sigma-Aldrich
Tetramethylethylenediamine (TEMED)	OmniPur/EMD
Tris	Bio Basic Inc.
Tris-HCl (0.125M, pH 6.8)	Bio-Rad
Triton X-100	Sigma-Aldrich
Trypan Blue Stain (0.4%)	GIBCO Life Technologies
Trypsin (0.25%, +1mM EDTA)	GIBCO Life Technologies
Tween 20	Fisher Scientific
UltraPure Water	Invitrogen
Xylenes	Fisher Scientific

2.1.1 Buffers and Solutions

The buffers and solutions commonly used for this thesis, and their composition, are listed in the table below.

Table 2.2 Common Buffers and Solutions

Buffer / Solution	**Composition**
1x SDS Extraction Buffer	0.125M Tris-HCK pH 6.8, 2% SDS, 10% Glycerol, 5% β-Mercaptoethanol
4x Seperating Buffer	1.5M Tris pH8.8, 0.4% SDS
4x Stacking Buffer	0.5M Tris pH 6.8, 0.4% SDS
Carbonate Transfer Buffer	10mM $NaHCO_3$, 3mM Na_2CO_3, 20% Methanol
Citrate Buffer pH 6.0	10mM Sodium Citrate Dihydrate, 0.05% Tween 20
Fixing Solution	1x PBS, 4% Paraformaldehyde
Gel Running Buffer	25mM Tris, 200mM Glycine, 0.1% SDS
Hank's Buffer	HBSS, 1.5% HEPES, 0.3% Penicillin-Streptomycin
HFN Basal Media	MEM, 10% FBS, 1mM L-Glutamine, 1mM Sodium Pyruvate, 1x NEAA, 1% Sucrose, 1% Penicillin-Streptomycin, 0.1% Fungizone

HFN Non-Serum Media	MEM, 1mM L-Glutamine, 1mM Sodium Pyruvate, 1x NEAA, 1% Sucrose
IF Blocking Solution	1x PBS, 2% BSA, 0.5% Saponin
IF Wash Solution	PBS++, 0.2% BSA, 0.1% Triton X-100
IHC Blocking Buffer for Human Tissue	1x TBS-T, 5% Goat Serum, 1% BSA
IHC Blocking Buffer for Mouse tissue	1x TBS-T, 5% Goat Serum, 5% Mouse Serum
Laemmli (Sample) Buffer	60mM Tris pH 6.8, 2% SDS, 10% Glycerol, 5% β-Mercaptoethanol, 0.01% Bromophenol Blue
Mononuclear Cell Basal Media	AIM-V Medium (1X), 1% Penicillin-Streptomycin
Mononuclear Cell Washing Buffer	1x PBS, 2% FBS
NT2 Basal Media	DMEM, 10% FBS, 1% Penicillin-Streptomycin, 0.1% Fungizone
Rat Neuron Basal Media	MEM, 2% FBS, 0.3mM L-Glutamine, 1.5mM Sodium Pyruvate, 1.5% HEPES, 1% N-2 Supplement0.3% Penicillin-Streptomycin
Tris Buffered Saline-Triton X-100 (1x TBS-T)	10mM Tris pH 8.0, 0.15M NaCl, 0.05% Triton X-100
Western Blocking Solution	1x PBS, 2% BSA
Western Blot Antibody Solution	1x TBS-T, 2% Milk (Carnation, skim milk powder)

2.1.2 Antibodies

Primary and secondary antibodies, and their working concentration applied in Western Blot, Immunohistochemistry and Immunocytochemistry of this study, were listed in the tables below.

Table 2.3 Primary Antibodies

Antibody	Supplier	Host	Antibody Clonality	Working Dilution	Appli-cation	Species Reactivity
BECN1	Santa Cruz	Mouse	Polyclonal	1:200	WB	Hu, Ms, Rt

BiP	BD	Mouse	Monoclonal	1:1000	WB	Dg, Hu, Ms, Rt
BiP	Abcam	Rabbit	Monoclonal	1:100	IHC	Hu, Ms
Calnexin	Dr. Luc Berthiaume's Lab	Rabbit	Polyclonal	1:1000	WB	---
Calreticulin	Thermo	Rabbit	Polyclonal	1:1000	WB	Hu, Ms, Rt
Caspase 3 (8G10)	Cell Signaling	Rabbit	Monoclonal	1:1000	WB	Hu, Ms, Rt
Caspase 8 (1C12)	Cell Signaling	Mouse	Monoclonal	1:1000	WB	Hu
CD3	BD	Mouse	Monoclonal	1:1000	TA	Hu
CD28	BD	mouse	Monoclonal	1:100000	TA	Hu
CHOP (9C8)	ENZO	Mouse	Monoclonal	1:1000	WB	Hu, Ms
CHOP (9C8)	Thermo	Mouse	Monoclonal	1:100	IHC	Hu, Ms, Rt
DNM1L (Drp1)	Abcam	Mouse	Monoclonal	1:1000	WB	Hu, Rt
Flag	Rockland	Mouse	Monoclonal	1:100	IF	---
GRP75/HSPA9B	Affinity BioReagents	Mouse	Monoclonal	1:1000	WB	Hu, Mk, Ms
GRP94	Millipore	Rabbit	Polyclonal	1:1000	WB	Hu, Mk, Rt
Lc3B (D11)	Cell Signaling	Rabbit	Monoclonal	1:1000	WB	Hu, Ms, Rt
MFN2	Abnova	Mouse	Monoclonal	1:1000	WB	Hu, Ms, Rt
Nucleo-porin p62	BD	Mouse	Monoclonal	1:2000	WB	Ch, Hu, Ms, Rt
PACS2	Protein Tech	Rabbit	Polyclonal	1:600	WB	Hu, Ms, Rt
Phospho-DRP1 (Ser637)	Cell Signaling	Rabbit	Polyclonal	1:1000	WB	Ms, Mk, Rt
Rab32	Dr. John Scott's Lab	Rabbit	Polyclonal	1:1000	WB/IHC	Hu
Rab32	Protein Tech	Rabbit	Polyclonal	1:200	IHC	Hu

Rab38	Abnova	Mouse	Monoclonal	1:1000	WB	Hu
Rab38	Abcam	Rabbit	Polyclonal	1:1000	WB	Ch, Cw, Hu, Ms, Rt
Rab7L1	Abnova	Mouse	Monoclonal	1:1000	WB	Hu
Rab7L1	Abcam	Mouse	Monoclonal	1:1000	WB	Hu
SMI 312R	Covance	Mouse	Monoclonal	1:1000	IHC	Hu, Ms
SMI 32R	Covance	Mouse	Monoclonal	1:1000	IHC	Mm, Ms
α-Tubulin	Millipore	Mouse	Monoclonal	1:2000	WB	Ch, Gr, Hu, Ms, Rt

WB: Western Blot

ICC: Immunocytochemistry

IF: Immunofluorescence

IHC: Immunohistochemistry

TA: T cell activation

Hu: Human	Ch: Chicken	Dg: Dog
Ms: Mouse	Cw: Cow	Gr: Gerbil
Rt: Rat	Mk: Monkey	Mm: Mammalian

Table 2.4 Secondary Antibodies

Antibody	**Supplier**	**Host**	**Antibody Clonality**	**Working Dilution**	**Application**
Alexa Fluor 750 anti-Rabbit	Invitrogen-Molecular Probes	Goat	Polyclonal	1:5000	WB
Alexa Fluor 680 anti-Mouse	Invitrogen-Molecular Probes	Goat	Polyclonal	1:5000	WB
Alexa Fluor 594 anti-Mouse	Invitrogen-Molecular Probes	Goat	Polyclonal	1:2000	IHC
Alexa Fluor 488 anti-Rabbit	Invitrogen-Molecular Probes	Goat	Polyclonal	1:2000	IHC
Alexa Fluor 488 anti-Mouse	Invitrogen-Molecular Probes	Goat	Polyclonal	1:2000	IF

2.1.3 Plasmids

The plasmid vectors and small hairpin RNAs (shRNAs) used in this study are listed in the tables below.

Table 2.5 Plasmids

Plasmid Name	Tag	Vector	Bacterial Resistance	Promoter	Plasmid type	Supplier
Rab32 WT	Flag	pcDNA3	Ampicillin	CMV	Mammalian Expression	Dr. John Scott's Lab
Rab32 Q85L	Flag	pcDNA3	Ampicillin	CMV	Mammalian Expression	Dr. John Scott's Lab
Rab32 T39N	Flag	pcDNA3	Ampicillin	CMV	Mammalian Expression	Dr. John Scott's Lab
pmaxGFP	GFP	pmaxGFP	Kanamycin	PCMV	Mammalian Expression	Lonza
pDsRed2-Mito	DsRed2	pDsRed2	Kanamycin	CMV	Mammalian Expression	Clontech
pEYFP-Mito	YFP	pEYFP	Kanamycin	CMV	Mammalian Expression	Clontech

Table 2.6 shRNAs

Name	ID	Reporter Gene	Vector	Selecting Marker	Target Species	Supplier
RAB32 RSH054438	RSH054438-1-CH1	eGFP	psi-H1	Puromycin	Rat	Gene Copoeia
RAB32 RSH054438	RSH054438-2-CH1	eGFP	psi-H1	Puromycin	Rat	Gene Copoeia
RAB32 RSH054438	RSH054438-3-CH1	eGFP	psi-H1	Puromycin	Rat	Gene Copoeia
RAB32 RSH054438	RSH054438-4-CH1	eGFP	psi-H1	Puromycin	Rat	Gene Copoeia
shRNA Scrambled Control Clone	CSHCTR001-CH1	eGFP	psi-H1	Puromycin	Rat	Gene Copoeia

RAB32 HSH001118	HSH001118-1-mH1	mCherry	psi-mH1	Puromycin	Human	Gene Copoeia
RAB32 HSH001118	HSH001118-2-mH1	mCherry	psi-mH1	Puromycin	Human	Gene Copoeia
RAB32 HSH001118	HSH001118-3-mH1	mCherry	psi-mH1	Puromycin	Human	Gene Copoeia
RAB32 HSH001118	HSH001118-4-mH1	mCherry	psi-mH1	Puromycin	Human	Gene Copoeia
shRNA Scrambled Control Clone	CSHCTR001-mH1	mCherry	psi-mH1	Puromycin	Human	Gene Copoeia

2.1.4 Cell Model and Human Tissue

The cell lines, primary cell cultures purified from embryo tissues and patient autopsy tissue samples used in this study are listed in the tables below. Patient autopsy tissue samples are identified according to patient clinical information.

Table 2.7 Primary Cell Culture and Cell Line

Mammalian Cell Line	**Source**
NT2 human teratocarcinoma cell line	ATCC
Primary Cell Culture	**Source**
Human fetal neuron	15-19 weeks human fetal brain
Rat cortical neuron	18 days rat embryos
T cell	Donated blood from volunteers
Bacterial Cell	**Source**
DH5α *E. Coli*	Dr. Gary Eitzen, University of Alberta

Table 2.8 Human Brain Tissue Source

Patient I. D.	**Age**	**Gender**	**Disease Course**
NP12-50	54	Male	Secondary Progressive MS
NP13-10	44	Male	Relapsing-Remitting MS

2.1.5 Multicomponent System, Software and Equipment

The multicomponent kit, software and equipment used in this study are listed in the tables below.

Table 2.9 Multicomponent System

Multicomponent system	**Supplier**
Amaxa Basic Nucleofector Kit (Primary Neurons)	Lonza
Amaxa Rat Neuron Nucleofector Kit	Lonza
Human CD4+ T Cell Enrichment Cocktail	RosetteSep
Human CD8+ T Cell Enrichment Cocktail	RosetteSep
QIAGEN Plasmid Midi Kit	QIAGEN
Vybrant Multicolor Cell-Labeling Kit	Invitrogen

Table 2.10 Detection and Analysis Software

Software	Supplier
Adobe Photoshop CS5	Adobe
Axiovision 4 Acquisition Software	Carl Zeiss
Microsoft Excel 2010-Data Analysis	Microsoft
ImageJ Software	Rasband, W.S., ImageJ, U.S. National Institutes of Health, http://rsb.info.nih.gov/ij/
Image Studio Lite Ver 3.1	LI-COR
Odyssey InFrared Imaging System	LI-COR

Table 2.11 Equipment

Equipment	**Supplier**
550 Sonic Dismembrator	Fisher Scientific
Axio Observer Wide-field Microscope	Carl Zeiss

Centrifuge	Beckman
Li-Cor Scanner	LI-COR
Microcentrifuge	Eppendorf
NanoDrop Spectrophotometer ND1000	Thermo Scientific
Nucleofector 2b Device	Lonza

2.2 METHODS

2.2.1 Mammalian Cell Culture Techniques

2.2.1.1 Maintenance and Differentiation of NT2 Cell Line

A human embryonic teratocarcinoma cell line, NT2, was maintained in NT2 basal medium (Table 2.2). Cells were incubated at 37°C in an environment of 95% air and 5% CO_2 and were passaged twice per week using 0.25% trypsin/1mM EDTA (Table 2.1).

NT2 cells were induced to differentiate into neuronal phenotypes after four weeks of treatment with 10μM Retinoic Acid (RA, Table 2.1) in aggregate cultures. Then cells were purified roughly and seeded into proper containers pre-coated with 1x poly-L-ornithine (Table 2.1). Following a two-week treatment with 25μM Cytosine Arabinoside (AraC, Table 2.1), NT2 neuron grew into proper phenotypes and was ready for use.

2.2.1.2 Isolation and Maintenance of Primary Neuron Cultures

Human fetal neuron (HFN) culture was prepared from 15-19 weeks fetal brains obtained with consent (approved by the University of Alberta Ethics Committee) [144]. In short, fetal brain tissues were dissected and meninges were removed. A single cell suspension was prepared by trituration of the tissues through serological pipettes, followed by digestion for 30 minutes with 0.25% trypsin and 0.2 mg/ml DNase I (Table 2.1), and was then passed through a 70-μm cell strainer (BD). Cells were washed 2 times

with fresh HFN basal medium (Table 2.2) and seeded in proper containers pre-coated with poly-L-ornithine at 60-80 million cells/flask. 25μM AraC was added to the basal medium for growing HFN and preventing the growth of astrocytes.

Rat cortical neuron culture was prepared from 18 days embryos (E18) obtained with consent (approved by the University of Alberta Ethics Committee). Briefly, embryos were removed from pregnant rat and cortices of the embryonic brains were isolated with removed skin, washed with Hank's buffer (Table 2.2). The cortices were then digested in 0.25% trypsin for 16 min and disrupted by glass Pasteur pipette. Cells were washed twice with HBSS medium (Table 2.1) and plated in proper container pre-coated with poly-L-ornithine at 3 million cells/flask. The medium for growing rat cortical neurons was rat neuron basal medium (Table 2.2).

2.2.2 Human Frozen Brain Tissues

Tissues of three frozen MS brains collected from two identified patients (Table 2.8) and one unidentified patient, as well as tissues from a frozen ALS brain were obtained from Brain Bank in MS Clinic, University of Alberta. The post-mortem brain tissue (NP12-50, Table 2.8) was kindly donated by Dr. Christopher Power and Dr. Jian-Qiang Lu at the University of Alberta and collected as described in [145].

2.2.2.1 Protein Extraction from Human Frozen Brain Tissues

Proteins were extracted from human frozen brain tissues in 1x SDS extraction buffer (Table 2.2). Following a one-minute brief vortex, samples were sonicated twice by 550 Sonic Dismembrator (Table 2.11) for 5-10 minutes. Supernatants were collected and

protein concentrations were measured by NanoDrop Spectrophotometer ND1000 (Table 2.11) at Absorbance 280nm.

2.2.2.2 Sectioning of Autopsy Brain Tissues

Surgical specimens were formalin-fixed, paraffin-embedded and sectioned at 5 μm. The fixed tissue sections were mounted onto slides and stained using immunohistochemistry techniques described below (see Section 2.2.4).

2.2.3 Protein Immunoblot

2.2.3.1 Sodium Dodecyl Sulfate-Polyacrylamide Gel Electrophoresis (SDS-PAGE)

Extracted protein samples from frozen brain tissues were denatured during extraction and separated by SDS-PAGE technique. In brief, protein samples and standards were separated using 4% stacking gels and 8, 12 or 15% separating gels, depending on the size of proteins of interest. The stacking gel is composed of 3% acrylamide (Table 2.1), 1x stacking buffer (Table 2.2), 0.1% TEMED (Table 2.1) and 0.2% APS (Table 2.1). The separating gel is composed of 1x separating buffer (Table 2.2), 0.1% TEMED, 0.1% APS and proper concentration of acrylamide. SDS-PAGE was done using the Mighty Small II gel running system (Amersham) under 150V for 70-120 minutes, depending on the gel percentage.

2.2.3.2 Western Blot

Following separation of the protein samples by SDS-PAGE, gels were transferred onto a nitrocellulose membrane (Table 2.1) using a Mini Transblot Cell apparatus (Bio-

Rad) in Carbonate Transfer Buffer (Table 2.2) at 400mA for 2 hours at 4°C. The membrane was then incubated in Western Blocking Solution (Table 2.2) for 1 hour at room temperature. After blocking, the membrane was incubated in primary antibodies (Table 2.3) diluted into proper concentration using Western Blot Antibody Solution (Table 2.2), either overnight at 4°C or 1 hour at room temperature, according to specifications of each antibody. On the following day, the membrane was washed 3 times with 1x TBS-T (Table 2.2) for 5 minutes each at room temperature with gentle shaking. Secondary antibody incubation was performed for 1 hour in secondary antibodies (Table 2.4) diluted into proper concentration using Western Blot Antibody Solution. Finally, the membrane was washed again as described above and sat in distilled water before detection.

Detection was performed using Li-Cor scanner (Table 2.11) and basic analysis was performed by an Odyssey Infrared Imaging System (Table 2.10).

2.2.4 Immunohistochemistry

Sample sections from each specimen collected (as described in Section 2.2.2) were stained with hematoxyline and eosin (H&E) to identify demyelinated lesion area [145]. Selected sections of tissue blocks with chronic active lesion were deparaffinised 2 times in xylene for 5 minutes each and rehydrated in decreasing concentrations of ethanol 2 times for 5 minutes each. Antigen retrieval was conducted by dipping the slides in boiling 10mM citrate buffer (pH 6.0, Table 2.2) for 20 minutes. The slides were blocked in IHC blocking buffer (Table 2.2) and then probed for Rab32, CHOP, BiP and neurofilament by primary antibodies (Table 2.3) diluted into proper concentration using IHC blocking

buffer, according to standard protocol and manufacturer's instruction. Fluorescent double-staining was carried out by detecting with goat-anti mouse/rabbit secondary antibodies conjugated to Alexafluor 488/594 (Table 2.4). Nuclei counterstaining was performed by incubating sections in 0.1% 4',6-Diamidino-2-Phenylindole (DAPI, Table 2.1) for 15min. Fluorescent microscopy was achieved by an Axiocam on an Axio observer microscope (Table 2.11) with either 10x or 20x plan-Apochromat lens. All images were processed by Axiovision 4 Acquisition Software using Z-stack correction and deconvolution functions and images were enhanced with Adobe Photoshop CS5 (Table 2.11) using levels function only, until reaching saturation in the most intense areas of the image.

2.2.5 Transfection and immunofluorescence microscopy

2.2.5.1 Nucleofection

Electroporation was carried out using Amaxa Basic Nucleofector Kit for primary neurons or Amaxa Rat Neuron Nucleofector Kit (Table 2.9) according to the manufacturer's instructions. In brief, NT2, HFN or rat neurons were incubated in 0.25% trypsin for 3-5 minutes, followed by deactivation of trypsin using basal medium. Collected cell supernatant was pelleted and re-suspended in non-serum medium to a concentration of 4-5 million cells/ml for primary neurons or 3.5 million cells/ml for NT2 neurons. After re-pellet, 5 million neurons were suspended in 100µl of pre-mixed Nucleofector Solution from the kit and mixed with 2-4 µg of plasmid (Table 2.5) or small hairpin RNA (shRNA, Table 2.6). Rab7L1 Wild Type (WT), Rab32 WT, Rab32 T39N (dominant negative mutant), Rab32 Q85L (dominant active mutant) or Rab32 shRNA

(sh-Rab32) plasmids (Table 2.5 & 2.6) were used in transfection of either type of cells. Fluorescent mitochondrial signal was achieved by either stain of neurons with MitoTracker Red CMXRos (Table 2.1) or transfection of neurons with pDsRed2-Mito plasmid (Table 2.5). For each cell type, the manufacturer suggested programs of nucleofector device (Table 2.11) were applied, and the most proper programs were determined based on cell viability and transfection efficiency for each type of cells. Ultimately, according to optimization results, A33, C03 and O03 programs were chosen for NT2 neurons, HFN and rat neurons, respectively. A recovery step was applied to improve cell viability by adding 500ul Roswell Park Memorial Institute medium (RPMI, Table 2.1) immediately into electroporated cells followed by 10-minute incubation at 37 °C [146]. Cells were seeded on coverslips pre-coated with poly-L-ornithine and cultured for 24 to 72 hours at 37 °C before immune-staining and microscopy analysis.

2.2.5.2 Immunocytochemistry

Following a 24 to72-hour growth, cells were incubated with 0.5 µl/ml MitoTracker Red at 37°C for 30 minutes if necessary, washed 3 times with PBS (Table 2.1) and fixed in 2ml fixing solution (Table 2.1 & 2.2) for 20 minutes at room temperature. After fixation, cells were washed with 2ml IF washing solution (Table 2.2) for 1-2 minutes if stained by MitoTracker dye, and washed twice with PBS. Cells transfected with auto-fluorescent protein tagged plasmids, including GFP (Table 2.5 & 2.6), pDsRed (Table 2.5), YFP (Table 2.5) and mCherry (Table 2.6), are stored in PBS until all transfection groups are ready for DAPI staining and mounting. On the other hand, cells transfected with Flag-tagged plasmids (Table 2.5) were blocked with IF blocking solution (Table 2.2)

for 10 minutes at room temperature. The primary antibody solution was prepared by diluting primary antibodies (Table 2.3) in IF blocking solution and 100 µl of the antibody solution was dropped to cover per coverslip. The coverslip was incubated for 1-2 hours at room temperature in the dark, washed 2 times in PBS for 5 minutes each and incubated in secondary antibody solution for 30 minutes at room temperature in the dark. The secondary antibody solution was prepared by diluting secondary antibodies (Table 2.4) in IF blocking solution and 100 µl of the antibody solution was dropped to cover per coverslip. Cells were then washed twice in PBS for 5 minutes each and sat in PBS until they are ready for counterstaining and mounting. All coverslips were incubated in PBS with 5ng/ml of DAPI for 10 minutes at room temperature. For mounting, glass slides were labeled and approximately 20µl mounting PLAF resin (Table 2.1) was dropped on top for each coverslip. After putting coverslips on resin drops, slides were allowed to dry overnight in the dark at room temperature and stored in 4°C before analysis.

2.2.5.3 Fluorescent Microscopy and Image Quantification

Immunofluorescent microscopy detection was achieved by an Axiocam on an Axio Observer microscope (Table 2.11) with either 40x, 63x or 100x plan-Apochromat lens. All images were processed by Axiovision 4 Acquisition Software using Z-stack correction and deconvolution functions and images were enhanced with Adobe Photoshop CS5 (Table 2.11) using levels function only, until reaching saturation in the most intense areas of the image. For consistency, sh-Rab32 signal detected under RFP channel was converted to green and pEYFP-Mito signal detected under GFP channel was converted to red as displayed in the following figures. Analysis of axonal growth and

mitochondrial morphology was performed using ruler and count functions. Analysis of transfection rate and cell viability was achieved by count function in the Photoshop and particle analysis function in the ImageJ software.

2.2.6 Bacterial Transformation

Bacterial host cell used in this protocol was competent DH5α *E. coli* bacteria (Table 2.7) stored in -86°C. Competent cells were thawed on ice for 15-20 minutes and 100µl of which was added to 1-2.5 µl of plasmid (Table 2.5) or shRNA (Table 2.6) and incubated on ice for 20 minutes. Bacteria were heat-shocked in a 45°C water bath for 45 seconds and mixed with 1ml of sterile LB broth (Table 2.1), prepared according to manufacturer's instructions. In the case of DNA, cells were centrifuged down using a microcentrifuge (Table 2.11) at maximum speed for 30 seconds, and then re-suspended in 100µl of LB, and plated onto pre-poured LB agar (Table 2.1) containing appropriate antibiotic. LB agar plates were incubated overnight at 37°C.

2.2.6.1 Bacterial Culture

Colonies of DH5α *E. coli* containing the transformed plasmid were picked using sterile pipette tips and grown in 50ml of LB broth containing appropriate antibiotic overnight at 37°C in a 220 rpm rotary shaker. In the morning of next day, the 50ml broth with bacteria were pelleted down and either stored frozen at -20°C for a short period of time or at -87°C for a long period of time, or conducted to DNA isolation protocol (see below).

2.2.6.2 Isolation of Plasmid from Bacteria

The QIAGEN Plasmid Midiprep Kit (Table 2.9) was applied to isolate plasmid from frozen pellets centrifuged from 50ml bacterial cultures, according to the manufacturer's instructions with modifications.

2.3 STATISTICAL ANALYSES

Data were analyzed statistically using the Student's t test and one-way analysis of variance (ANOVA). T-test was used when comparing two sample means for one factor assuming equal variance and ANOVA was used when comparing more than two sample means for one factor. Error bars illustrate standard deviations of the mean. Microsoft Excel 2010 (Table 2.10) was used for data analyses.

CHAPTER 3:

Human Tissue Studies

3. HUMAN TISSUE STUDIES

3.1 BACKGROUND AND RATIONALE

As stated in Section 1.1.3, ER stress could play a role in the pathogenesis of MS where it complements pre-lesion alterations and lesion development in response to inflammation [117, 118]. Prolonged ER stress down-regulates global protein synthesis, distorts calcium homeostasis and accelerates cell apoptosis through multiple signaling pathways [109, 110]. Accordingly, I propose that ER stress is essential for massive CNS cell death in MS, including neurons. Rab32, a small GTPase mediating ER-mitochondrial interaction and calnexin enrichment at MAM [136], contributes to downstream pathways of ER stress signals and regulates apoptosis. It has been shown that, in neuronal cells, Rab32 is up-regulated in response to induced ER stress under hypoxia. In a mouse study of acute brain inflammation, Rab32 is substantially induced along with pro-inflammatory cytokines increment in the brain, suggesting a potential linkage between Rab32 and inflammation [147]. Moreover, one of the Rab32 family proteins has been identified in genetic level as a risk marker in patients with most common subtypes of MS, RR-MS and SP-MS [48]. Thus, these evidences encourage me to study the potential role of Rab32 in MS pathology in association with ER stress and inflammation.

However, not much is known about Rab32 other than its AKAP function at MAM and involvement in post-Golgi transport. The mechanisms of Rab32 in these cellular compartments are not well studied, making it challenging to study this protein as a biomarker of a complicated disease such as MS.

3.2 RESULTS

3.2.1 Expression of Rab proteins, ER stress and apoptosis markers in brain tissue of MS patients.

3.2.1.1 Rab32 family proteins expression in MS brain tissue.

Rab32 protein is a small GTPase in the Rab subfamily of Ras small molecular weight G-protein, and is detected ubiquitously in mammalian organs and tissues [136, 137]. Its universal expression reveals its vital role in common pathways of cellular metabolism in different types of cells. To study a potential role of Rab32 in MS pathology, we first need to investigate the presence and variation of Rab32 protein in human brains of MS patients.

In order to detect Rab32 protein expression in MS brain tissues, total protein was extracted from either lesion or NAWM samples of frozen brain tissues of the three MS patients, and analyzed by SDS-PAGE and Western blot. Rab32 protein was observed to be universally expressed in NAWM and lesion of brain tissue from the three MS patients (Fig. 3.1A). Interestingly, Rab32 expression was significantly induced in the acute lesion where immune cell infiltration was active and activated resident microglia were present compared to surrounding NAWM (Fig. 3.1B). However, in chronic lesions where inflammation diminished and tissue damage dominated, the expression of Rab32 was relatively inhibited compared to peri-lesional NAWM (Fig. 3.1B). In fact, acute lesions are characterized by suffering from relatively high-level immune cell infiltration and inflammation compared to surrounding area, as well as in peri-lesion region of chronic lesions where inflammation is more dominant compared to the lesion center [84, 117]. Thus, Rab32 up-regulation is likely associated with inflammation as observed in acute lesion and NAWM of chronic lesion.

Expression levels of Rab38 and Rab7L1 proteins were probed as well considering their evolutionary and functional relationship with Rab32 and the relevance of RAB38 gene to MS disease onset. The level of both Rab38 and Rab7L1 proteins were markedly increased in the active lesion compared to NAWM, while the variation of expression was relatively inconspicuous in chronic lesions compared to that of Rab32 (Fig. 3.1A&B). The diminution of Rab38 and Rab7L1 signal could be observed clearly in one of the three chronic samples, while, in the other two samples, the expression level of both proteins in either NAWM or lesion was low (Fig. 3.1A). Quantitative analysis of band intensities represents similar expression tendency where the difference between chronic lesion and NAWM is really mild in either Rab38 or Rab7L1 protein-levels (Fig. 3.1B). Thus, I conclude that proteins in Rab32 subfamily, Rab32, Rab38 and Rab7L1, are present in human brain tissues and their variation of expression depends on the inflammatory status of the tissue.

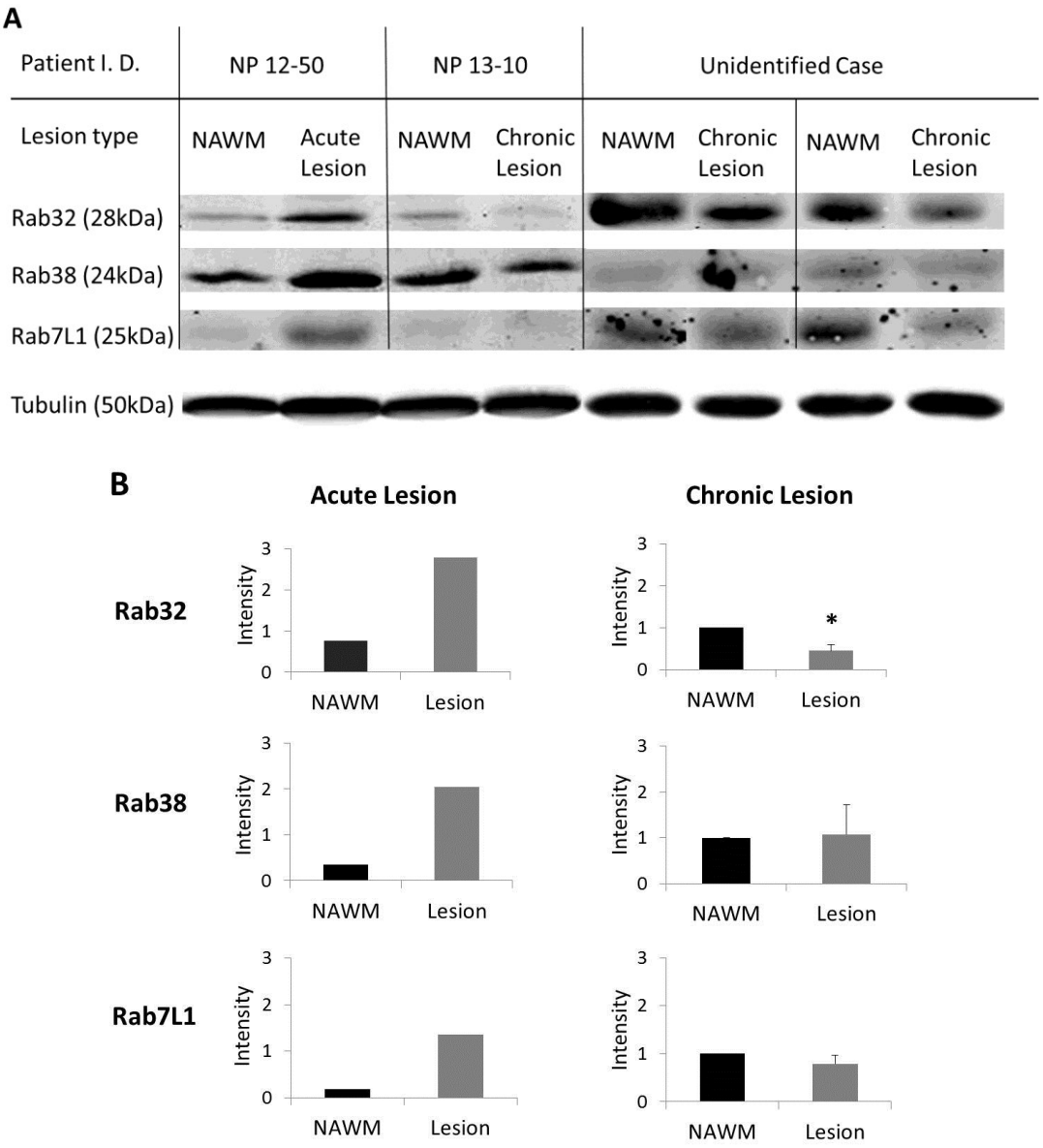

Figure 3.1 Identification of Rab proteins in human brain tissues. A. Western blots of MS brain tissue samples. Extracted protein samples from MS brains with chronic and acute lesions were probed by anti-α-tubulin for microtubule subunit protein tubulin (50kDa), anti-Rab32 for human Rab32 (28kDa), anti-Rab38 for human Rab38 (24kDa) and anti-Rab7L1 for human Rab7L1 or rat Rab29 (25kDa) antibodies, and were detected using goat-anti mouse/rabbit secondary antibodies conjugated to Alexafluor 680/750 on an Odyssey infrared imaging system (LI-COR). Tubulin was used as a loading control. Clinical details of each patient are listed in Table 2.8. **B**. Quantitative analysis of band intensities of each protein. Quantification was performed using Image Studio Lite software. Band intensities of one acute and three chronic lesion samples were collected and corrected

according to the level of the loading control. Fold changes in chronic lesions were normalized relative to control NAWM, and mean values were plotted. Error bars indicate standard error of mean values.

3.2.1.2 Detection of essential ER stress and apoptosis associated proteins

With the same protein samples used in section 3.2.1.1, I then probed for several typical ER stress-associated proteins. As stated in section 1.3.1.2, the ER chaperone BiP is an early signaling marker in response to ER stress, and prolonged stress induces production of this protein for further signaling [109]. Calnexin is another ER chaperone assisting protein coding and quality control, whereas accumulation of improperly-folded proteins accelerates calnexin production and retention in the ER lumen [148]. CHOP is an indicator of active cell apoptosis responding to ER stress whose function is to block transcription of several genes and to facilitate transcriptional regulator production [110]. From the blotting image, the expression of ER stress markers calnexin and BiP increased in all four lesion samples compared to NAWM regardless of inflammation severity (Fig. 3.2A). The increase in chronic lesion and NAWM samples becomes moderate when band intensities of these proteins were quantitatively evaluated (Fig. 3.2B). CHOP was expressed in relative low-level in all tissue samples (Fig. 3.2A), whereas the protein level in acute lesion is clearly increased compared to that in surrounding NAWM (Fig. 3.2B). In chronic lesion samples, the quantification results of band intensities indicated a relatively mild increase in CHOP compared to that in NAWM (Fig. 3.2B). This is conceivable because in acute lesion where inflammation is dominant, ER stress is heavily induced compared to less-affected NAWM, while in and around chronic lesions, both cellular damage and inflammation are present, leading to an overall high-level of ER

stress. Thus, the up-regulation of Rab32 protein level associates with induced ER stress in the acute lesion whereas in chronic lesions, Rab32 expression was occluded under relatively moderate ER stress. Combining with the information of inflammation, these findings suggested that Rab32 production is promoted under ER stress corresponding to inflammation severity.

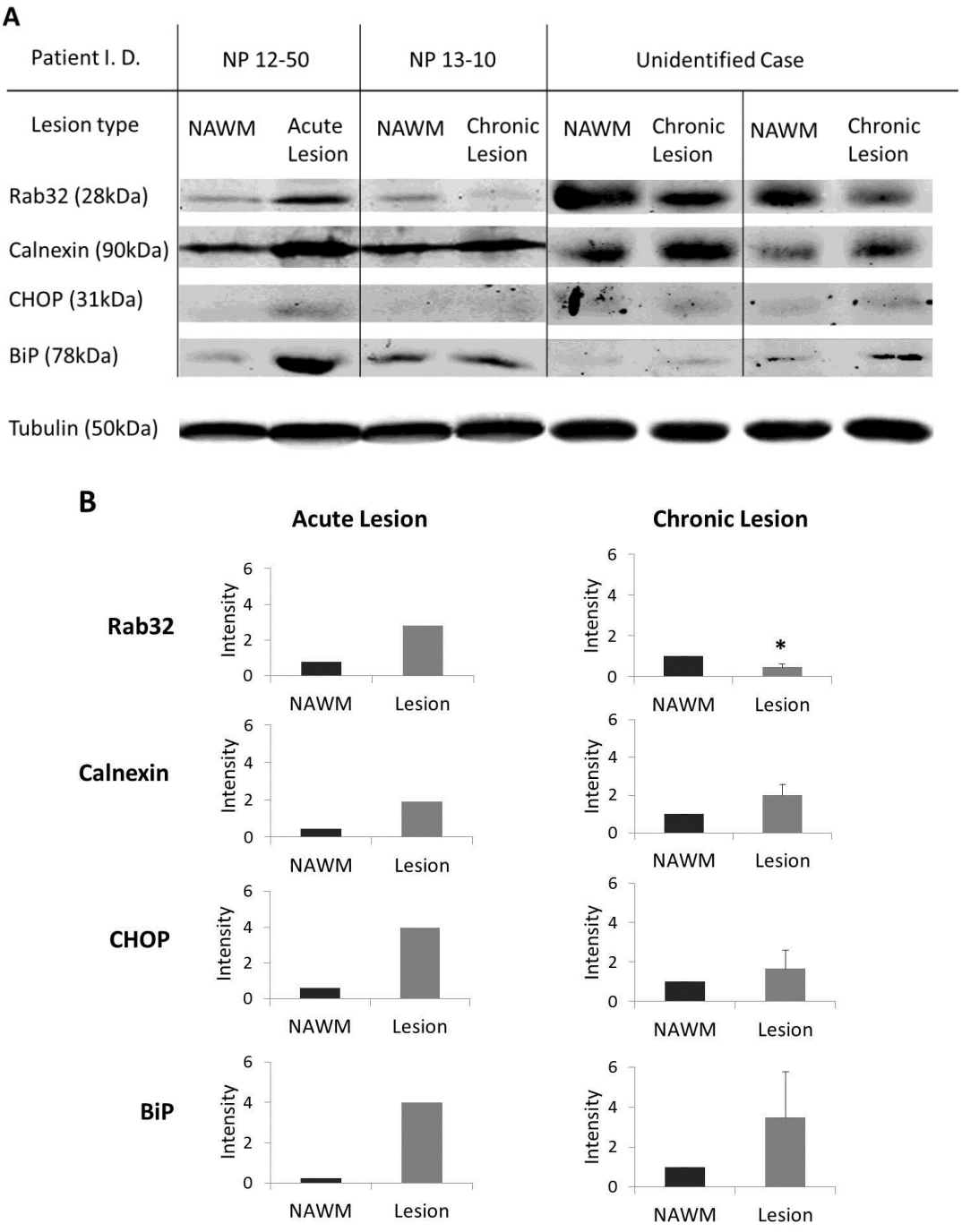

Figure 3.2 Rab32 protein level varies upon ER stress in chronic and acute lesions of MS brain tissue. A. Western blots of MS brain tissue samples. Same extracted protein samples described in figure 3.1 were probed by anti-Rab32, anti-calnexin for ER chaperone calnexin (90kDa), anti-CHOP for transcription factor CHOP(31kDa), and anti-BiP for ER chaperone and stress sensor BiP (78kDa) antibodies, and were detected as described in figure 3.1. Tubulin was used as a loading control. **B**. Quantitative analysis of band

intensities of each protein. Quantification was performed using Image Studio Lite software. Band intensities of one acute lesion sample and three chronic lesion samples were collected and corrected according to the level of the loading control. Fold changes in chronic lesions were normalized relative to control NAWM, and mean values were plotted. Error bars indicate standard error of mean values. n=3, *p<0.01.

3.2.1.3 Detection of other ER and mitochondrial proteins associated with ER stress, ER-mitochondrial interaction and mitochondrial membrane dynamics.

In addition, I probed for several other ER stress associated chaperones and some proteins involved in ER-mitochondrial communication and mitochondrial dynamics to further analyze the ER stress condition and mitochondrial alteration in MS. Glucose-regulated protein 94 (Grp94) is a molecular chaperone closely interacting with BiP that has roles in folding, stabilizing and secreting proteins in the ER and associated degradation pathways, and is ER stress-inducible [148]. Glucose-regulated protein 75 (Grp75), a member of the heat shock protein 70 (Hsp70) family, is a mitochondrial chaperone involved in ER-mitochondria interaction and protein folding and translocation in mitochondria, whose expression level is up-regulated under ER stress [149]. A multifunctional sorting protein, phosphofurin acidic cluster sorting protein 2 (PACS-2), integrates ER homeostasis and the ER-mitochondria interaction, and initiates a sequence of mitochondria-mediated apoptotic pathways [125]. Moreover, PACS-2 is identified to contribute to the enrichment of calnexin at MAM, which is believed to cause cell apoptosis [150]. Mfn2 and Drp1 are essential proteins in mitochondrial fission/fusion mechanisms [95].

In this study, one acute MS lesion case and one chronic MS lesion case were incorporated and protein detection was performed in the same fashion as described in

section 3.2.1.1. ER stress-associated chaperones, Grp75 and Grp94, were induced in both acute and chronic lesions compared to NAWMs (Fig. 3.3A&B), while the increase was relatively moderate in chronic lesion compared to the acute sample (Fig. 3.3B). This upward tendency agreed with the observed increase of other ER stress markers calnexin, BiP and CHOP, indicating a similar pattern of ER stress condition in acute and chronic lesion and surrounding tissue concluded in section 3.2.1.2. Besides, PACS-2 expressed in low level in all but the acute lesion sample (Fig. 3.3A), and its quantitative analysis of band intensity presented an apparent increase in both lesion samples compared to their NAWM (Fig 3.3B). Interestingly, bands of mitochondrial fusion protein Mfn2 showed overall low-level of its expression in both acute and chronic samples compared to those of fission protein Drp1 (Fig. 3.3A). Both Mfn2 and Drp1 increased their expression in acute lesion whereas this trend was reversed in chronic lesion compared to surrounding NAWMs (Fig. 3.3B). This might indicate an up-regulation of mitochondrial membrane dynamics in response to inflammation as well as an inhibition of production and activity of mitochondrial dynamics-related proteins in the area of cell degradation. It is also noteworthy that the variation of Drp1 expression has a similar tendency to that of Rab32 in these samples, suggesting a potential partnership of these two proteins in cellular mechanisms of MS pathogenesis.

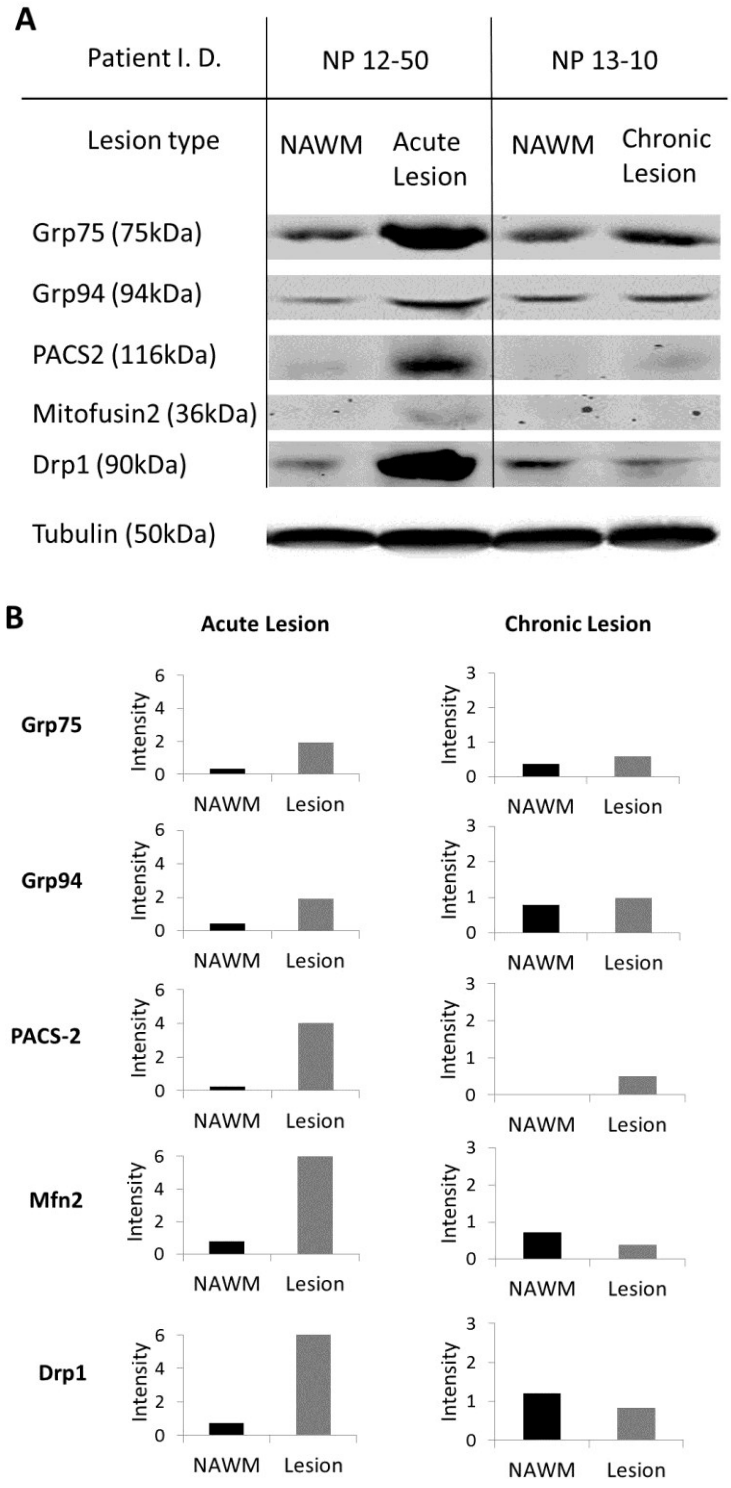

Figure 3.3 Detection of other ER and mitochondrial related proteins in chronic and acute lesions of MS brain tissue. A. Western blots of MS brain tissue samples. Two of the extracted protein samples described in figure 3.1 were probed by anti-GRP75 for mitochondrial chaperone Grp75 (75kDa), anti-GRP94 for ER chaperone Grp94

(94kDa), anti-PACS2 for the apoptotic marker PACS-2 (116kDa), anti-DNM1L for mitochondrial fission protein Drp1 (90kDa), and anti-MFN2 for mitochondrial fusion protein Mfn2 (36kDa) antibodies, and were detected as described in figure 3.1. Tubulin was used as a loading control. **B**. Quantitative analysis of band intensities of each protein. Quantification was performed using Image Studio Lite software. Band intensities of one acute lesion sample and one chronic lesion samples were illustrated.

3.2.2 Localization of Rab32 in brain tissue of MS patients

3.2.2.1 Co-localization of Rab32 with apoptotic marker CHOP

Following the blotting results showing that Rab32 expression is up-regulated in response to ER stress and inflammation, I examined the location of its expression variation in MS lesion tissues. To highlight the localization of ER stress, CHOP was chosen as a marker because of its very low expression within cells in non-stressful conditions compared to the other ER chaperones and its role in ER stress induced apoptotic mechanisms. The detection of CHOP indicates prolonged ER stress and ongoing apoptosis.

Immunohistochemistry was performed on surgical tissue sections of one MS patient brain (NP12-50, Table 2.8). A sample section from each case was stained for general cell structures (cell nuclei and cytoplasm) and myelin structure using a combination of H&E and Luxol Fast Blue (LFB). Chronic active WM lesion, lesion border and NAWM were identified in appendix figure 7.1 in terms of coverage of myelin sheath (Fig. 7.1, blue) and tissue destruction (Fig. 7.1, pink).

Immunofluorescent detection was then applied in adjacent sections to define the localization of Rab32 and CHOP. As observed, CHOP was expressed more at the border of chronic active lesions where immune cell infiltration and activation dominated,

suggesting high-level ER stress and inflammation in this area (Fig. 3.4B). It is worth noting that induction of Rab32 protein co-localized with the expression of CHOP at the lesion border (Fig. 3C&F). However, in NAWM and chronic lesion areas, the co-localization was unlikely (Fig. 3C). Thus, the increase of Rab32 at active lesion border coincided with ER stress-induced apoptosis, suggesting inflammation-associated production and activation of this protein in response to prolonged ER stress.

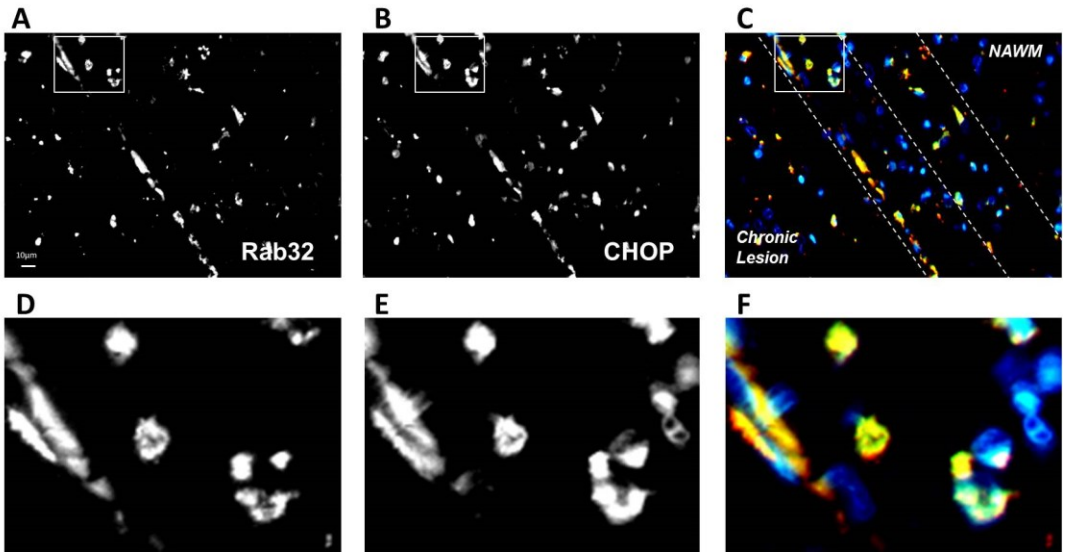

Figure 3.4 Rab32 co-localizes with the pro-apoptotic, ER stress-associated transcription factor CHOP on the border of chronic active lesions in MS tissue. Autopsy tissue sections from an MS patient (NP 12-50) brain with chronic active lesions were probed with anti-Rab32 and anti-CHOP antibodies and nuclei were counterstained with DAPI. Sections were detected by immunofluorescence using goat-anti mouse/rabbit secondary antibodies conjugated to Alexafluor 488/594 and fluorescent microscopy. Images were taken under 20x magnification. **A**: Rab32; **B**: CHOP; **C**: Merge in yellow, Rab32 in red, CHOP in green and nuclei in blue. Chronic lesion, lesion border and NAWM were identified using H&E and LFB stain of adjacent sections as described in figure 7.1. The dashed lines in **C** represent the area of active lesion border. Highlighted areas in **A**, **B** and **C** were zoomed in and presented as **D, E** and **F**, respectively. Scale bar: **A, B, C** = 10µm.

3.2.2.2 Rab32 expression in neurons

According to previous results showing that Rab32 protein levels were up-regulated in lesion tissue of MS patient brain in response to inflammation and ER stress, the next step was to determine whether this variation of expression was localized in neurons. To answer this question, adjacent tissue sections from surgical specimens of the same patient brain used in section 3.2.2.1 were tested for axonal and non-phosphorylated neurofilament, as well as Rab32. Rab32 was expressed in relatively high-level at border of chronic active lesion compared to other areas of the lesion within the section (Fig. 3.5A), which is consistent with my previous findings (Fig. 3.4A). Neurofilament was universally expressed while a relatively diminished signal was observed in the chronic lesional area (Fig. 3.5C). Some swollen axons were observed at the lesion border (Fig. 3.5B arrows), indicating an ongoing axonal degeneration within this area of the lesion in response to active inflammation. When we consider the merged images, signals of Rab32 and neurofilament were only partially overlapping throughout the tissue section (Fig. 3.5C&E). Interestingly, the co-localization appeared mainly in swollen axons at the active lesion border (Fig. 3.5C arrows). These swollen axons were surrounded by some nuclei that might have come from infiltrated immune cells (Fig. 3.5E, blue), and were possibly indicating active inflammatory-mediated focal degeneration. This suggests that Rab32 increases its production and plays a role in the inflammation-initiated axonal injury. Overall, it is possible that up-regulation of Rab32 occurs not necessarily in neurons but some other type of CNS cells as well. Moreover, an increase of Rab32

protein level in swollen axons indicates that Rab32-associated neuropathology in MS could be inflammation-dependent axonal injury.

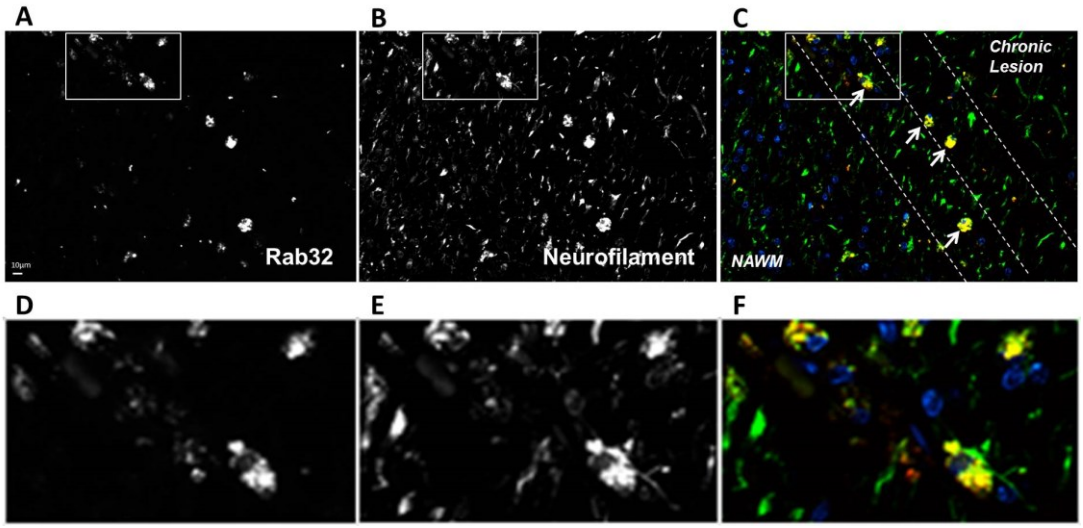

Figure 3.5 Rab32 expresses in neurons of MS brain tissue. Autopsy tissue sections from the same brain as stated in figure 3.4 were probed with anti-Rab32 and anti-SMI312/32R antibodies and DAPI stain was applied. SMI312/32R antibody cocktail was applied to indicate pan-axonal phosphorylated (pathological) and non-phosphorylated (normal) neurofilaments. Sections were detected by immunofluorescence using goat-anti mouse/rabbit secondary antibodies conjugated to Alexafluor 488/594 and fluorescent microscopy. Images were taken under 20x magnification. **A**: Rab32; **B**: neurofilament; **C**: Merge in yellow, Rab32 in red, neurofilament in green and nuclei in blue. Chronic lesion, lesion border and NAWM were identified using H&E and LFB stain of adjacent sections as described in figure 7.1. The dashed lines in **C** represent the area of active lesion border. White arrows in **B** and **C** indicate swollen axons. Highlighted areas in **A**, **B** and **C** were zoomed in and presented as **D, E** and **F**, respectively. Scale bar: **A, B, C** = 10µm.

3.3 SUMMARY

Knowledge of ER stress and mitochondrial dynamics alteration in MS pathology remains limited. In this project, we examined a potential biomarker, Rab32, to study neglected cellular mechanism in neurodegeneration of the disease. The study of Rab32-

mediated mechanisms allows us to link inflammation, ER stress and mitochondrial dynamics impairment all together and to have a better understanding of MS neuropathology. Rab32 at protein-level was altered in MS lesions in response to inflammation severity brought on by prolonged ER stress. It co-localized with ER stress and apoptotic marker at the border of MS lesions, emphasizing its metabolic functions in relation to inflammation and ER stress induced apoptosis. Furthermore, the observed localization of Rab32 within neurons of MS brain tissue suggests possible contribution of this protein in neurodegenerative mechanisms of MS leading to permanent disability.

CHAPTER 4:

Cellular Studies

4. CELLULAR STUDIES

4.1 BACKGROUND AND RATIONALE

Since I found altered Rab32 levels in neurons at active MS lesion border, I then decided to determine the function of Rab32 in neurons. Rab32 is identified as an A-kinase anchoring protein (AKAP) regulating phosphorylation and inactivation of Drp1 [136, 137], and the majority of endogenous Rab32 proteins are mitochondrial or ER membrane associated [136]. It has been predicted that, in a human immortal cancer cell line, overexpression and inactivation of Rab32 increases phosphorylation of Drp1 at Ser656, which is known to inhibit mitochondrial fission and cell apoptosis [95]. In contrast, the blockage of Rab32 protein expression was shown to promote aberrant fragmentation of mitochondria [136], which would destroy mitochondrial function and induce cell apoptosis. Furthermore, activation of Rab32 was also observed to induce cell apoptosis onset through regulation of calcium homeostasis and calnexin localization in ER and MAM [136]. A suggested mechanism of active Rab32 at MAM is related to mitochondrial dynamics, where it drives Drp1 recruitment at mitochondrial communication sites of ER membrane to promote mitochondrial fragmentation and subsequent cell apoptosis [140]. It has also been observed that overexpressed active Rab32 lowered mitochondrial membrane potential in Hela cells, suggesting retarded ATP production and energy deficiency in these cells (unpublished data). In conclusion, these findings propose a vital role of Rab32 in regulating the normal mitochondrial dynamics and cell metabolism, whose abnormality in production and activity would lead to cell apoptosis.

4.2 RESULTS

4.2.1 Function of Rab32 protein within neurons

To examine the function of Rab32 in neurons, either wild type or mutant of this protein has to be overexpressed to amplify cellular alterations. As a great cell model, human fetal neuron mimics the complex bio-physiological condition and biochemical mechanisms of human cells. However, because of limited availability of human tissue, rat cortical neurons were also a good neuronal model for cellular analyses in vitro.

4.2.1.1 Modification of nucleofection conditions

We chose nucleofection as our ideal transfection technique because of the high consistency and efficiency of the technique with low cytotoxicity to primary mammalian neurons and its suitability for the study of both transient and permanent transfected cells [146]. However, because primary rat cortical and human fetal neurons are sensitive to the environment and are relatively hard to transfect, control experiments were performed to find appropriate transfection conditions for these cells.

Firstly, nucleofection of rat cortical neurons with GFP control vector was performed to improve viability and adherence of transfected neurons. Transfection of neurons with or without plasmid showed no effect on cell viability (Fig. 4.1A&B), whereas a recovery step applied following transfection was able to protect cells from electroporation-mediated damage as described in section 2.2.5.1 (Fig. 4.1B&C). According to manufacturer suggestions, two of the programs in the nucleofector device (Table 2.10), O-03 and G-13, were tested. A mild improvement of transfection efficiency was observed

in O-03 transfection group compared to G-13 (Fig. 4.1C&E or 4.1D&F). Adherence of neurons onto the coverslip is important for cell viability and subsequent analysis. Two methods of coverslip-coating were examined and results showed no significant difference on neuron viability and morphology (Fig. 4.1C&D or 4.1E&F). Thus, O-03 program was selected to efficiently transfect rat neurons followed by a recovery step.

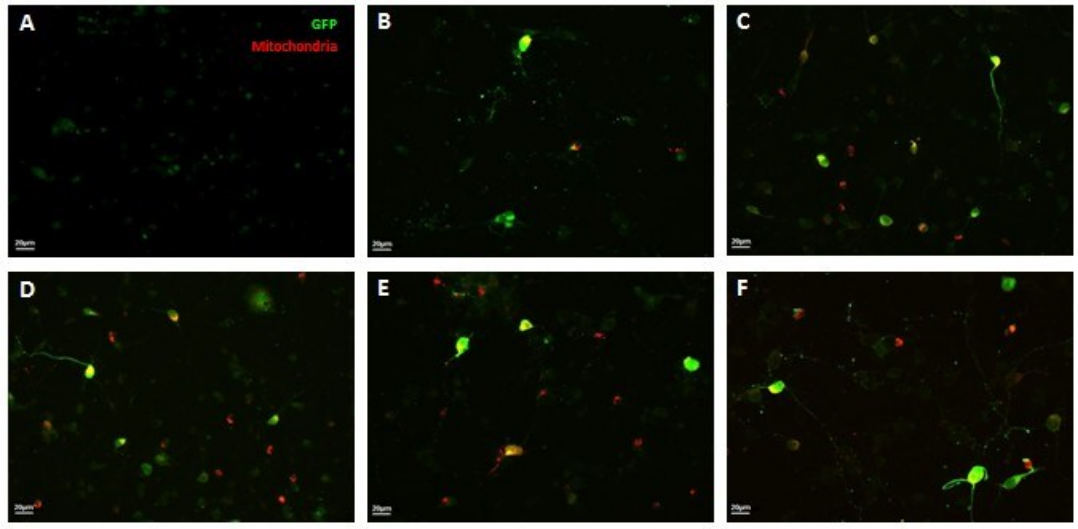

Figure 4.1 Modification of transfection conditions for primary neurons. Rat cortical neurons were electroporated using two different programs of the nucleofector device (Table 2.10) according to manufacturer's suggestions, where different conditions of coverslip-coating and post-transfection recovery steps were applied. Transfection was performed for 4.5 million cells per program with either pmaxGFP vector, pDsRed2-Mito plasmid or both (Table 2.5), and grew for 72 hours on coverslips pre-coated with poly-L-ornithine (poly-O) post-transfection. After fixation, cells expressing inserted plasmids were detected by immunofluorescence microscopy. As illustrated in images **A** to **F**, GFP expressing cells show green signal and mitochondria show red signal, and the merged show yellow signal. Images show portions of cells. **A**. Neurons were transfected using program O-03 with no plasmid added; coverslip-coating was 2 hours, 37°C. **B**. Neurons were transfected using program O-03 with both of the plasmids; coverslip-coating was 2 hours, 37°C. **C**. Neurons were transfected using program O-03 with both of the plasmids followed by a recovery step that 500ul RPMI (Table 2.1) was added to electroporated cells followed

by the incubation at 37°C for 15 minutes before seeding; coverslip-coating was 2 hours, 37°C. **D**. Most conditions were performed in the same way as described in **C**, except that coverslip-coating was 3 hours at room temperature. **E**. Neurons were transfected using program G-13 with both of the plasmids followed by a recovery step; coverslip-coating was 2 hours, 37°C. **F**. Most conditions were performed in the same way as described in **E**, except that coverslip-coating was 3 hours at room temperature. The most proper transfection condition was chosen based on viability, neuron morphology and growth, and relative transfected cell number per unit area. Scale bar = 20μm.

For human neurons, a similar control experiment was performed using six different nucleofector programs, and other steps were carried out as in rat neurons. After evaluating cell viability and transfected cell number and morphology, C-03 program was selected as the most suitable program for HFN transfection (Fig. 4.2).

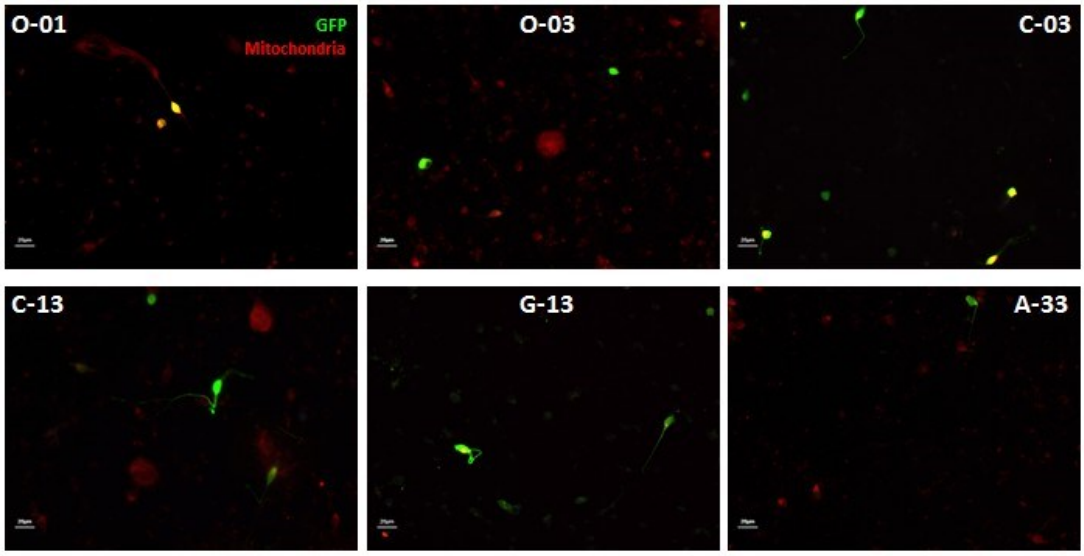

Figure 4.2 Selection of nucleofection program for human fetal neurons. Human fetal neurons were electroporated using six different programs of the nucleofector device according to manufacturer's suggestion. Double transfection was performed for 4 million cells per program with pmaxGFP vector and pDsRed2-Mito plasmid, and grew for 72 hours on coverslips post-transfection. Coverslips were pre-coated with poly-O for 3 hours

at 37°C. After fixation, cells expressing inserted plasmids were detected using immunofluorescence microscopy. As illustrated in all six images, GFP expressing cells show green signal and mitochondria show red signal, and the merged show yellow signal. Nucleofector device program applied is labeled in white on the top of each image. Images show portions of cells. The most proper program was chosen based on viability, neuron morphology and growth. Scale bar = 20μm.

Moreover, transfection efficiency was examined in HFN for four types of Rab32 plasmids and a control GFP vector. Transfection efficiency could be affected by different plasmid applied, and relied on purity and amount of the plasmid [146]. As observed in figure 4.3, both GFP and Rab32WT transfection groups had a relatively high efficiency with more green-signaling cells present, while the Rab32WT group showed high viability compared to other groups (Fig. 4.3A). In Rab32Q85L and sh-Rab32 transfection groups, both cell viability (Fig. 4.3A) and transfection efficiency (Fig. 4.3B) decreased. Rab32T39N had a moderate efficiency in terms of cell viability (Fig. 4.3A&B). In quantitative comparison with control GFP vector, Rab32 Q85L and sh-Rab32 plasmids were the most difficult to transfect and express in HFN, whereas Rab32 WT and T39N plasmids had higher efficiencies (Fig. 4.3B).

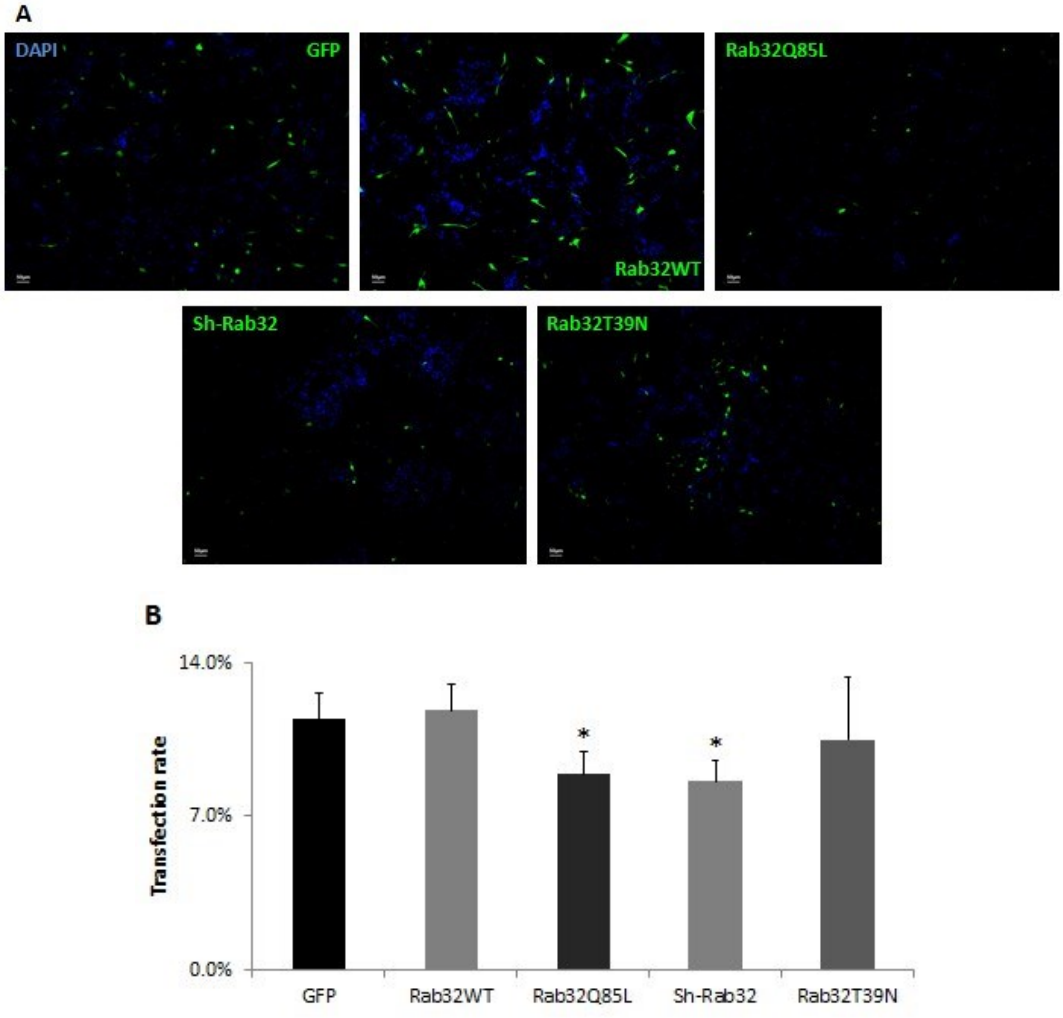

Figure 4.3 Evaluation of transfection efficiency of different plasmids in HFNs using C-03 program. HFNs were electroporated as described in figure 4.2 using C-03 program. Transfection was performed for 5 million cells per program with pmaxGFP vector as well as Rab32 WT, Rab32 Q85L, sh-Rab32 and Rab32 T39N plasmids (Table 2.5&2.6) and grew for 24 hours on coverslips post-transfection. After fixation, nuclear staining was performed and cells expressing inserted plasmids were detected using immunofluorescence microscopy. **A**. Neurons transfected with each plasmid under the same transfection conditions. Green signal shows the expression of specific plasmid as labeled on the top left corner of each image, and DAPI signal (blue) shows nuclear staining. Scale bar = 50μm. **B**. Quantification of transfection efficiency for each plasmid. Under 10x magnification, five positions were randomly selected for each transfection group and the ratio of transfected cell (green) number over total cell (DAPI) number within the observed area was plotted as the transfection rate for each plasmid. n = 5; *p<0.05.

4.2.1.2 The role of Rab32 in neuronal growth and mitochondrial dynamics

Considering that Rab32 plays a role in regulating mitochondrial dynamics and cell apoptosis, I then wanted to determine whether these functions have been preserved in neurons. Thus, transfected neurons were analyzed using fluorescent microscopy at high magnification to evaluate neurite outgrowth and mitochondrial morphology and distribution. Both a GFP control group and a corresponding negative-control group were selected as normal controls to be compared with Rab32 transfected groups. The negative control was defined as neurons on the same coverslip of Rab transfected neurons expressing only mitochondrial plasmid. Thus, GFP transfection group was used as a universal control to retain cellular alterations caused by double insertion and expression of plasmids, while negative control was used to control for confounding factors of GFP transfection and isolate changes caused by abnormal expression and activity of Rab32 proteins. A significant difference between Rab32 transfected neurons and either GFP or negative control could provide insight on Rab32's function in cellular mechanisms within neurons. As observed in figure 4.4, there was no difference between GFP-negative control and GFP-positive cells in either neurite outgrowth or mitochondrial distribution (Fig. 4.4B), suggesting that they were both reasonable controls and the effect of double-transfection was negligible on neuronal morphology.

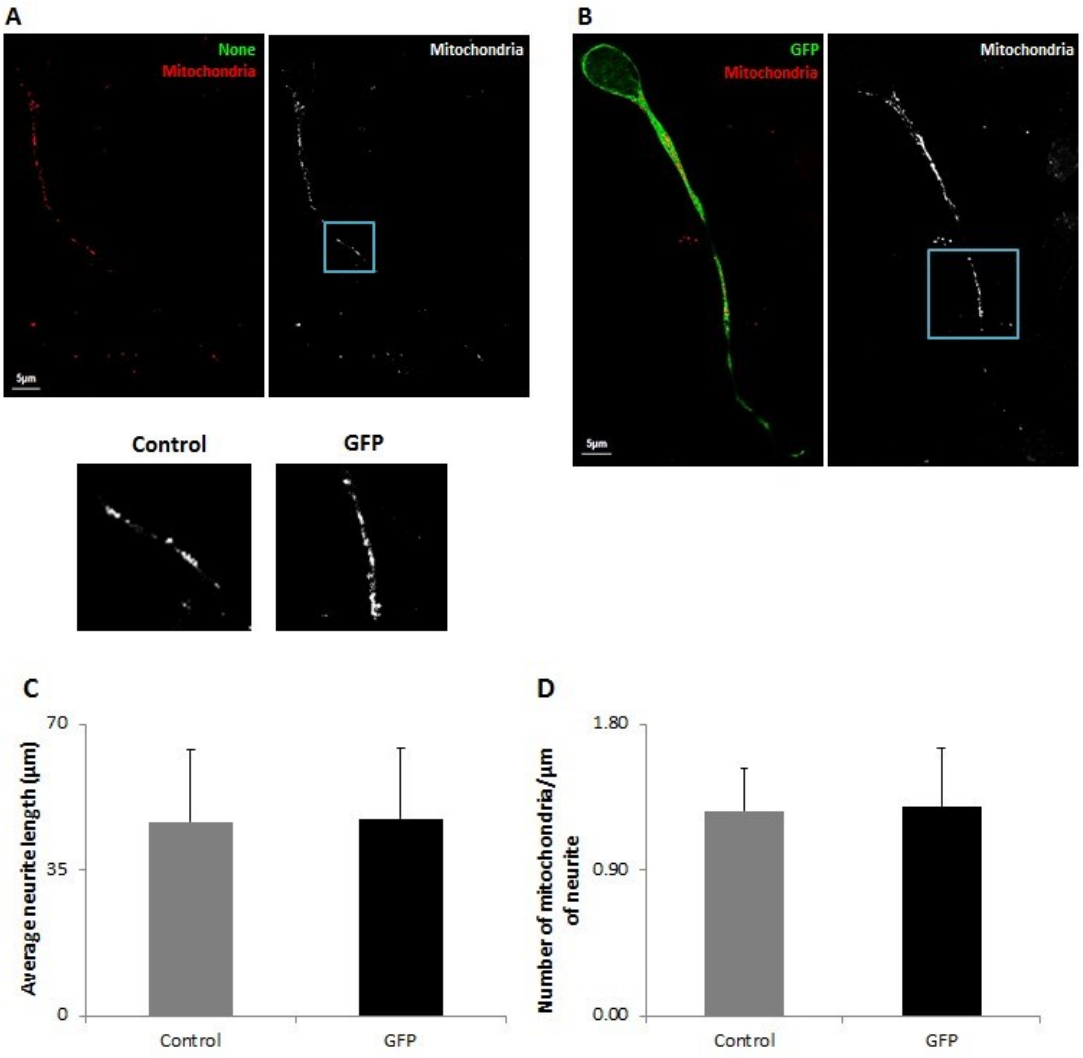

Figure 4.4 Control transfection of HFN with GFP vector. HFNs were co-electroporated with pDsRed2-Mito and pmaxGFP vectors. 24-hour post transfection, cells were fixed and processed for immunofluorescence microscopy. **A**. Neurons that express mitochondrial vector only. Merged channel image shows expression of mitochondrial plasmid but no GFP since only red signal was observed. The black and white image shows mitochondria distribution in the soma and axon of neurons. **B**. Neurons that express both GFP and mitochondrial plasmids. Merged channel image shows expression of both of the plasmids, GFP in green and mitochondria in red. Highlighted area of mitochondrial distribution images in **A** and **B** was enlarged as presented below the top panel. **A**, **B**: scale bar = 5μm. The longest neurite length of each Mito-expressing neuron with or without GFP was measured using Adobe Photoshop (Table 2.11), as well as the count of

mitochondria in each of its neurites. **C**. Quantification of average length of the neurite. **D**. Quantification of the number of mitochondria per unit length of the neurite. **C**, **D**: n=10.

To examine cellular alteration caused by abnormal protein-level and activity of Rab32, human or rat neurons were electroporated with either WT, shRNA, dominant active Q85L mutant or dominant negative T39N mutant plasmids. In each transfection group, tens of neurons expressing mitochondrial plasmid with or without Rab32 protein signal were captured for further study. Some of these cells appeared to be transected in the images. This was due to overlapping of the cells, which caused them to be partially covered. To evaluate neuronal growth and mitochondria distribution, respectively, for each transfected neuron captured, the length of the longest neurite and the count of mitochondria per unit length in the same neurite were measured.

As observed in most transfected neurons, mitochondria were evenly distributed throughout the neurite (Fig. 4.5-4.8). In the enlarged region of interest (ROI) of mitochondria, a relative decrease of their size was observed in Rab32Q85L transfected neurons (Fig. 4.5B) but not in others (Fig. 4.6-4.8B) compared to corresponding negative controls (Fig. 4.5-4.8A), suggesting induced mitochondria fragmentation associated with activation of Rab32.

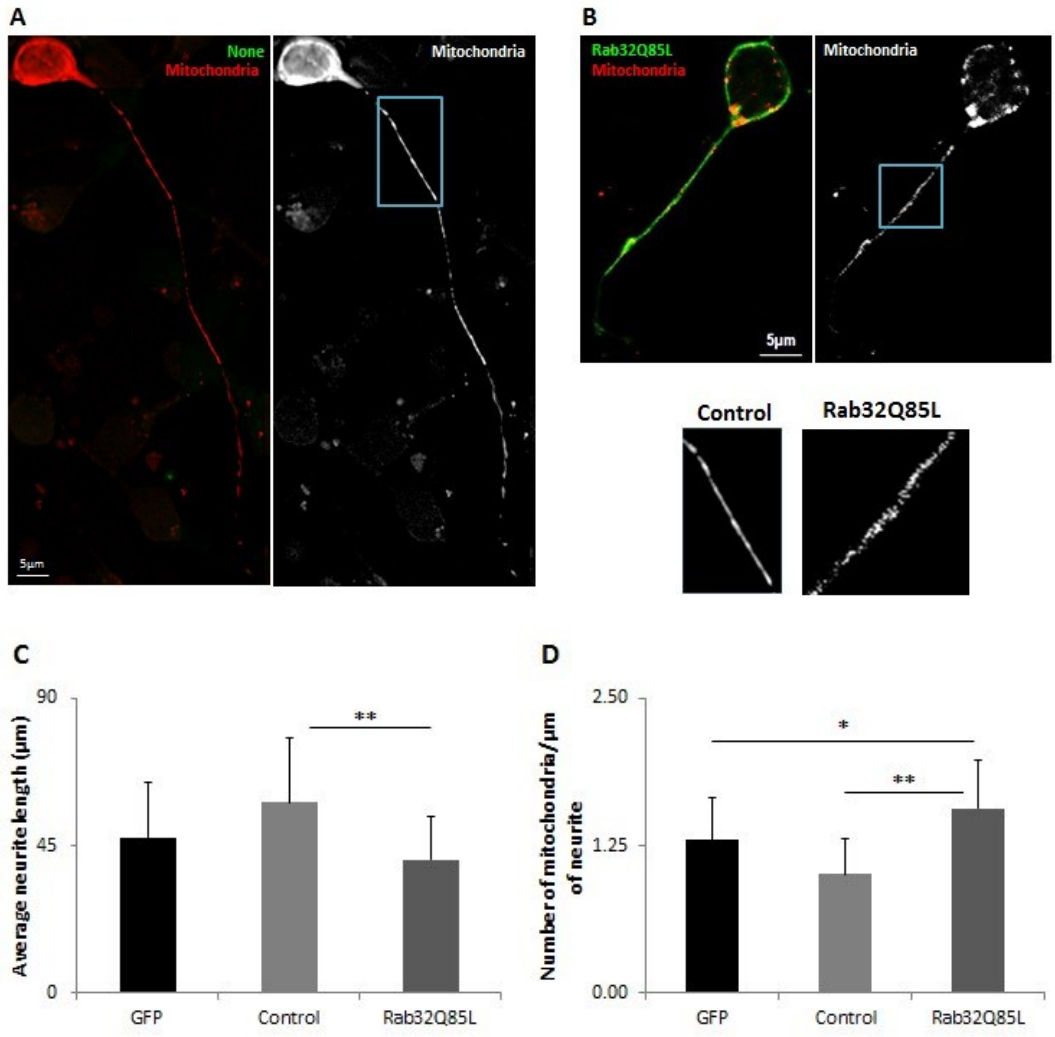

Figure 4.5 Activation of Rab32 inhibits neurite outgrowth and induces mitochondria fragmentation in human neurons. HFNs were co-electroporated with pDsRed2-Mito and dominant active Rab32 Q85L plasmids. 24-hour post transfection, cells were fixed and processed for immune-staining and fluorescence microscopy. **A**. Neurons that express mitochondrial vector only. Merged channel image shows expression of mitochondrial plasmid but no Rab32Q85L since only red signal was observed. The black and white image shows mitochondria distribution in the soma and axon of neurons. **B**. Neurons that express both Rab32Q85L and mitochondrial plasmids. Merged channel image shows expression of both of the plasmids, Rab32Q85L in green and mitochondria in red. Highlighted area of mitochondrial distribution images in **A** and **B** was enlarged as presented below the top panel. **A**, **B**: scale bar = 5μm. The longest neurite length of each Mito-expressing neuron with or without Rab32Q85L was measured as well as the count of mitochondria in each of its neurites. **C**. Quantification of average length of the neurite.

GFP was used as an alternative control. **D**. Quantification of the number of mitochondria per unit length of the neurite. **C**, **D**: n=16; *p<0.05, **p<0.01.

Quantitative analysis of neurite length showed significant difference along with overexpression and/or activation of Rab32 in comparison with negative controls (Fig. 4.5&4.6), where neuron growth was promoted with high-level of Rab32 (Fig 4.6C) but was inhibited in Rab32-activated neurons (Fig. 4.5C). However, these effects were really mild when comparing to GFP control. Thus, the effect of abnormal Rab32 expression and activity on neuron growth is not clear and needs further analyses.

Moreover, an increased number of mitochondria was observed in neurites expressing over-activated Rab32 compared to both controls (Fig. 4.5D). In contrast, a reduction of mitochondria count was present in neurites expressing inactive Rab32 when compared to its negative control, while this reduction disappeared when compared to GFP control (Fig. 4.7D). In other transfected neurons, no significant effect was present in mitochondrial distribution within the neurites (Fig. 4.6&4.8D). In conclusion, these results imply that Rab32 over-activation plays an important role in regulating mitochondrial fragmentation and distribution in neurons, and affects neurite outgrowth. Overexpression or inactivation of this protein was shown to contribute to similar alterations of neurons but the effect was not significant.

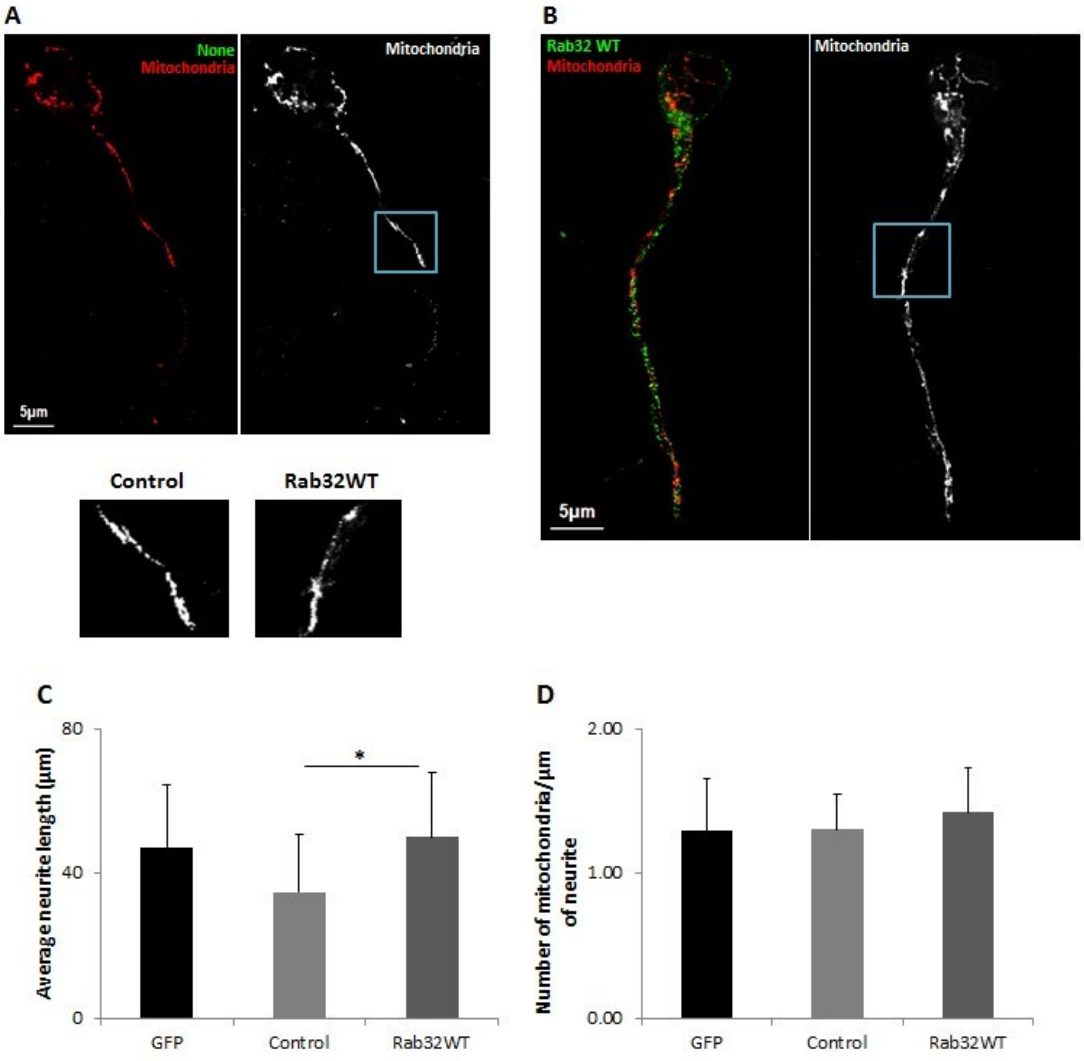

Figure 4.6 Overexpression of Rab32 has moderate effect on neurite outgrowth but not mitochondrial distribution. HFNs were co-electroporated with pDsRed2-Mito and Rab32 WT plasmids. 24-hour post transfection, cells were fixed and processed for immune-staining and fluorescence microscopy. **A**. Neurons that express mitochondrial vector only. Merged channel image shows expression of mitochondrial plasmid but no Rab32WT since only red signal was observed. The black and white image shows mitochondria distribution in the soma and axon of neurons. **B**. Neurons that express both Rab32WT and mitochondrial plasmids. Merged channel image shows expression of both of the plasmids, Rab32WT in green and mitochondria in red. Highlighted area of mitochondrial distribution images in **A** and **B** was enlarged as presented below the top panel. **A**, **B**: scale bar = 5µm. The longest neurite length of each Mito-expressing neuron with or without Rab32WT was measured as well as the count of mitochondria in each of its

neurites. **C**. Quantification of average length of the neurite. GFP was used as an alternative control. **D**. Quantification of the number of mitochondria per unit length of the neurite. **C**, **D**: n=12; **p*<0.05.

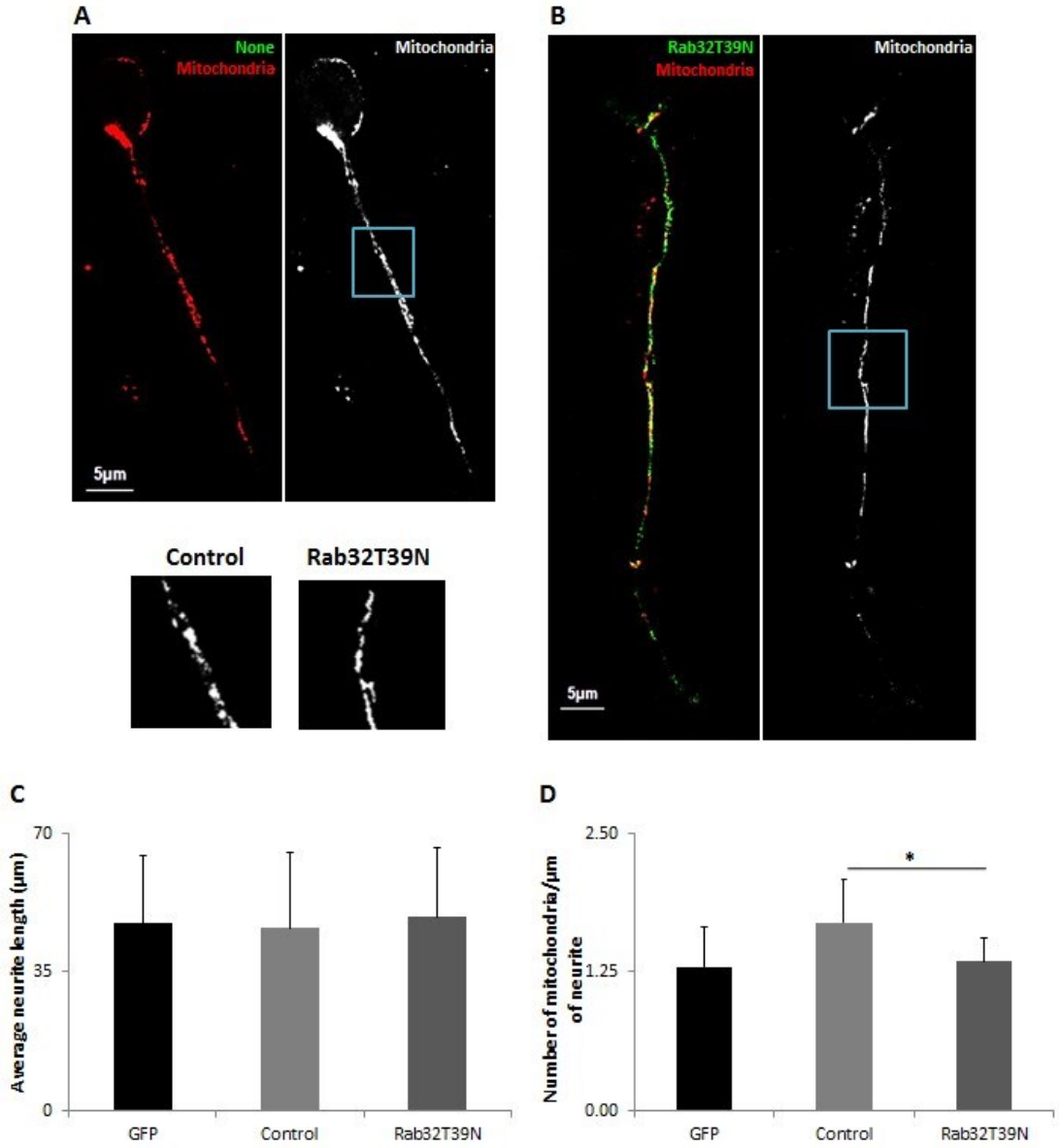

Figure 4.7 Inactivation of Rab32 has moderate effect on mitochondrial distribution but not neuron morphology. HFNs were co-electroporated with pDsRed2-Mito and dominant negative Rab32 T39N plasmids. 24-hour post transfection, cells were fixed and processed for immune-staining and fluorescence microscopy. **A**. Neurons that express mitochondrial vector only. Merged channel image shows expression

of mitochondrial plasmid but no Rab32T39N since only red signal was observed. The black and white image shows mitochondria distribution in the soma and axon of neurons. **B**. Neurons that express both Rab32T39N and mitochondrial plasmids. Merged channel image shows expression of both of the plasmids, Rab32T39N in green and mitochondria in red. Highlighted area of mitochondrial distribution images in **A** and **B** was enlarged as presented below the top panel. **A**, **B**: scale bar = 5μm. The longest neurite length of each Mito-expressing neuron with or without Rab32T39N was measured as well as the count of mitochondria in each of its neurites. **C**. Quantification of average length of the neurite. GFP was used as an alternative control. **D**. Quantification of the number of mitochondria per unit length of the neurite. **C**, **D**: n=11; *p<0.05.

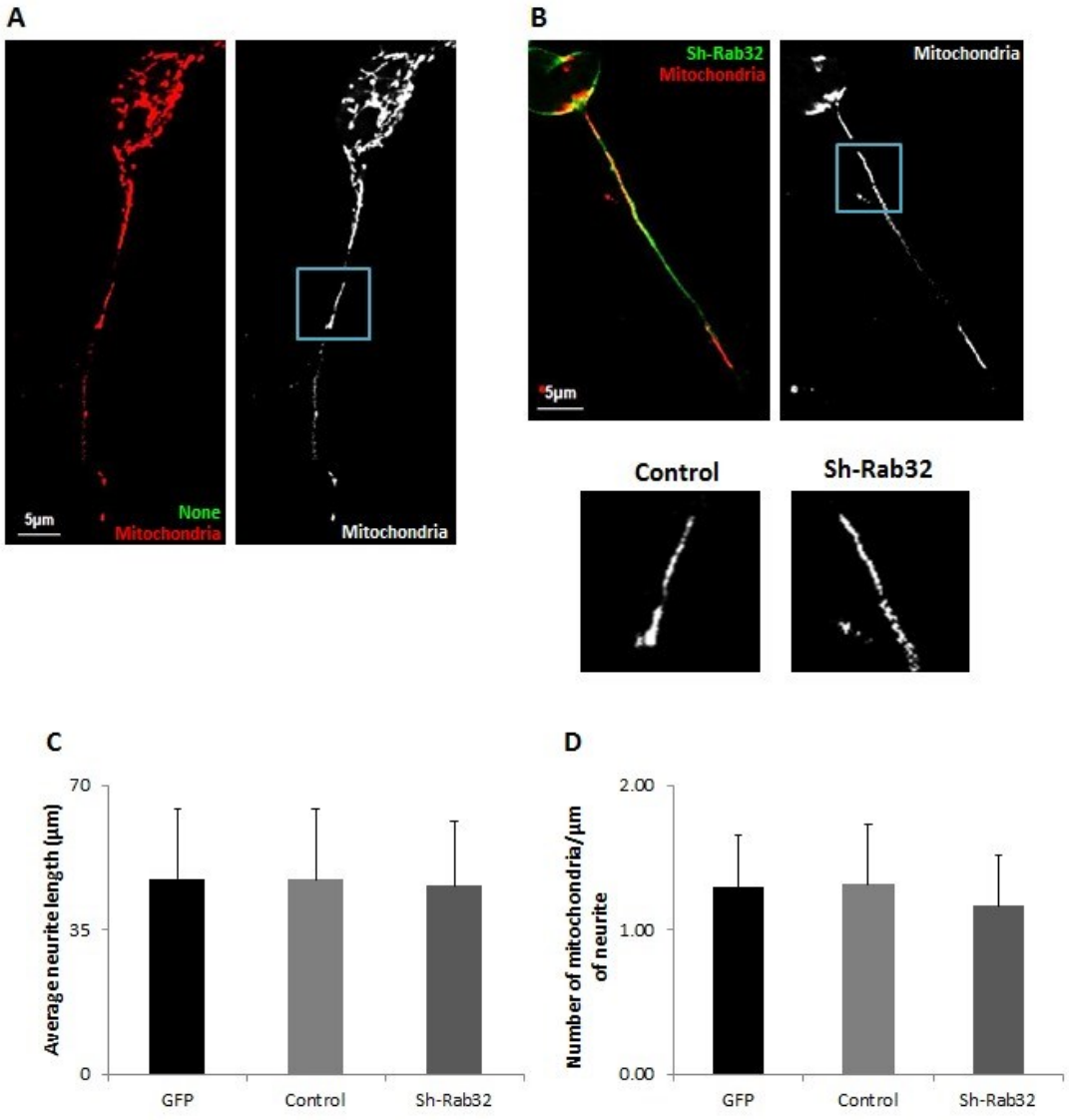

Figure 4.8 Depletion of Rab32 has no significant effect on neuron morphology and mitochondria distribution. HFNs were co-electroporated with pEYFP-Mito and sh-Rab32 plasmids. 24-hour post transfection, cells were fixed and processed for immunofluorescence microscopy. For consistency, signal color of each plasmid was interconverted as described in section 2.2.5.3. **A**. Neurons that express mitochondrial vector only. Merged channel image shows expression of mitochondrial plasmid but no sh-Rab32 since only red signal was observed. The black and white image shows mitochondria distribution in the soma and axon of neurons. **B**. Neurons that express both sh-Rab32 and mitochondrial plasmids. Merged channel image shows expression of both of the plasmids, sh-Rab32 in green and mitochondria in red. Highlighted area of mitochondrial distribution

images in **A** and **B** was enlarged as presented below the top panel. **A**, **B**: scale bar = 5μm. The longest neurite length of each Mito-expressing neuron with or without sh-Rab32 was measured as well as the count of mitochondria in each of its neurites. **C**. Quantification of average length of the neurite. GFP was used as an alternative control. **D**. Quantification of the number of mitochondria per unit length of the neurite. **C**, **D**: n=11.

In addition, rat cortical neurons were transfected with sh-Rab32 plasmid to compare and verify the findings in human neurons. Rat neurons transfected with small hairpin RNA vector were used as the only control instead of GFP control. In observation, both vector and sh-Rab32 transfected neurons were in low viability whose mitochondria were evenly distributed but more abundant in the region of neurites close to soma (Fig. 4.9A&B). It is worth noting that Rab32-depleted neurons grew in a sub-healthy status with relatively shorter neurites compared to the control (Fig. 4.9C). Mitochondria were distantly distributed in these neurites but the effect was not statistically significant (Fig. 4.9D). Moreover, by measuring and comparing the size (length) of individual mitochondrion within the neurites, its difference between Rab32 knock-out and control neurons was not significant (Fig. 4.9E). More than half of mitochondria were shorter than 0.5 μm in Rab32-depleted neurons, whereas less than half was shorter in control neurons (Fig. 4.9F). Thus, depletion of Rab32 protein could have a more severe effect on mitochondrial dynamics and growth of rat neurons when compared to human neurons.

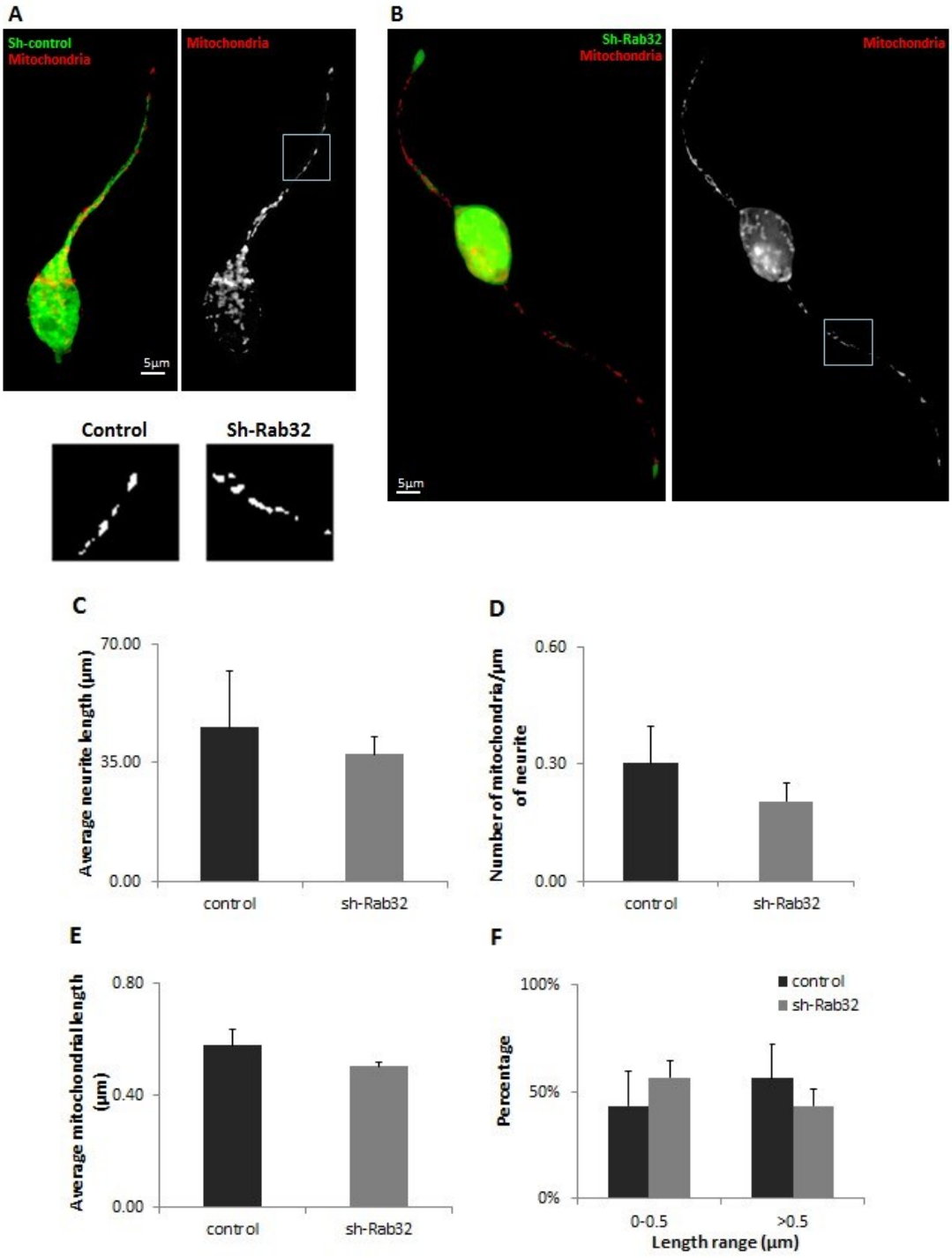

Figure 4.9 Mitochondrial distribution and morphology are relatively preserved in Rab32-depleted rat neurons. Rat cortical neurons were co-electroporated with pDsRed2-Mito and either sh-Rab32 (rat, Table 2.6) or sh-control (rat, Table 2.6) plasmids. 72-hour post transfection, cells were fixed and processed for immunofluorescence microscopy. **A**. Neurons that express sh-control and mitochondria plasmids. Merged

channel image shows expression of both of the plasmids, sh-control in green and mitochondria in red. The black and white image shows mitochondria distribution in soma and axon of neurons. **B**. Neurons that express both Rab32sh-Rab32 and mitochondria plasmids. Merged channel image shows expression of both of the plasmids, sh-Rab32 in green and mitochondria in red. Highlighted area of mitochondrial distribution images in **A** and **B** was enlarged as presented below the top panel. **A**, **B**: scale bar = 5μm. The longest neurite length of each Mito-expressing neuron with sh-control or sh-Rab32, the count of mitochondria and the length of mitochondria in each of these neurites were measured. **C**. Quantification of average length of the neurite. **D**. Quantification of the number of mitochondria per unit length of the neurite. **E**. Quantification of average length of mitochondria in the neurite. **F**. Quantification of proportion of mitochondria with the length less or over than 0.5μm in each transfection group. Percentage was calculated according to the following formula: Percentage of less than 0.5 μm length of mitochondria = (number of mitochondria with length shorter than 0.5 μm in the longest neurite) / (total number of mitochondria in this neurite). **C**, **D**, **E**, and **F**: n=5.

4.2.1.3 Long-term effect of Rab32and its mutants on neuron survival.

Rab32 protein is also identified to regulate cell apoptosis through multiple mechanisms [136]. One of the possible mechanisms is the regulation of calcium transport at MAM and subsequent metabolic activities of mitochondria, including ATP production [136]. Other mechanisms involve calnexin relocation-signaling cascades inducing apoptotic reactions and up-regulation of apoptotic markers [136].

To examine long-term effects of Rab32 on the induction of neuronal apoptosis, a timeline experiment was performed. Rab32 WT, Rab32 Q85L, Rab32 T39N and sh-Rab32 plasmids were used as different transfection groups and GFP vector as a control (Fig. 4.10A, vertically). Four time points were selected to measure cell viability after transfection, which were 24, 40, 48 and 72 hours (Fig. 4.10A, horizontally). The viability at each time point was quantitatively analyzed with a normalization and a correction

based on total cell number and positive cell number at 24 hours. Details are described in figure 4.10 legend. It was observed that either activation or inactivation of Rab32 promoted neuronal death as early as 48 hours after the insertion of the plasmids (Fig. 4.10B). Overexpression of this protein showed an effect on neuronal killing at 72 hours (Fig. 4.10B). However, no significant effect was observed on neuronal viability in GFP control and Rab32-depletion groups (Fig. 4.10B). Thus, these findings suggest that Rab32 plays a role in accelerating neuronal apoptosis.

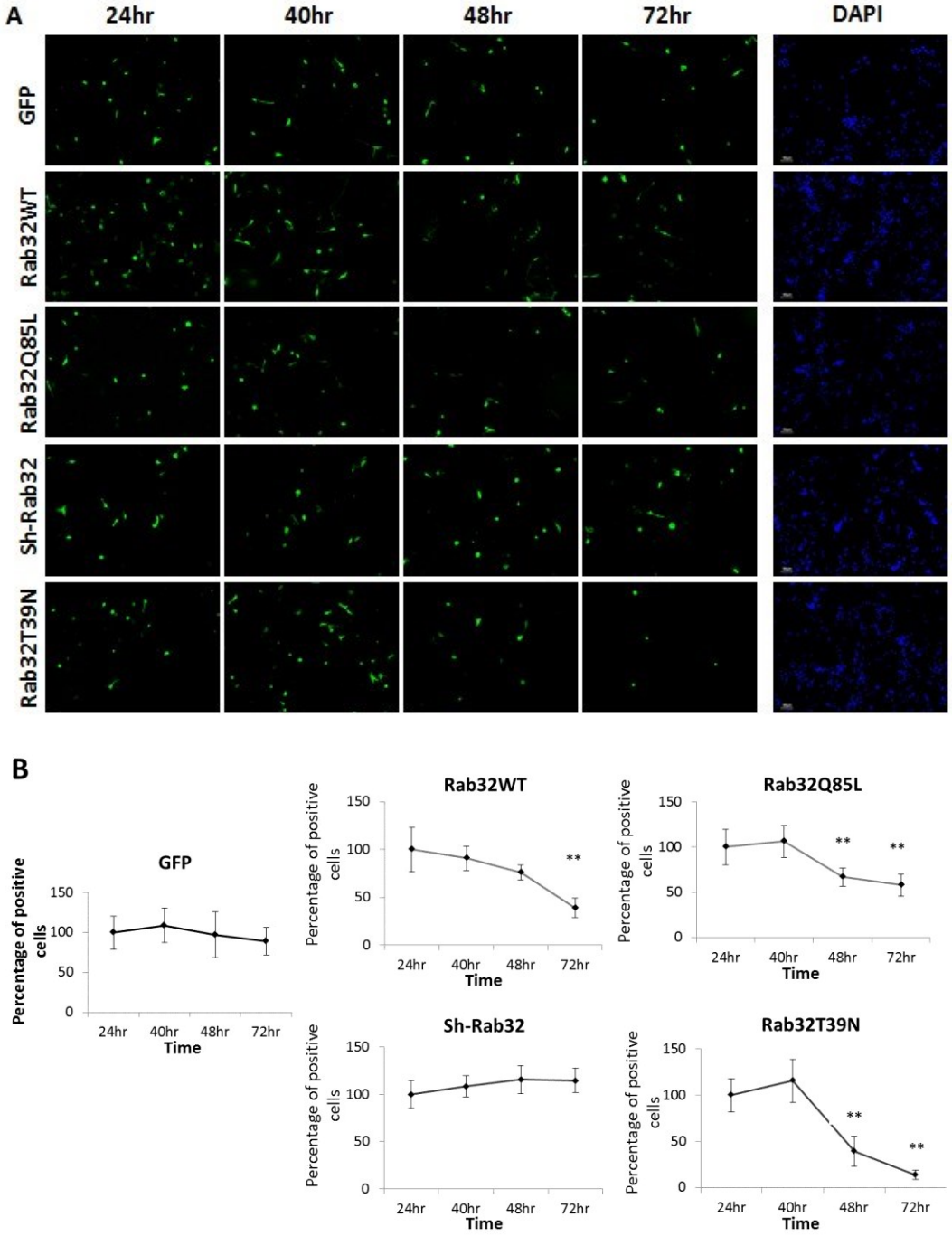

Figure 4.10 Viability of neurons expressing different mutants of Rab32. HFNs were co-electroporated with either pmaxGFP, Rab32 WT, Rab32 Q85L, sh-Rab32 or Rab32 T39N plasmids. 24-hour, 40-hour, 48-hour or 72-hour post transfection, cells were fixed and processed for immune-staining and fluorescence microscopy. **A**. Viability of neurons transfected with each plasmid at different time points. Transfection groups with different plasmids are displayed vertically and time points are arranged horizontally.

Viability is estimated by number of transfected cells with green signal in each picture. DAPI stain shows total number of cells in each transfection group at 24 hours. Scale bar = 50μm. **B**. Quantification of time-dependent viability of transfected cells. Under 20x magnification, ten positions were randomly selected for each transfection group at each time point. Normalization factor (nf) for each transfection group was calculated: nf = (total cell number at 24 hour) / (total cell number at any time points). Normalized number of transfected cells representing cell viability was calculated by multiplying observed number of transfected cells with nf at each time point. Normalized cell number at 40, 48 and 72 hours were then evaluated based on that at 24hr by taking the ratio: percentage of positive cell = (normalized cell number at any time points) / (normalized cell number at 24hr), thus to indicate the variation of positive cell count since initial time-point (100% at 24hr). The percentages were plotted in y-axis and time points in x-axis. n=10; $**p<0.01$.

4.3 SUMMARY

Rab32 protein possibly has different functions in different cell types [151, 152]. In this part of the project, I found that Rab32 has similar function in regulating mitochondrial dynamics and cell apoptosis to that observed in human cancer cell lines [136]. Dominant-activation of Rab32 protein had a significant effect on mitochondrial fragmentation and distribution and neurite outgrowth while these cellular mechanisms were barely affected by other Rab32 mutants. Moreover, the alteration of protein expression and activity showed long-term effect on neuronal viability, suggesting a role of Rab32 in neurodegenerative mechanisms and progression of MS. To sum up, I suggest that Rab32 is a potential bio-marker and target in MS pathology and therapeutic treatments.

CHAPTER 5:

Discussion and Future Directions

5. DISCUSSION AND FUTURE DIRECTIONS

5.1 DISCUSSION

5.1.1 Rab32 protein expression is altered in MS brain tissue

Our results demonstrated that Rab proteins, Rab32, Rab38 and Rab7L1, were present in MS patient brains and the level of expression varied according to the inflammatory status of the tissue. This finding suggests a potential role of Rab32 family proteins in the pathology of MS in response to inflammation. Furthermore, Rab32 protein is up-regulated in association with high-level ER stress within active lesions where inflammation and immune cell infiltration dominate, implying a potential involvement of Rab32 in inflammation-associated ER stress and downstream mechanisms. However, in chronic lesions, Rab32 protein-level decreased under preserved high-level ER stress. A possible explanation could be that, in these lesions, the massive loss of neurons and other CNS cells could be due to activation of apoptosis through other mediator pathways and necrosis. Indeed, infiltrating activated immune cells gradually diffuse into the surrounding NAWM as disease progresses, leading to induced inflammation in NAWM rather than in chronic lesions [84, 117]. However, in the central area of chronic lesions, active inflammation becomes rare and severe tissue disruption takes place instead [84, 117]. Thus, in place of an up-regulation in the center of chronic lesions, the relative high-level of Rab32 in chronic NAWM represents inflammation diffusion, which confirms some of the MRI results observed in MS patient brains [153]. Furthermore, in MS brain tissues, Rab32 co-localizes with ER stress and apoptotic marker CHOP at active inflammatory region of lesions. These results are suggestive of a primary function of

Rab32 in the initiation of ER stress-mediated cell apoptosis in response to high-level inflammation.

Intriguingly, a recent study on acute inflammation in mouse brain represented a potential relationship between Rab32 protein and inflammation. They found that Rab32 protein was substantially up-regulated during the acute phase of inflammation in response to pro-inflammatory cytokines and returned to a relatively normal level after early inflammation [147]. However, the experiments in this study [147] were performed only for a 24-hour-period and were not reflective of the chronic inflammatory responses occurring in most MS brains. In chronic disease stages, Rab32 expression is down-regulated within lesions compared to the NAWM, suggesting a relatively slow and inactive apoptotic status and degeneration of large amount of CNS cells. My findings showing that Rab32 protein expression is elevated in the active stage of acute lesion and depressed in the chronic lesions, are suggestive of a role of Rab32 protein in the early disease progression following the initial inflammation in MS. Furthermore, the increment and reduction of Rab38 protein suggests a potentially similar role to Rab32.

In addition to the previous observations, Rab32 was found to be mainly up-regulated in swollen axons at the active inflammatory lesion border, indicating its contribution to the early axonal injury in MS neuropathology. Accumulation of axonal loss subsequently leads to neurodegeneration and irreversible neurological disability in MS. The immune-staining data of expression localization of Rab32 in MS brain tissue and its up-regulation in neurons of active inflammatory MS lesions are highly suggestive of a potential role of Rab32 in neurodegenerative progression of MS in response to inflammation.

A mechanism can be proposed based on the available literature and my findings. The infiltration and activation of immune cells induce neuroinflammation in acute lesions or surrounding NAWM of chronic lesions within MS brains. Under the attack of activated immune cells, CNS resident cells activate BiP signaling pathways in ER to coordinate the extracellular stress conditions. The activation of these pathways, as an indicator of induced ER stress, signals a cascade of events to accelerate the production of ER chaperones, such as XBP-1 and BiP, involved in the quality-control cycle in the attempt to rescue the cell. However, sensing irreversible signal of prolonged ER stress, cell starts cascades of reactions that will lead to cell death in response to inflammatory environment. The elevated synthesis and release of the ER stress-associated pro-apoptotic marker CHOP blocks transcription of several genes crucial to cell metabolism and survival, subsequently inducing cell apoptosis. Meanwhile, induction and activation of Rab32 in response to long-term ER stress indirectly lead to cell death through impaired mitochondrial dynamics and function.

5.1.2 Rab32 protein alters cellular metabolism and mitochondrial distribution in neurons

My results from the intracellular studies in rat and human neurons indicated cellular alterations associated with abnormal expression and activity of Rab32. Over-activation of Rab32 was shown to significantly increase mitochondrial number in neurons through a mechanism of increased fragmentation. Inhibition of Rab32 activity reduced mitochondrial count and relatively protected mitochondria against fragmentation, which was in agreement with the finding in Hela cells where dominant negative Rab32 mutant

caused phosphorylation and inactivation of Drp1 [136]. However, depletion of Rab32 protein in human neurons had less obvious effect on mitochondrial morphology and distribution whereas the influence became apparent in rat neurons. This suggests the presence of other proteins functionally related to Rab32 in human neurons. On the other hand, in rat neurons, Rab32 plays a dominant role in these mechanisms. Thus, inhibition of Rab32 production is possibly a therapeutic target for treating neurodegeneration in MS patients caused by overexpression and abnormal activity of Rab32.

An interesting phenomenon of mitochondria content in response to demyelination and remyelination in MS brain tissue was observed by Zambonin *et al.* Their findings indicated that axonal content of mitochondria, including size and number, was significantly induced in demyelinated axons, while remyelination of these axons did not recover mitochondrial content with preserving high-level of mitochondrial number [74]. This suggests that mitochondrial dynamics are impaired independently of myelin and remyelination does not affect neurodegeneration in MS. Thus, understanding the mechanisms of mitochondrial axonal transportation in neurons, a mechanism that could be impaired in MS, would contribute to better understanding the pathological alterations at disease onset and shed new light on a potential treatment target for MS.

Mitochondrial-ER membrane associated proteins are well positioned to play a key role in coordinating and regulating diverse mitochondrial functions [154]. It is not surprising that the Rab32 protein, which is mostly ER and mitochondrial membrane associated [136], performs numerous organelle related functions, including regulation of mitochondrial fission [137], modulation of ER calcium handling and disruption of specific enrichment of calnexin on the mitochondria-associated membrane [136],

regulating ER stress-associated and mitochondrial impairment-triggered cell apoptosis [136], and microtubule-based mitochondrial transportation [134]. My data from the intracellular studies indicate a consistent appearance of abnormal mitochondria morphology and distribution in neurons with overexpression of dominant-active Rab32 protein, and the impaired mitochondrial dynamics affected neurite outgrowth and the phenotype to a certain extent. These results suggest an energy deficit status of these neurons characterized by smaller and disoriented mitochondria and inhibited growth. These observations are in agreement with the finding of energy deficiency described in Hela cells associated with diminished mitochondrial membrane potential (unpublished data). Accordingly, it is conclusive that Rab32 protein is essential to maintain regular mitochondrial functions, and the impairment of mitochondrial dynamics in neurons of MS patients is potentially related to Rab32 protein alterations.

Moreover, the timeline experiment performed to examine cell viability showed long-term effect in neurons. Induced mortality in neurons with altered activity of Rab32 showed toxicity of these mutants potentially related to the impairment in mitochondrial dynamics. In addition, overexpression of this protein induces cell death in the long-term, suggesting a vital role of Rab32 in preserving normal cellular activities and neuronal survival. I observed that, in neurons overexpressing Rab32, neurite outgrowth was transiently enhanced. Thus, linking to my finding that Rab32 overexpression accelerates neuronal apoptosis in the long-term, it is possible that this protein is involved in multiple pathways and regulates neuron growth and death in a time-dependent manner.

According to the literature and published protocols, transfected neurons using the nucleofector system were ready for analysis as early as 24 hours. This time point was

applied in our study to analyze intracellular alteration such as mitochondrial morphology and distribution. A long-term analysis over 40 hours post-transfection is not suggested because of induced cell apoptosis in some transfection groups leading to a decrease in sample sizes and missing information at onset. However, a time course experiment is important to study Rab32 alteration and function in MS disease progression. MS is a chronic inflammatory disease where inflammation triggers a slowly progressing neuronal death and tissue damage. Prolonged effect of Rab32 on neuron viability was comparable with the chronic progression of MS, indicating a potential role of this protein in linking early CNS inflammation with late-stage neurodegeneration in this disease.

5.1.3 Genetic association of Rab protein family with MS

There is a risk gene identified in MS whose protein product has a Rab-GTPase regulatory activity, which may be related to the variation of Rab protein levels in MS brain tissues. A recent GWAS study conducted by the International Multiple Sclerosis Genetics Consortium has identified a number of putative MS susceptibility genes [155]. Among them, 21 SNPs that are located in the GFI1-EVI5-RPL5-FAM69A locus, and the ecotropic viral integration site 5 (EVI5) is the most likely candidate as a risk gene for MS [48, 156, 157]. EVI5 gene encodes Evi5 protein homolog which has a domain stimulating and up-regulating Rab GTPases activity, termed as GTPase-activating protein (GAP). Evi5 protein is mostly known as a Rab11-GAP [158] while it targets several other Rab proteins including Rab5 [159], Rab6 [159], Rab10 [160], Rab23 [161] and Rab35 [162] *in vitro*. Although there was no evidence showing a regulatory function of Evi5 protein on Rab32, Rab38 or Rab7L1, indirect regulation might exist due to its multi-targeting

property. Evi5 is also a nuclear zinc-finger protein that functions as a transcriptional repressor that is possibly a part of the centrosome stability and dynamics [156]. This suggested a potential regulatory role of Evi5 protein in the transcription of functional membrane associated motor proteins, and implied a possibility of Evi5 in modulating mitochondrial movement and distribution in neurons. Moreover, another possibility of EVI5 in MS is that it facilitates the regulation at genetic level, where EVI5 gene may modulate alternative transcription of the other MS risk genes.

5.1.4 Potential impairment of mitochondrial dynamics in MS brain tissue

Another protein functionally related to Rab32 in regulating mitochondrial dynamics is Drp1. Drp1 is highly expressed in neurons compared to other types of cells [94] and regulates mitochondrial fission associated with neuronal apoptosis [163]. Rab32 regulates the activation of Drp1 thus indirectly modulates mitochondrial dynamics [136]. Interestingly, alterations of Drp1 expression in MS brain tissues showed the same tendency as Rab32 in both acute and chronic samples, suggesting a partnership of these two proteins in cellular mechanisms. Another mitochondrial dynamics-related protein, Mfn2, showed similar change of its expression as Drp1 in MS tissues, which indicated dysfunction of mitochondria dynamics in MS patient brains in response to inflammation severity. There is a possibility that the reduction of Rab32 and Drp1 in chronic lesion is related to the significant loss of neurons and the deficit of functional cellular proteins in the late-stage chronic MS brain. Even though the mechanism of Rab32 protein in neurons is not clear, it is noteworthy that Rab32 proteins have potential roles in regulation of mitochondrial mobility and inflammatory-induced neuronal apoptosis in MS.

5.2 LIMITATIONS

There were limitations in my experiments and the way data was collected. High cell viability was achieved through modification of transfection conditions, whereas the transfection efficiency of primary neurons was consistently low and further modification of the technique is needed for improvement. Also, the standard deviations were relatively large in the statistical analysis of the data. One reason could be that there are multiple populations of neurons in the cortex and it is hard to differentiate these populations only through neuron morphology. A large sample size could not be achieved by considering only one population of neurons under very low transfection efficiency, leading to less significant difference between treatment groups. The short growth period of neurons for only 24 hours might not allow a notable variation in mitochondrial phenotype as a consequence of the Rab32 dysfunction. However, long-term treatment led to death of transfected neurons caused by toxicity of expressing plasmid and was not suitable for evaluating cellular alteration at early-stage. The transfection techniques and cut-off time need to be improved and deliberated to obtain more analyzable data.

In addition, detection of Rab32 expression was performed in a limited number of MS cases without healthy control cases due to shortage of post-mortem tissue. Increasing the sample size of each type of lesion and incorporating healthy controls are among the steps that could be taken to obtain statistically analyzable data.

5.3 CONCLUSIONS

Rab32 family proteins were detected in human MS brain and their expression level varied with different pathological conditions. Rab32 protein-level was induced in association with inflammation severity in MS lesion tissues in response to prolonged ER stress. In these tissues, Rab32 was observed to co-localize with ER stress and apoptotic marker at the active lesion border, emphasizing that its metabolic mechanism was related to both ER and inflammation. These results suggested a role of this protein in inflammation-initiated and ER stress-induced cell apoptosis during MS progression. Furthermore, the observed localization of Rab32 within neurons in the same lesion tissue indicated possible contribution of this protein in neurodegenerative mechanism in MS leading to permanent disabilities and death of patients.

Dominant-active Rab32 protein had a significant effect on mitochondrial distribution and neurite outgrowth while these cellular mechanisms were affected moderately by other Rab32 mutants. It was shown that mitochondria were fragmented and crowded in Rab32-activated neurites. These neurites were shorter in length, suggesting inhibited neuron growth caused by mitochondrial impairment. When neuron expressed inactivated Rab32, mitochondria tended to distribute further in the axons. Moreover, alteration of Rab32 expression and activity showed long-term effect on neuron viability. Over- or under-activation of Rab32 caused induction in cell apoptosis since 48 hours post-transfection, while this decreased viability was observed in neurons overexpressed Rab32 at 72 hours post-transfection. This is suggestive of a role of this protein in neurodegenerative pathways and chronic progression of MS. Thus, Rab32 is likely a potential bio-marker and therapeutic target in MS pathology and treatments.

5.4 FUTURE DIRECTIONS

Our exciting results are encouraging and they inspire many potential new experiments to further understand the mechanism of Rab32-regulated mitochondrial dynamics and neuronal apoptosis in MS.

Firstly, a better human cell model can be introduced with relative consistency in neuron morphology and mimicry of brain environment, such as induced pluripotent stem cells (iPSC) [164]. This type of stem cell can be obtained and derived from fibroblasts [164] or white blood cells [165] of MS patients and it is able to be differentiated into different types of CNS cells. A mixed culture of iPSC-derived CNS cells from MS patients can preserve genetic information while presenting cellular alterations caused by single protein mutation, such as Rab32, and external variations, such as inflammation. Other good human neuronal models, such as dorsal root ganglion (DRG) neurons, are good for their stable morphology and large size of axons, thus can make observing mitochondrial alterations more steadily and easily.

Moreover, MS animal models such as EAE should be included to study behavioral and pathological changes caused by alteration of our target protein. We could try to develop different types of Rab32 transgenic mouse and incorporate techniques of humanized immune system [166], and study pathological effect of this protein in more complex living organisms. The use of animal model also allows us to mimic the neuroinflammatory condition in MS patients with infiltration of peripheral immune cells and chronic activation of resident microglia, linking Rab32-associated machinery to inflammation in MS directly.

Last but not least, more biological replicates need to be done to further confirm our findings.

BIBLIOGRAPHY

1. Murray, T.J., *The History of Multiple Sclerosis: the Changing Frame of the Disease over the centuries.* J. Neuro. Sci., 2009. **277 Suppl 1**: p. S3-8.
2. Murray, T.J., *Multiple Sclerosis: The History of a Disease*2005, New York: Demos Health. 580.
3. Lassmann, H., *Mechanisms of Neurodegeneration shared between Multiple Sclerosis and Alzheimer's Disease.* J. Neural Transm., 2011. **118**: p. 747-752.
4. Sospedra, M., & Martin, R., *Immunology of multiple sclerosis.* Annu. Rev. Immunol. , 2005. **23**: p. 275-286.
5. Dutta, R., & Trapp, B. D. , *Mechanisms of neuronal dysfunction and degeneration in multiple sclerosis.* Progress in neurobiology, 2011. **93**(1): p. 1-12.
6. Hauser, S.L., & Oksenberg, J. R., *The neurobiology of multiple sclerosis: genes, inflammation, and neurodegeneration.* Neuron, 2006. **52**: p. 61-76.
7. Noseworthy, J.H., *Progress in determining the causes and treatment of multiple sclerosis.* Nature, 1999. **399**: p. A40-A47.
8. Trapp, B.D., & Nave, K. A., *Multiple sclerosis: an immune or neurodegenerative disorder?* Annu. Rev. Neurosci., 2008. **31**: p. 247-269.
9. Weinshenker, B.G., *Natural history of multiple sclerosis.* Ann. Neurol., 1998. **36**: p. S6-S11.
10. Noseworthy, J.H., Lucchinetti, C., Rodriguez, M., & Weinshenker, B. G., *Multiple sclerosis.* N. Engl. J. Med., 2000. **343**: p. 938-952.
11. O'Gorman, C., Lucas, R., & Taylor, B., *Environmental risk factors for multiple sclerosis: a review with a focus on molecular mechanisms.* International journal of molecular sciences, 2012. **13**(9): p. 11718-52.
12. Eikelenboom, M.J., Killestein, J., Kragt, J. J., Uitdehaag, B. M., & Polman, C. H., *Gender Diferences in Multiple Sclerosis: Cytokines and Vitamin D.* J. Neuro. Sci., 2009. **286**(1-2): p. 40-42.
13. Kurtzke, J.F., *Rating Neurologic Impairment in Multiple Sclerosis: an Expanded Disability Status Scale (EDSS).* Neurology, 1983. **33**(11): p. 1444-1452.
14. Compston, A., Confavreux, C., Lassmann, H., McDonald, L., Miller, D., Noseworthy, J., ... Wekerle, H., *McAlfine's Multiple Sclerosis*. 4th ed2006, USA: Elsevier.
15. Fox, R.J., & Cohen, J. A., *Multiple sclerosis: the importance of early recognition and treatment.* Cleve. Clin. J. Med., 2001. **68**: p. 171-175.
16. Lassmann, H., & van Horssen, J., *The molecular basis of neurodegeneration in multiple sclerosis.* FEBS letters, 2011. **585**(23): p. 3715-3723.
17. Beebe, G.W., Kurtzke, J. F., Kurland, L. T., Auth, T. L., & Nagler, B., *Studies on the natural history of multiple sclerosis. 3. Epidemiologic analysis of the army experience in World War II.* . Neurology, 1967. **17**: p. 1-17.
18. Nagata, C., Fujita, S., Iwata, H., Kurosawa, Y., Kobayashi, K., Kobayashi, M., ... Nose, T., et al., *Systemic lupus erythematosus: A case-control epidemiologic study in Japan.* Int. J. Dermatol., 1995. **34**(5): p. 333-337.

19. Compston, A., *Genetic epidemiology of multiple sclerosis.* J. Neurol. Neurosurg. Psychiatry, 1997. **62**: p. 553-561.
20. Kurtzke, J.F., *A reassessment of the distribution of multiple sclerosis. Part one.* . Acta. Neurol. Scand. , 1975. **51**: p. 110-136.
21. Simpson, S., Jr. Blizzard, L., Otahal, P., van der Mei, I., & Taylor, B. , *Latitude is significantly associated with the prevalence of multiple sclerosis: a meta-analysis.* J. Neurol. Neurosurg. Psychiatry, 2011. **82**: p. 1132-1141.
22. Koutsouraki, E., Costa, V., & Baloyannis, S., *Epidemiology of multiple sclerosis in Europe: a review.* Int. Rev. Psychiatry, 2010. **22**: p. 2-13.
23. Ahlgren, C., Lycke, J., Odén, A., & Andersen, O., *High risk of MS in Iranian immigrants in Gothenburg, Sweden.* Multiple Sclerosis, 2010. **16**: p. 1079-1082.
24. Cabre, P., Signate, A., Olindo, S., Merle, H., Caparros-Lefebvre, D., Béra, O., & Smadja, D., *Role of return migration in the emergence of multiple sclerosis in the French West Indies.* Brain, 2005. **128**: p. 2899-2910.
25. Dean, G., & Elian, M., *Age at immigration to England of Asian and Caribbean immigrants and the risk of developing multiple sclerosis.* J. Neurol. Neurosurg. Psychiatry, 1997. **63**: p. 565-568.
26. Gale, C.R., & Martyn, C. N., *Migrant studies in multiple sclerosis.* Prog. Neurobiol., 1995. **47**: p. 425-448.
27. Guimond, C., Dyment, D. A., Ramagopalan, S. V., Giovannoni, G., Criscuoli, M., Yee, I. M., ... Sadovnick, A. D., *Prevalence of MS in Iranian immigrants to British Columbia, Canada.* . J. Neurol., 2010. **257**: p. 667-668.
28. Kahana, E., Alter, M., & Zilbe, N., *Environmental factors determine multiple sclerosis risk in migrants to Israel.* Mult. Scler., 2008. **14**(1): p. S69-S70.
29. McLeod, J.G., Hammond, S. R., & Kurtzke, J. F., *Migration and multiple sclerosis in immigrants to Australia from United Kingdom and Ireland: A reassessment. I. Risk of MS by age at immigration.* J. Neurol., 2011. **258**: p. 1140-1149.
30. Wallin, M.T., Page, W. F., & Kurtzke, J. F., *Migration and multiple sclerosis in Alaskan military veterans.* J. Neurol., 2009. **256**: p. 1413-1417.
31. Hewagama, A., & Richardson, B., *The genetics and epigenetics of autoimmune diseases.* J. Autoimmun., 2009. **33**: p. 3-11.
32. Wallin, M.T., Culpepper, W. J., Coffman, P., Pulaski, S., Maloni, H., Mahan, C. M., Haselkorn, J. K., & Kurtzke, J. F., *Veterans Affairs Multiple Sclerosis Centres of Excellence Epidemiology Group. The Gulf War era multiple sclerosis cohort: Age and incidence rates by race, sex and service.* Brain, 2012. **135**: p. 1778-1785.
33. Munger, K.L., Zhang, S. M., O'Reilly, E., Hernan, M. A., Olek, M. J., Willett, W. C., & Ascherio, A., *Vitamin D intake and incidence of multiple sclerosis.* . Neurology, 2004. **62**: p. 60-65.
34. Munger, K.L., Levin, L. I., Hollis, B. W., Howard, N. S., & Ascherio, A., *Serum 25-hydroxyvitamin D levels and risk of multiple sclerosis.* . J. Am. Med. Assoc., 2006. **296**: p. 2832-2838.
35. Ascherio, A., Munger, K. L., & Simon, K. C., *Vitamin D and multiple sclerosis.* Lancet. Neurol., 2010. **9**(6): p. 599-612.
36. Lonergan, R., Kinsella, K., Fitzpatrick, P., Brady, J., Murray, B., Dunne, C., ... Tubridy, N., *Multiple sclerosis prevalence in Ireland: relationship to vitamin D*

status and HLA genotype. J. Neurol. Neurosurg. Psychiatry, 2011. **82**(3): p. 317-322.
37. Lysandropoulos, A.P., Jaquiery, E., Jilek, S., Pantaleo, G., Schluep, M., & Du Pasquier, R. A., *Vitamin D has a direct immunomodulatory effect on CD8+ T cells of patients with early multiple sclerosis and healthy control subjects.* J. Neuroimmunol., 2010. **233**(1-2): p. 240-244.
38. Solomon, A.J., & Whitham, R. H., *Multiple sclerosis and vitamin D: a review and recommendations.* Curr. Neurol. Neurosci. Rep., 2010. **10**(5): p. 389-396.
39. Marrie, R.A., Horwitz, R. I., Cutter, G., Tyry, T., & Vollmer, T., *Smokers with multiple sclerosis are more likely to report comorbid autoimmune diseases.* Neuroepidemiology, 2011. **36**: p. 85-90.
40. Vessey, M.P., Villard-Mackintosh, L., & Yeates, D., *Oral contraceptives, cigarette smoking and other factors in relation to arthritis.* Contraception, 1987. **35**: p. 457-464.
41. Holt, P.G., *Immune and inflammatory function in cigarette smokers.* . Thorax, 1987. **42**: p. 241-249.
42. Sopori, M., Goud, N., & Kaplan, A., *Effects of Tobacco Smoke on the Immune System*1994, NY, USA: Raven Press: New York.
43. Chen, J.L., Wei, L., Bereczki, D., Hans, F. J., Otsuka, T., Acuff, V., ... Fenstermacher, J. D., *Nicotine raises the influx of permeable solutes across the rat blood-brain barrier with little or no capillary recruitment.* J. Cereb. Blood Flow Metab. , 1995. **15**: p. 687-698.
44. Grunwald, F., Schrock, H., & Kuschinsky, W., *The influence of nicotine on local cerebral blood flow in rats.* Neurosci. Lett., 1991. **124**: p. 108-110.
45. Granieri, E., & Casetta, I. , *Selected reviews common childhood and adolescent infections and multiple sclerosis.* Neurology, 1997. **49**: p. S42-54.
46. Kakalacheva, K., Munz, C., & Lunemann, J. D. , *Viral triggers of multiple sclerosis.* Biochim. Biophys. Acta., 2011. **1812**: p. 132-140.
47. Djelilovic-Vranic, J., & Alajbegovic, A., *Role of early viral infections in development of multiple sclerosis.* Med. Arh., 2012. **66**: p. 37-40.
48. Baranzini, S.E., & Nickles, D. , *Genetics of multiple sclerosis: swimming in an ocean of data.* Current opinion in neurology, 2012. **25**(3): p. 239-245.
49. Ebers, G.C., Bulman, D. E., Sadovnick, A. D., Paty, D. W., Warren, S., Hader, W., ... Brunet, D., *A population-based study of multiple sclerosis in twins.* N. Engl. J. Med., 1986. **315**: p. 1638-1642.
50. Oksenberg, J.R., & Baranzini, S. E., *Multiple sclerosis genetics--is the glass half full, or half empty?* Nature reviews: neurology, 2010. **6**(8): p. 429-437.
51. Damal, K., Stoker, E., & Foley, J. F., *Optimizing therapeutics in the management of patients with multiple sclerosis: a review of drug efficacy, dosing, and mechanisms of action.* Biologics, 2013. **7**: p. 247-258.
52. Minagar, A., *Current and Future Therapies for Multiple Sclerosis.* Scientifica (Cairo), 2013(2013): p. 249101.
53. Granger, D.N., & Senchenkova, E., *Inflammation and Microcirculation*2010, San Rafael (CA): Morgan & Claypool Life Sciences.
54. Scott, A., Khan, K. M., Cook, J. L., & Duronio, V., *Waht is "Infllamtion"? Are We Ready to Move Beyond Celsus?* Br. J. Sports Med., 2004. **38**: p. 248-249.

55. Van Lint, P., & Libert, C., *Chemokine and cytokine processing by matrix metalloproteinases and its effect on leukocyte migration and inflammation.* Journal of leukocyte biology, 2007. **82**(6): p. 1375-1381.
56. Bakshi, R., Thompson, A. J., Rocca, M. A., Pelletier, D., Dousset, V., Barkhof, F., ... Filippi, M., *MRI in multiple sclerosis: current status and future prospects.* Lancet. Neurol., 2008. **7**: p. 615-625.
57. Stadelmann, C., *Multiple sclerosis as a neurodegenerative disease: pathology, mechanisms and therapeutic implications.* Current opinion in neurology, 2011. **24**(3): p. 224-229.
58. Nikić, I., Merkler, D., Sorbara, C., Brinkoetter, M., Kreutzfeldt, M., Bareyre, F. M., ... Kerschensteiner, M., *A reversible form of axon damage in experimental autoimmune encephalomyelitis and multiple sclerosis.* Nature medicine, 2011. **17**(4): p. 495-499.
59. Goldsby, R.A., Kindt, T. J., & Osborne, B. A., *Kuby Immunology: vaccines*. 4th ed2000, New York: Freeman & Co.
60. Compston, A., & Coles, A., *Multiple sclerosis.* Lancet, 2008. **372**: p. 1502-1517.
61. Bar-Or, A., *The immunology of multiple sclerosis.* Seminars in neurology, 2008. **28**: p. 29-45.
62. Libbey, J.E., McCoy, L. L., & Fujinami, R. S., *Molecular mimicry in multiple sclerosis.* Int. Rev. Neurobiol., 2007. **79**: p. 127-147.
63. Myoung, J., Kang, H. S., Hou, W., Meng, L., Dal Canto, M. C., & Kim, B. S., *Epitope-specific CD8+ T cells play a differential pathogenic role in the development of a viral disease model for multiple sclerosis.* Journal of virology, 2012.
64. Sallusto, F., Impellizzieri, D., Basso, C., Laroni, A., Uccelli, A., Lanzavecchia, A., & Engelhardt, B., *T-cell trafficking in the central nervous system.* Immunological reviews, 2012. **248**(1): p. 216-217.
65. Man, S., Ubogu, E. E., & Ransohoff, R. M., *Inflammatory Cell Migration into the Central Neuvous System: a few new twists on an old table.* Brain Pathology, 2007. **17**(2): p. 243-250.
66. Androdias, G., Reynolds, R., Chanal, M., Ritleng, C., Confavreux, C., & Nataf, S., *Meningeal T cells associate with diffuse axonal loss in multiple sclerosis spinal cords.* Ann. Neurol., 2010. **68**: p. 465-476.
67. Magliozzi, R., Howell, O. W., Reeves, C., Roncaroli, F., Nicholas, R., Serafini, B., ... Reynolds, R., *A gradient of neuronal loss and meningeal inflammation in multiple sclerosis.* Ann. Neurol., 2010. **68**(4): p. 477-493.
68. Frischer, J.M., Bramow, S., Dal-Bianco, A., Lucchinetti, C. F., Rauschka, H., Schmidbauer, M., ... Lassmann, H., *The relation between inflammation and neurodegeneration in multiple sclerosis brains.* Brain, 2009. **132**(Pt 5): p. 1175-1189.
69. Schirmer, L., Antel, J. P., Brück, W., & Stadelmann, C., *Axonal loss and neurofilament phosphorylation changes accompany lesion development and clinical progression in multiple sclerosis.* Brain pathology, 2011. **21**(4): p. 428-440.
70. Sawcer, S., Hellenthal, G., Pirinen, M., Spencer, C. C., Patsopoulos, N. A., Moutsianas, L., ... Compston, A., *Genetic risk and a primary role for cell-*

mediated immune mechanisms in multiple sclerosis. Nature, 2011. **476**(7359): p. 214-219.
71. Bitsch, A., Schuchardt, J., Bunkowski, S., Kuhlmann, T., & Brück, W., *Acute axonal injury in multiple sclerosis. Correlation with demyelination and inflammation.* Brain, 2000. **123**(6): p. 1174-1183.
72. Bjartmar, C., Wujek, J. R., & Trapp, B. D., *Axonal loss in the pathology of MS: consequences for understanding the progressive phase of the disease.* J. Neuro. Sci., 2003. **206**(2): p. 165-171.
73. Lappe-Siefke, C., Goebbels, S., Gravel, M., Nicksch, E., Lee, J., Braun, P. E., ... Nave, K. A., *Disruption of Cnp1 uncouples oligodendroglial functions in axonal support and myelination.* Nature genetics, 2003. **33**(3): p. 366-374.
74. Zambonin, J.L., Zhao, C., Ohno, N., Campbell, G. R., Engeham, S., Ziabreva, I., ... Mahad, D. J., *Increased mitochondrial content in remyelinated axons: implications for multiple sclerosis.* Brain, 2011. **134**(Pt 7): p. 1901-1913.
75. Copper, G.M., *The Cell: A Molecular Approach*, 2000, Sinauer Associates: Sunderland (MA).
76. Witte, M.E., Mahad, D. J., Lassmann, H., & van Horssen, J., *Mitochondrial dysfunction contributes to neurodegeneration in multiple sclerosis.* Trends in Molecular Medicine, 2014. **20**(3): p. 179-187.
77. Martin, L.J., *Mitochondrial and Cell Death Mechanisms in Neurodegenerative Diseases.* Pharmaceuticals (Basel), 2011. **3**(4): p. 839-915.
78. Piaceri, I., Rinnoci, V., Bagnoli, S., Failli, Y., & Sorbi, S., *Mitochondria and Alzheimer's Disease.* Journal of the Neurological Sciences, 2012. **322**(1-2): p. 31-34.
79. Cleveland, D.W., & Rothstein, J. D., *From Charcot to Lou Gehrig: Deciphering Selective Motor Neuron Death in ALS.* Nature Reviews Neuroscience, 2001. **2**(11): p. 806-819.
80. Di Filippo, M., Chiasserini, D., Tozzi, A., Picconi, B., & Calabresi, P., *Mitochondria and the link between neuroinflammation and neurodegeneration.* Journal of Alzheimer's Disease, 2010. **20**: p. S369-S379.
81. van Horssen, J., Witte, M. E., Schreibelt, G., & de Vries, H. E., *Radical changes in multiple sclerosis pathogenesis.* Biochimica et biophysica acta, 2011. **1812**(2): p. 141-150.
82. Witte, M.E., Geurts, J. J. G., de Vries, H. E., van der Valk, P., & van Horssen, J., *Mitochondrial dysfunction: a potential link between neuroinflammation and neurodegeneration?* Mitochondrion, 2010. **10**(5): p. 411-418.
83. Campbell, G.R., Ziabreva, I., Reeve, A. K., Krishnan, K. J., Reynolds, R., Howell, O., ... Mahad, D. J., *Mitochondrial DNA deletions and neurodegeneration in multiple sclerosis.* Annals of neurology, 2011. **69**(3): p. 481-492.
84. Mahad, D.J., Ziabreva, I., Campbell, G., Lax, N., White, K., Hanson, P. S., Lassmann, H., & Turnbull, D. M., *Mitochondrial changes within axons in multiple sclerosis.* Brain, 2009. **132**: p. 1161-1174.
85. Qi, X., Lewin, A. S., Sun, L., Hauswirth, W. W., & Guy, J., *Mitochondrial protein nitration primes neurodegeneration in experimental autoimmune encephalomyelitis.* J. Biol. Chem., 2006. **281**(42): p. 31950-31962.

86. Stommel, E.W., van Hoff, R. M., Graber, D. J., Bercury, K. K., Langford, G. M., & Harris, B. T., *Tumor necrosis factor-a induces changes in mitochondrial cellular distribution in motor neurons.* Neuroscience, 2007. **146**(3): p. 1013-1019.
87. Swarup, V., Das, S., Ghosh, S., & Basu, A., *Tumor necrosis factor receptor-1-induced neuronal death by TRADD contributes to the pathogenesis of Japanese encephalitis.* J. Neurochem., 2007. **103**(2): p. 771-783.
88. Trapp, B.D., & Stys, P. K., *Virtual hypoxia and chronic necrosis of demyelinated axons in multiple sclerosis.* Lancet Neurol., 2009. **8**: p. 280-291.
89. Campbell, G.R., & Mahad, D. J., *Mitochondrial changes associated with demyelination: consequences for axonal integrity.* Mitochondrion, 2012. **12**(2): p. 173-179.
90. Cai, Q., & Sheng, Z. H., *Mitochondrial transport and docking in axons.* Experimental neurology, 2009. **218**(2): p. 257-267.
91. Hollenbeck, P.J., *The pattern and mechanism of mitochondrial transport in axons.* Front Biosci., 1996. **1**: p. d91-102.
92. Chen, H., & Chan, D. C., *Mitochondrial dynamics--fusion, fission, movement, and mitophagy--in neurodegenerative diseases.* Human molecular genetics, 2009. **18**(R2): p. R169-176.
93. Saxton, W.M., & Hollenbeck, P. J., *The axonal transport of mitochondria.* Journal of cell science, 2012. **125**(Pt 9): p. 2095-2104.
94. Reddy, P.H., Reddy, T. P., Manczak, M., Calkins, M. J., Shirendeb, U., & Mao, P., *Dynamin-related protein 1 and mitochondrial fragmentation in neurodegenerative diseases.* Brain research reviews, 2011. **67**(1-2): p. 103-118.
95. Ong, S.B., & Hausenloy, D. J., *Mitochondrial morphology and cardiovascular disease.* Cardiovascular Research, 2010. **88**(1): p. 16-29.
96. Otera, H.C., Wang, M. M., Cleland, K., Setoguchi, S., Yokota, R. J., & Mihara, K., *Mff is an essential factor for mitochondrial recruitment of Drp1 during mitochondrial fission in mammalian cells.* J. Cell Biol., 2010. **191**: p. 1141-1158.
97. Chen, H., Detmer, S. A., Ewald, A. J., Griffin, E. E., Fraser, S. E., & Chan, D. C., *Mitofusins Mfn1 and Mfn2 coordinately regulate mitochondrial fusion and are essential for embryonic development.* J. Cell. Biol., 2003. **160**: p. 189-200.
98. Ishihara, N., Eura, Y., & Mihara, K., *Mitofusin 1 and 2 play distinct roles in mitochondrial fusion reactions via GTPase activity.* J. Cell Sci., 2004. **117**: p. 6535-6546.
99. de Brito, O.M., & Scorrano, L., *Mitofusin 2 tethers endoplasmic reticulum to mitochondria.* Nature, 2008. **456**: p. 605-610.
100. Chang, D.T.W., & Reynolds, I. J., *Mitochondrial trafficking and morphology in healthy and injured neurons.* Progress in neurobiology, 2006. **80**(5): p. 241-268.
101. Manczak, M., Calkins, M. J., & Reddy, P. H., *Impaired mitochondrial dynamics and abnormal interaction of amyloid beta with mitochondrial protein Drp1 in neurons from patients with Alzheimer's disease: implications for neuronal damage.* Hum. Mol. Genet., 2011. **20**: p. 2495-2509.
102. Reddy, P., *Inhibitors of Mitochondrial Fission as a Therapeutic Strategy for Diseases with Oxidative Stress and Mitochondrial Dysfunction.* Journal of Alzheimer's Disease, 2014. **40**(2): p. 245-256.

103. Magrané, J., & Manfredi, G., *Mitochondrial function, morphology, and axonal transport in amyotrophic lateral sclerosis.* Antioxid. Redox Signal., 2009. **11**(7): p. 1615-1626.
104. Liang, C.L., Wang, T. T., Luby-Phelps, K., & German, D. C., *Mitochondria mass is low in mouse substantia nigra dopamine neurons: implications for Parkinson's disease.* Exp. Neurol., 2007. **203**: p. 370-380.
105. Exner. N., T., B., Paquet, D., Holmstrom, K., Schiesling, C., Gispert, S., ... Haass, C., *Loss-of-function of human PINK1 results in mitochondrial pathology and can be rescued by parkin.* J. Neurosci., 2007. **27**(45): p. 12413-12418.
106. Su, Y.C., & Qi, X., *Inhibition of excessive mitochondrial fission reduced aberrant autophagy and neuronal damage caused by LRRK2 G2019S mutation.* Hum. Mol. Genet., 2013. **22**(22): p. 4545-4561.
107. Amiri, M., & Hollenbeck, P. J., *Mitochondrial biogenesis in the axons of vertebrate peripheral neurons.* Dev. Neurobiol., 2008. **68**: p. 1348-1361.
108. Alberts, B., Johnson, A., Lewis, J., Raff, M., Roberts, K., & Walter, P., *Molecular Biology of the Cell*, 2002, Garland Science: New York.
109. Xu, C., Bailly-Maitre, B., & Reed, J., *Endoplasmic reticulum stress: cell life and death decisions.* Journal of Clinical Investigation, 2005. **115**(10): p. 2656-2664.
110. Li, S., Yang, L., Selzer, M. E., & Hu, Y., *Neuronal endoplasmic reticulum stress in axon injury and neurodegeneration.* Annals of neurology, 2013. **00**: p. 1-10.
111. Halliday, M., & Mallucci, G. R., *Targeting the unfolded protein response in neurodegeneration: a new approach to therapy.* Neuropharmacology, 2014. **76**(Pt A): p. 169-174.
112. Nijholt, D.A., de Graaf, T. R., van Haastert, E. S., Oliveira, A. O., Berkers, C. R., Zwart, R., ... Scheper, W., *Endoplasmic reticulum stress activates autophagy but not the proteasome in neuronal cells: implications for Alzheimer's disease.* Cell Death Differ., 2011. **18**(6): p. 1071-1081.
113. Nijholt, D.A., van Haastert, E. S., Rozemuller, A. J., Scheper, W., & Hoozemans, J. J., *The unfolded protein response is associated with early tau pathology in the hippocampus of tauopathies.* J. Pathol., 2012. **226**: p. 693-702.
114. Hetz, C., Russelakis-Carneiro, M., Maundrell, K., Castilla, J., & Soto, C., *Caspase-12 and endoplasmic reticulum stress mediate neurotoxicity of pathological prion protein.* EMBO J., 2003. **22**: p. 5435-5445.
115. Wang, X., Shi, Q., Xu, K., Gao, C., Chen, C., Li, X. L., ... Dong, X. P., *Familial CJD associated PrP mutants within transmembrane region induced Ctm-PrP retention in ER and triggered apoptosis by ER stress in SH-SY5Y cells.* PLoS One, 2011. **6**(1): p. e14602.
116. Orsi, A., Fioriti, L., Chiesa, R., & Sitia, R., *Conditions of endoplasmic reticulum stress favor the accumulation of cytosolic prion protein.* J. Biol. Chem., 2006. **281**: p. 30431-30438.
117. Cunnea, P., Mhaille, A. N., McQuaid, S., Farrell, M., McMahon, J., & FitzGerald, U., *Expression profiles of endoplasmic reticulum stress-related molecules in demyelinating lesions and multiple sclerosis.* Multiple Sclerosis, 2011. **17**(7): p. 808-818.

118. McMahon, J.M., McQuaid, S., Reynolds, R. & FitzGerald, U. F., *Increased expression of ER stress- and hypoxia-associated molecules in grey matter lesions in multiple sclerosis.* Multiple sclerosis, 2012. **18**(10): p. 1437-1447.
119. Ni Fhlathartaigh, M., McMahon, J., Reynolds, R., Connolly, D., Higgins, E., Counihan, T., & FitzGerald, U., *Calreticulin and other components of endoplasmic reticulum stress in rat and human inflammatory demyelination.* Acta. Neuropathol. Commun., 2013. **1**(1): p. 37.
120. Csordas, G., Renken, C., Varnai, P., Walter, L., Weaver, D., Buttle, K. F., ... Hajnoczky, G., *Structural and functional features and significance of the physical linkage between ER and mitochondria.* The Journal of cell biology, 2006. **174**: p. 915-921.
121. Birner, R., Burgermeister, M., Schneiter, R., & Daum, G., *Roles of phosphatidylethanol- amine and of its several biosynthetic pathways in Saccharomyces cerevisiae.* Mol. Biol. Cell, 2001. **12**: p. 997-1007.
122. Steenbergen, R., Nanowski, T. S., Beigneux, A., Kulinski, A., Young, S. G., & Vance, J. E., *Disruption of the phosphatidylserine decarboxylase gene in mice causes embryonic lethality and mitochondrial defects.* J. Biol. Chem., 2005. **280**: p. 40032-40040.
123. Raturi, A., & Simmen, T., *Where the endoplasmic reticulum and the mitochondrion tie the knot: The mitochondria-associated membrane (MAM).* Biochim. Biophys. Acta., 2013. **1833**(1): p. 213-224.
124. Cardenas, C., Miller, R. A., Smith, I., Bui, T.,Molgo, J., Muller, M., ... Foskett, J. K., *Essential regulation of cell bioenergetics by constitutive InsP3 receptor Ca2+ transfer to mitochondria.* Cell, 2010. **142**: p. 270-283.
125. Simmen, T., Aslan, J. E., Blagoveshchenskaya, A. D., Thomas, L., Wan, L., Xiang, Y., ... Thomas, G., *PACS-2 controls endoplasmic reticulum-mitochondria communication and Bid-mediated apoptosis.* The EMBO journal., 2005. **24**: p. 717-729.
126. Bernardi, P., & Rasola, A., *Calcium and cell death: the mitochondrial connection.* Sub-cellular biochemistry, 2007. **45**: p. 481-506.
127. Boehning, D., Patterson, R. L., Sedaghat, L., Glebova, N. O., Kurosaki, T., & Snyder, S. H., *Cytochrome c binds to inositol (1,4,5) trisphosphate receptors, amplifying calcium-dependent apoptosis.* Nature cell biology, 2003. **5**: p. 1051-1061.
128. Schon, E.A., & Area-Gomez, E., *Mitochondria-associated ER membranes in Alzheimer disease.* Molecular and Cellular Neurosciences, 2013. **55**: p. 26-36.
129. Cheung, K.H., Shineman, D., Muller,M., Cardenas, C., Mei, L., Yang, J., ... Foskett, J. K., *Mechanismof Ca2+ disruption in Alzheimer's disease by presenilin regulation of InsP3 receptor channel gating.* Neuron, 2008. **58**: p. 871-883.
130. McCaffrey, M.W.L., A. J., *Rab Family.* Encyclopedia of Biological Chemistry, 2004. **3**: p. 629-634.
131. Zerial, M., & McBride, H., *Rab proteins as membrane organizers.* Nat. Rev. Mol. Cell. Biol., 2001. **2**(2): p. 107-117.
132. Brighouse, A., Dacks, J. B., & Field, M. C., *Rab protein evolution and the history of the eukaryotic endomembrane system.* Cellular and molecular life sciences: CMLS, 2010. **67**(20): p. 3449-3465.

133. Novick, P., Medkova, M., Dong, G., Hutagalung, A., Reinisch, K., & Grosshans, B., *Interactions between Rabs, tethers, SNAREs and their regulators in exocytosis.* Biochem. Soc. Trans., 2006. **34**: p. 683-686.
134. Bao, X., Faris, A. E., Jang, E. K., & Haslam, R. J., *Molecular cloning, bacterial expression and properties of Rab31 and Rab32 New blood platelet Rab proteins.* Eur. J. Biochem., 2002. **271**: p. 259-271.
135. Ambrosio, A.L., Boyle, J. A., & Di Pietro, S. M., *Mechanism of platelet dense granule biogenesis: study of cargo transport and function of Rab32 and Rab38 in a model system.* Blood, 2012. **120**: p. 4072-4081.
136. Bui, M., Gilady, S. Y., Fitzsimmons, R. E. B., Benson, M. D., Lynes, E. M., Gesson, K., ... Simmen, T., *Rab32 modulates apoptosis onset and mitochondria-associated membrane (MAM) properties.* J. Bio. Chem., 2010. **285**(41): p. 31590-31602.
137. Alto, N.M., Soderling, J., & Scott, J. D., *Rab32 is an A-kinase anchoring protein and participates in mitochondrial dynamics.* The Journal of cell biology, 2002. **158**(4): p. 659-668.
138. Grohm, J., Kim, S. W., Mamrak, U., Tobaben, S., Cassidy-Stone, A., Nunnari, J., ... Culmsee, C., *Inhibition of Drp1 provides neuroprotection in vitro and in vivo.* Cell Death Differ., 2012. **19**(9): p. 1446-1458.
139. Yoshimura, S., Egerer, J., Fuchs, E., Haas, A. K., & Barr, F. A., *Functional dissection of Rab GTPases involved in primary cilium formation.* J. Cell Biol., 2007. **178**(363-369).
140. Sandoval, C.O., & Simmen, T., *Rab proteins of the endoplasmic reticulum: functions and interactors.* Biochem. Soc. Trans., 2012. **40**: p. 1426-1432.
141. Fujikawa, K., Satoh, A., & Kawamura, S., *Molecular and functional characterization of a unique Rab protein, RABRP1, containing the WDIAGQE sequence in a GTPase motif.* Zoological science., 2002. **19**: p. 981-993.
142. Marks, M.S., *Organelle biogenesis: en BLOC exchange for RAB32 and RAB38.* Current Biology, 2012. **22**(22): p. R963-965.
143. Gan-Or, Z., Bar-Shira, A., Dahary, D., Mirelman, A., Kedmi, M., Gurevich, T., ... Orr-Urtreger, A., *Association of Sequence Alterations in the Putative Promoter of Rab7L1 With a Reduced Parkinson Disease Risk.* Arch. Neurol., 2012. **69**(1): p. 105-110.
144. Zhu, Y., Vergote, D., Pardo, C., Noorbakhsh, F., McArthur, J. C., Hollenberg, M. D., ... Power, C., *CXCR3 activation by lentivirus infection suppresses neuronal autophagy: neuroprotective effects of antiretroviral therapy.* FASEB J., 2009. **23**(9): p. 2928-2941.
145. Lu, J.Q., Wilson, B., Yong, V. W., Pugh, J., & Mehta, V., *Immune cell infiltrates in atypical teratoid/rhabdoid tumors.* The Canadian journal of neurological sciences, 2012. **39**(5): p. 605-612.
146. Zeitelhofer, M., Vessey, J. P., Xie, Y., Tübing, F., Thomas, S., Kiebler, M., & Dahm, R., *High-efficiency transfection of mammalian neurons via nucleofection.* Nature Protocols, 2007. **2**(7): p. 1692-1704.
147. Liang, Y., Lin, S., Zou, L., Zhou, H., Zhang, J., Su, B., & Wan, Y., *Expression profiling of Rab GTPases reveals the involvement of Rab20 and Rab32 in acute brain inflammation in mice.* Neuroscience letters, 2012. **572**(2): p. 110-114.

148. Groenendyk, J., & Michalak, M., *Endoplasmic reticulum quality control and apoptosis.* Acta. Biochim. Pol., 2005. **52**(2): p. 381-395.
149. Grimm, S., *The ER–mitochondria interface: The social network of cell death.* Biochimica et Biophysica Acta, 2012. **1823**(2): p. 327-334.
150. Lynes, E.M., & Simmen, T, *Urban planning of the endoplasmic reticulum (ER): How diverse mechanisms segregate the many functions of the ER.* Biochimica et Biophysica Acta, 2011. **1813**(10): p. 1893-1905.
151. Cohen-Solal, K.A., Sood, R., Marin, Y., Crespo-Carbone, S. M., Sinsimer, D., Martino, J. J., ... Chen, S., *Identification and characterization of mouse Rab32 by mRNA and protein expression analysis.* Biochim. Biophys. Acta., 2003. **1651**(1-2): p. 68-75.
152. Bultema, J.J., & Di Pietro, S. M., *Cell type-specific Rab32 and Rab38 cooperate with the ubiquitous lysosome biogenesis machinery to synthesize specialized lysosome-related organelles.* Small GTPases, 2013. **4**(1): p. 16-21.
153. Vellinga, M.M., Vrenken, H., Hulst, H. E., Polman, C. H., Uitdehaaq, B. M., Pouwels, P. J., ... Geurts, J. J., *Use of ultrasmall superparamagnetic particles of iron oxide (USPIO)-enhanced MRI to demonstrate diffuse inflammation in the normal-appearing white matter (NAWM) of multiple sclerosis (MS) patients: an exploratory study.* Journal of Magnetic Resonance Imaging : JMRI, 2009. **29**(4): p. 774-779.
154. Misko, A., Jiang, S., Wegorzewska, I., Milbrandt, J., & Baloh, R. H., *Mitofusin 2 is necessary for transport of axonal mitochondria and interacts with the Miro/Milton complex.* The Journal of neuroscience, 2010. **30**(12): p. 4232-4240.
155. Hafler, D.A., Compston, A., Sawcer, S., Lander, E. S., Daly, M. J., De Japer, P. L., ... Hauser, S. L., *The International Multiple Sclerosis Genetics Consortium: risk alleles for multiple sclerosis identified by a genome wide study.* N. Engl. J. Med., 2007. **357**(9): p. 851-862.
156. Alcina, A., Fernández, O., Gonzalez, J. R., Catalá-Rabasa, A., Fedetz, M., Ndagire, D., ... Matesanz, F., *Tag-SNP analysis of the GFI1-EVI5-RPL5-FAM69 risk locus for multiple sclerosis.* European journal of human genetics : EJHG, 2010. **18**(7): p. 827-831.
157. Baranzini, S.E., Wang, J., Gibson, R. a, Galwey, N., Naegelin, Y., Barkhof, F., ... Oksenberg, J. R., *Genome-wide association analysis of susceptibility and clinical phenotype in multiple sclerosis.* Human molecular genetics, 2009. **18**(4): p. 767-778.
158. Laflamme, C., Assaker, G., Ramel, D., Dorn, J. F., She, D., Maddox, P. S., & Emery, G., *Evi5 promotes collective cell migration through its Rab-GAP activity.* The Journal of cell biology, 2012. **198**(1): p. 57-67.
159. Faitar, S.L., Dabbeekeh, J. T. S., Ranalli, T. A., & Cowell, J. K., *EVI5 is a novel centrosomal protein that binds to alpha- and gamma-tubulin.* Genomics, 2005. **86**(5): p. 594-605.
160. Itoh, T., Satoh, M., Kanno, E., & Fukuda, M., *Screening for target Rabs of TBC (Tre-2/Bub2/Cdc16) domain-containing proteins based on their Rab-binding activity.* Genes to cells: devoted to molecular & cellular mechanisms, 2006. **11**(9): p. 1023-1037.

161. Lim, Y.S., & Tang, B. L., *Investigating the roles and functions of Rab23 in primary ciliogenesis.* Cilia, 2012. **1**(Suppl 1): p. 33.
162. Fuchs, E., Haas, A. K., Spooner, R. A., Yoshimura, S., Lord, J. M., & Barr, F. A., *Specific Rab GTPase-activating proteins define the Shiga toxin and epidermal growth factor uptake pathways.* The Journal of cell biology, 2007. **177**(6): p. 1133-1143.
163. Gomez-Lazaro, M., Bonekamp, N. A., Galindo, M. F., Jordán, J., & Schrader, M., *6-Hydroxydopamine (6-OHDA) induces Drp1-dependent mitochondrial fragmentation in SH-SY5Y cells.* Free Radic. Biol. Med., 2008. **44**(11): p. 1960-1969.
164. Kim, S.U., Lee, H. J., & Kim, Y. B., *Neural stem cell-based treatment for neurodegenerative diseases.* Neuropathology, 2013. **33**(5): p. 491-504.
165. Wang, T., Choi, E., Monaco, M. C., Campanac, E., Medynsts, M., Do, T., ... Nath, A., *Derivation of Neural Stem Cells from Human Adult Peripheral CD34+ Cells for an Autologous Model of Neuroinflammation.* PloS One, 2014. **8**(11): p. e81720.
166. Zayoud, M., El Malki, K., Frauenknecht, K., Teinschek, B., Kloos, L., Karram, K., ... Kurschus, F. C., *Subclinical CNS inflammation as response to a myelin antigen in humanized mice.* J. Neuroimmune Pharmacol., 2013. **8**(4): p. 1037-1047.

APPENDIX

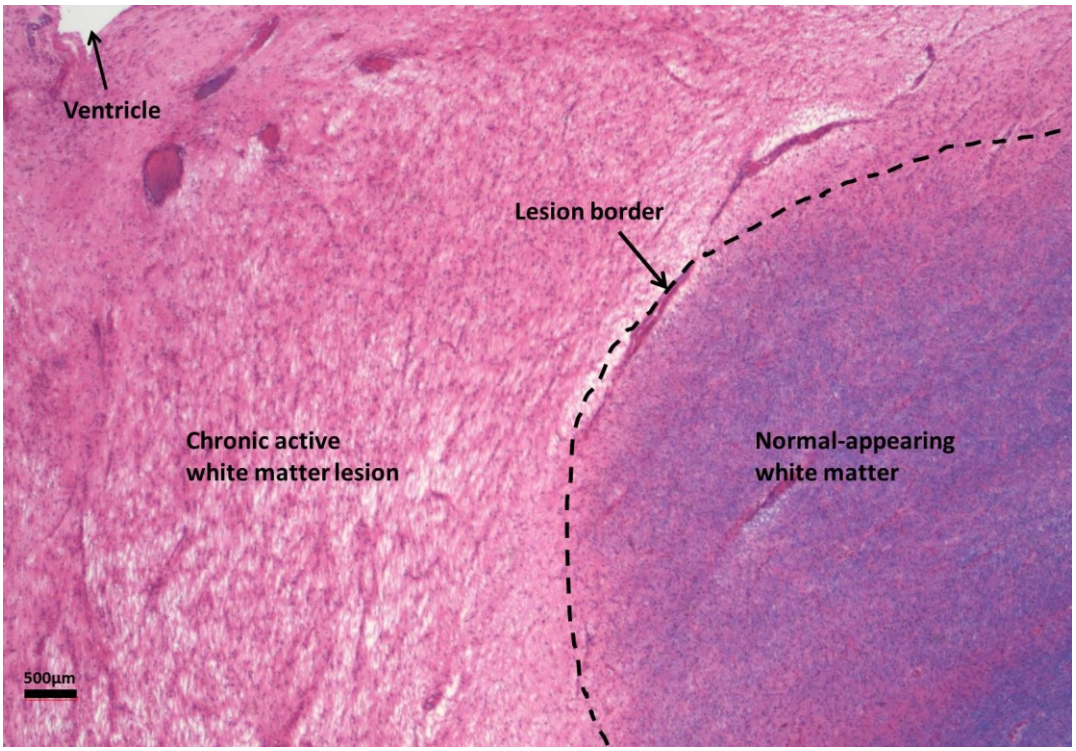

Figure 7.1 Identification of lesion and NAWM areas in surgical specimen tissue section of MS patient brain. Autopsy tissue sections from a MS patient (NP 12-50) brain with chronic active lesions were stained by hematoxylin and eosin (Table 2.1) for basic cellular structure and Luxol Fast Blue (Table 2.1) for myelin structure. In the image of the section, purple dots represent cell nucleus and pink area represents cytosolic tissue structure. The blue area on lower right corner represents myelin-covered normal-appearing white matter, and the peri-ventricular white matter area without myelin (blue) shows highly disruptive tissue structure, and is identified as a chronic active lesion. The junction between NAWM and lesion shows less destruction of the tissue without myelin sheath coverage is indicated as lesion border where cell degeneration is relatively mild but immune cell activation and inflammation are more dominated. The upper left cover of the section shows the ventricle. Scale bar = 500µm.